INTERNATIONAL ATOMIC ENERGY AGENCY
UNITED NATIONS EDUCATIONAL, SCIENTIFIC AND CULTURAL ORGANIZATION
INTERNATIONAL CENTRE FOR THEORETICAL PHYSICS
I.C.T.P., P.O. BOX 586, 34100 TRIESTE, ITALY, CABLE: CENTRATOM TRIESTE

SMR. 758 - 12

SPRING COLLEGE IN CONDENSED MATTER ON QUANTUM PHASES

(3 May - 10 June 1994)

==========

FURTHER MATERIAL for lectures on

NUMERICAL RENORMALIZATION GROUP STUDIES OF KONDO PROBLEMS

Barbara A. JONES
IBM Research Division
Almaden Research Centre
San Jose, CA 95120, U.S.A.

==========

These are preliminary lecture notes, intended only for distribution to participants.

==========

PHYSICAL REVIEW B VOLUME 21, NUMBER 3 1 FEBRUARY 1980

Renormalization-group approach to the Anderson model of dilute magnetic alloys. I. Static properties for the symmetric case

H. R. Krishna-murthy,* J. W. Wilkins, and K. G. Wilson
Physics Department, Cornell University, Ithaca, New York 14853
(Received 10 September 1979)

The temperature-dependent impurity susceptibility for the symmetric Anderson model is calculated for all physically relevant values of its parameters U (the Coulomb correlation energy) and Γ (the impurity-level width). It is shown that, when $U > \pi\Gamma$, for temperatures $T < U/(10k_B)$ the symmetric Anderson model exhibits a local moment and that its susceptibility maps neatly onto that of the spin-$\frac{1}{2}$ Kondo model with an effective coupling given by $\rho J_{\text{eff}} = -8\Gamma/\pi U$. Furthermore, this mapping is shown for remarkably large values of $|\rho J_{\text{eff}}|$. At very low temperatures (much smaller than the Kondo temperature) the local moment is frozen out, just as for the Kondo model, leading to a strong-coupling regime of constant susceptibility at zero termperature. The results also depict the formation of a local moment from the free orbital as T drops below U, a feature not present in the Kondo model. Finally, when $U << \pi\Gamma$ there is a direct transition from free-orbital regime for $T >> \Gamma$ to the strong-coupling regime for $T << \Gamma$. The calculations were performed using the numerical renormalization group originally developed by Wilson for the Kondo problem. In addition to the actual numerical calculations, analytic results are presented. In particular, the effective Hamiltonians, i.e., fixed-point Hamiltonian plus relevant and marginal operators, are constructed for the free-orbital, local-moment, and strong-coupling regimes. Analytic formulas for the impurity susceptibility and free energy in all three regimes are developed. The impurity specfic heat in the strong-coupling regime is calculated.

I. INTRODUCTION

The paper and the one following it are devoted to a detailed discussion of the application of renormalization-group techniques to the Anderson model[1] of dilute magnetic alloys and, in particular, to a calculation of the susceptibility. Previously we have published summaries of our calculations for the symmetric case[2]—the subject of this paper (I)—and the asymmetric case[3]—which is covered in the following paper (II). Accordingly we defer any summary of our results until the introduction of the following paper, where we compare and contrast the underlying physics of the symmetric and asymmetric Anderson models. The experimentalist or casual theoretically-inclined reader is directed to that introduction. At the same time we do not have space for a discussion of most of the previous theoretical effort in this area but instead refer the reader to available review articles[4] and the first published susceptibility calculation[5] for the Anderson model.

This work is an extension of the application[6] of the numerical renormalization-group techniques to the Kondo model. That the application is far from trivial can be judged by the length of these papers. Nonetheless, in an attempt to conserve space, we have not repeated in detail arguments from that work[6] which can be used here with essentially no change.

There is one aspect of the papers that may be initially confusing. Although there is extensive numerical work associated with this approach, we would stress that once the underlying fixed points[6] have been identified, many of the calculations can be done *analytically*, albeit in some cases using parameters deduced from the numerical calculations. In these two papers we have stressed the analytic underpinning of the work in the hope that it will offer insight to future research workers attempting to compute other properties such as the electrical resistivity.

The rest of the paper is organized as follows. In Sec. II, we summarize the techniques and transformations that convert the Anderson model into a (numerically and analytically) soluble proble. Section III contains a preliminary presentation of the numerical results, whereas in Sec. IV the analytic machinery is used to derive the effective Hamiltonian about each fixed point. Detailed quantitative results appear in Sec. V, followed by a very brief summary in Sec. VI which serves as a sendoff for the introduction in Paper II. Finally, there is a set of Appendices devoted to various technical details.

II. SUMMARY OF THE BASIC TECHNIQUES

A. Model Hamiltonian

The Anderson Hamiltonian[1] for a single magnetic impurity in a nonmagnetic metal is

$$\mathcal{H}_A \equiv \sum_{\vec{k}} \epsilon_{\vec{k}} c^\dagger_{\vec{k}\mu} c_{\vec{k}\mu} + \epsilon_d c^\dagger_{d\mu} c_{d\mu} + \sum_{\vec{k}} \left(V_{\vec{k}d} c^\dagger_{\vec{k}\mu} c_{d\mu} + V^*_{\vec{k}d} c^\dagger_{d\mu} c_{\vec{k}\mu} \right) + U (c^\dagger_{d\uparrow} c_{d\uparrow})(c^\dagger_{d\downarrow} c_{d\downarrow}) \quad . \tag{2.1}$$

$\epsilon_{\vec{k}}$ and ϵ_d are to be measured from the Fermi level. *Repeated spin indices are assumed to be summed over.*

We will prefer to write Eq. (2.1) in another equivalent form

$$\mathcal{H}_A = -\tfrac{1}{2} U + \sum_{\vec{k}} \epsilon_{\vec{k}} c^\dagger_{\vec{k}\mu} c_{\vec{k}\mu} + (\epsilon_d + \tfrac{1}{2} U) c^\dagger_{d\mu} c_{d\mu} + \sum_{\vec{k}} \left(V_{\vec{k}d} c^\dagger_{\vec{k}\mu} c_{d\mu} + V^*_{\vec{k}d} c^\dagger_{d\mu} c_{\vec{k}\mu} \right) + \tfrac{1}{2} U (c^\dagger_{d\mu} c_{d\mu} - 1)^2 \quad . \tag{2.2}$$

The equivalence of the two forms can be verified by expanding out the last term in Eq. (2.2) and making use of relations such as $(c^\dagger_{d\uparrow} c_{d\uparrow})^2 = c^\dagger_{d\uparrow} c_{d\uparrow}$.

In this paper a simplified version of Eq. (2.2) will be treated. The simplification is achieved by assuming that the Fermi surface is wholly contained in a single, isotropic ($\epsilon_{\vec{k}}$ depends only on $|\vec{k}|$) conduction band extending in energy from $-D$ to D, and that $V_{\vec{k}d}$ depends only on $|\vec{k}|$. This means that if one uses a set of spherical waves about the impurity site (taken to be at the origin) as the basis states for the conduction electrons, the impurity couples only to the s-wave states. For calculating the changes in various properties of the system due to the presence of the impurity the higher angular momentum states can hence be ignored. It is convenient to let the s-wave states be labeled by energy rather than by momentum. Dropping the constant term in Eq. (2.2), the simplified version of the Hamiltonian $\mathcal{H}_A$ that results when one goes through all the steps indicated above is given by

$$\mathcal{H}_A = \int_{-D}^{D} \epsilon a^\dagger_{\epsilon\mu} a_{\epsilon\mu} \, d\epsilon + (\epsilon_d + \tfrac{1}{2} U) c^\dagger_{d\mu} c_{d\mu} + \frac{1}{2} \frac{U}{D} (c^\dagger_{d\mu} c_{d\mu} - 1)^2 + \int_{-D}^{D} d\epsilon \, [\rho(\epsilon)]^{1/2} [V_d(\epsilon) a^\dagger_{\epsilon\mu} c_{d\mu} + V^*_d(\epsilon) c^\dagger_{d\mu} a_{\epsilon\mu}] \quad , \tag{2.3}$$

where $\rho(\epsilon)$ is the one-electron density of states per spin, and $V_d(\epsilon)$ is V_{kd} expressed as a function of the energy ϵ_k. $a^\dagger_{\epsilon\uparrow}$ creates an electron in an s-wave state (about the origin) of energy ϵ, and is supposed to be normalized as $\{a_{\epsilon\mu}, a^\dagger_{\epsilon'\nu}\} = \delta(\epsilon - \epsilon')\delta_{\mu\nu}$. Note that the Fermi level corresponds to $\epsilon = 0$.

We now further simplify Eq. (2.3) by ignoring the energy dependence of ρ and of V_d and replacing them by their values at the Fermi level. This is *not* a crucial approximation, and the effects of relaxing this assumption will be commented upon in a later section. It is also convenient to measure energies relative to the band edge D by working in terms of the variable $k = \epsilon/D$, and operators $a_{k\mu} = \sqrt{D}\, a_{\epsilon\mu}$ [this makes $\{a_{k\mu}, a_{k'\nu}\} = \delta_{\mu\nu}\delta(k - k')$]. The final version of the model Hamiltonian that results is

$$\mathcal{H}_A = D \left\{ \int_{-1}^{1} k a^\dagger_{k\mu} a_{k\mu} \, dk + \frac{1}{D} (\epsilon_d + \tfrac{1}{2} U) c^\dagger_{d\mu} c_{d\mu} + \frac{1}{2} \frac{U}{D} (c^\dagger_{d\mu} c_{d\mu} - 1)^2 + \left(\frac{\Gamma}{\pi D} \right)^{1/2} \int_{-1}^{1} dk \, (a^\dagger_{k\mu} c_{d\mu} + c^\dagger_{d\mu} a_{k\mu}) \right\} \quad , \tag{2.4}$$

where

$$\Gamma \equiv \pi \rho V_d^2 \quad . \tag{2.5}$$

In this form the Hamiltonian retains only the barest essential structure; only the dimensionless parameters (ϵ_d/D), (U/D), and (Γ/D) enter the theory, and the temperature-dependent properties of the Hamiltonian will be functions only of the ratio $(k_B T/D)$. Appendix A contains more details about the various transformations of the Hamiltonian discussed above.

The *results* to be presented in this paper will be confined to the *symmetric case*, which corresponds to choosing $\epsilon_d = -\frac{1}{2} U$ so that the second term in Eq. (2.4) is absent. (The asymmetric case will be considered in the next paper.) In this case $\mathcal{H}_A$ exhibits particle-hole symmetry; i.e., it remains invariant under the transformation $(a_{k\mu} \rightarrow a^\dagger_{-k\mu},\ c_{d\mu} \rightarrow -c^\dagger_{d\mu})$. Since the basic techniques to be summarized in the rest of this section are as applicable to the asymmetric case as to the symmetric case, the full Hamiltonian will be considered until we come to Sec. III.

B. Logarithmic discretization

The problem is to calculate the "impurity contribution" to the various properties of the system described by Eq. (2.4). The key to its solution lies in a logarithmic discretization of k space. One introduces a parameter $\Lambda (> 1)$ and divides up the k domain $[-1, 1]$ into a sequence of intervals as shown in Fig. 1. The nth interval (for positive k) extends from $\Lambda^{-(n+1)}$ to Λ^{-n}. One can now define a complete set of orthonormal functions spanning the k space by

setting up Fourier series in each of these intervals

$$\psi_{np}^{\pm}(k) = \begin{cases} \dfrac{\Lambda^{n/2}}{(1-\Lambda^{-1})^{1/2}} e^{\pm i\omega_n pk} & \text{if } \Lambda^{-(n+1)} < \pm k < \Lambda^{-n} \\ 0 & \text{if } k \text{ is outside the above interval} \end{cases} . \tag{2.6}$$

Here n, the interval index, takes values $0, 1, 2, \ldots$; p, the Fourier harmonic index, takes on all integral values from $-\infty$ to $+\infty$; the superscript $+$ $(-)$ denotes a basis function defined for positive (negative) k. ω_n, the *fundamental* Fourier frequency in the nth interval, is clearly

$$\omega_n = \frac{2\pi}{\Lambda^{-n} - \Lambda^{-(n+1)}} = \frac{2\pi\Lambda^n}{1-\Lambda^{-1}} . \tag{2.7}$$

The operators $a_{k\mu}$ can be expanded in this basis

$$a_{k\mu} = \sum_{np} [a_{np\mu}\psi_{np}^{+}(k) + b_{np\mu}\psi_{np}^{-}(k)] ; \tag{2.8}$$

$$a_{np\mu} = \int_{-1}^{1} dk\, [\psi_{np}^{+}(k)]^* a_{k\mu}; \quad b_{np\mu} = \int_{-1}^{1} dk\, [\psi_{np}^{-}(k)]^* a_{k\mu} . \tag{2.9}$$

The operators $a_{np\mu}$ and $b_{np\mu}$ form a complete set of independent, discrete, electron operators obeying standard anticommutation rules

$$\{a_{np\mu}, a_{n'p'\mu'}^{\dagger}\} = \delta_{nn'}\delta_{pp'}\delta_{\mu\mu'} , \ldots .$$

The Hamiltonian Eq. (2.4) can now be expressed in terms of the discrete operators $a_{np\mu}$ instead of the operators $a_{k\mu}$. It is straightforward to verify the following two results:

$$\int_{-1}^{1} k a_{k\mu}^{\dagger} a_{k\mu}\, dk = \tfrac{1}{2}(1+\Lambda^{-1}) \sum_{np} \Lambda^{-n}(a_{np\mu}^{\dagger} a_{np\mu} - b_{np\mu}^{\dagger} b_{np\mu}) + \frac{1-\Lambda^{-1}}{2\pi i} \sum_{n} \sum_{p \neq p'} \frac{\Lambda^{-n}}{p'-p} (a_{np\mu}^{\dagger} a_{np'\mu} - b_{np\mu}^{\dagger} b_{np'\mu}) \exp \frac{2\pi i (p'-p)}{1-\Lambda^{-1}} , \tag{2.10}$$

$$\int_{-1}^{1} a_{k\mu}\, dk = (1-\Lambda^{-1})^{1/2} \sum_{n} \Lambda^{-n/2}(a_{n0\mu} + b_{n0\mu}) . \tag{2.11}$$

From Eqs. (2.11) and (2.4) it is clear that the impurity couples directly only to the operators a_{n0} and b_{n0}. The operators a_{np} and b_{np} with $p \neq 0$ have to be considered only because the second term in Eq. (2.10) couples them to the operators a_{n0} and b_{n0}. Because of the factor $(1-\Lambda^{-1})/2\pi$, this coupling will be small if Λ is close to 1.

As a first approximation, one now neglects the terms in Eq. (2.10) containing a_{np} and b_{np} for $p \neq 0$. Calculations for the Kondo problem[6] have shown that this is actually a surprisingly good approximation even for Λ as large as 3. The resulting approximation to $\mathcal{H}_A$ is

$$\frac{\mathcal{H}_A}{D} \cong \tfrac{1}{2}(1+\Lambda^{-1}) \sum_{n=0}^{\infty} \Lambda^{-n}(a_{n\mu}^{\dagger} a_{n\mu} - b_{n\mu}^{\dagger} b_{n\mu}) + \frac{1}{D}(\epsilon_d + \tfrac{1}{2}U) c_{d\mu}^{\dagger} c_{d\mu} + \left(\frac{2\Gamma}{\pi D}\right)^{1/2} (f_{0\mu}^{\dagger} c_{d\mu} + c_{d\mu}^{\dagger} f_{0\mu}) + \frac{1}{2}\frac{U}{D}(c_{d\mu}^{\dagger} c_{d\mu} - 1)^2 , \tag{2.12}$$

where we have defined a new operator $f_{0\mu}$, using Eq. (2.11),

$$f_{0\mu} = \left[\tfrac{1}{2}(1-\Lambda^{-1})\right]^{1/2} \sum_{n=0}^{\infty} \Lambda^{-n/2}(a_{n\mu} + b_{n\mu}) \equiv \frac{1}{\sqrt{2}} \int_{-1}^{1} dk\, a_{k\mu} . \tag{2.13}$$

The subscript "0" for the operators a_{n0} and b_{n0} has been dropped in Eqs. (2.12) and (2.13), and will be omitted

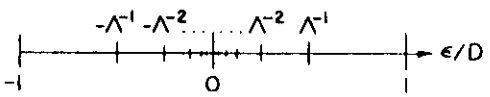

FIG. 1. Logarithmic discretization of the conduction bond. The Fermi energy is at zero and the top and bottom of the conduction bond at $k \equiv \epsilon/D = +1$ and -1, respectively.

hereafter. The factor of $1/\sqrt{2}$ in Eq. (2.13) is to normalize $f_{0\mu}$ so that $\{f_{0\mu}, f_{0\nu}^{\dagger}\} = \delta_{\mu\nu}$.

In going from the continuum Hamiltonian Eq. (2.4) to the discrete Hamiltonian Eq. (2.12), we have essentially replaced electrons with all possible energies between -1 and $+1$ by electrons with a discrete set of energies $\pm\Lambda^{-n}$. In this process energy values close to the Fermi level, which are the ones that determine the low-temperature ($k_B T \ll D$) properties of the system, *are* being well sampled. The motivation for the *logarithmic* discretization is that electron energies are thereby clearly separated into different "orders of magnitude," each of which contributes equally to logarithmic divergences found in perturbative solutions to the Anderson Hamiltonian.[4,5] See Sec. VII, Ref. 6, for a more detailed discussion regarding the motivation. The limit $\Lambda \to 1$ is the continuum limit in which the discretization ceases to be an approximation.

C. Conversion to a "hopping Hamiltonian"

In Eq. (2.12) the impurity is coupled only to the operator f_0, which is essentially the conduction-electron field operator at the impurity site. It is convenient to make a unitary transformation from the set of operators $(a_{n\mu}, b_{n\mu})$ to a new orthonormal set $(f_{n\mu})$ with $f_{0\mu}$ continuing to be given by Eq. (2.13). There are infinitely many such sets $(f_{n\mu})$. Since the conduction-electron kinetic-energy term in Eq. (2.12) is diagonal in the operators $(a_{n\mu}, b_{n\mu})$, any transformation away from this set of operators will lead to operators $(f_{n\mu})$ that are coupled to one another. The best one can do is choose such a transformation that the operators $(f_{n\mu})$ exhibit only nearest-neighbor coupling; i.e., $f_{n\mu}$ is coupled only to $f_{(n\pm1)\mu}$. Details of the derivation of such a transformation are given in Sec. VII, Ref. 6. The resulting expression for the discrete approximation to $\mathcal{H}_f$ is

$$\frac{\mathcal{H}_f}{D} = \tfrac{1}{2}(1+\Lambda^{-1}) \sum_{n=0}^{\infty} \Lambda^{-n/2} \xi_n [f_{n\mu}^{\dagger} f_{(n+1)\mu} + f_{(n+1)\mu}^{\dagger} f_{n\mu}] + \frac{1}{D}(\epsilon_d + \tfrac{1}{2}U) c_{d\mu}^{\dagger} c_{d\mu}$$
$$+ \left(\frac{2\Gamma}{\pi D}\right)^{1/2} (f_{0\mu}^{\dagger} c_{d\mu} + c_{d\mu}^{\dagger} f_{0\mu}) + \frac{1}{2}\frac{U}{D}(c_{d\mu}^{\dagger} c_{d\mu} - 1)^2 \ , \tag{2.14}$$

where the ξ_n's are Λ-dependent coefficients of order 1, given by

$$\xi_n = (1-\Lambda^{-n-1})(1-\Lambda^{-2n-1})^{-1/2}(1-\Lambda^{-2n-3})^{-1/2} \ , \tag{2.15}$$

which can essentially be replaced by 1 for large n.

Note that the transformation from the discrete Hamiltonian (2.12) to the hopping form (2.14) is an exact transformation. For later reference the expressions for the operators f_1 and f_2 will be recorded below. f_0 was defined earlier in Eq. (2.13).

$$f_{1\mu} = [\tfrac{1}{2}(1-\Lambda^{-3})]^{1/2} \sum_{n=0}^{\infty} \Lambda^{-3n/2}(a_{n\mu} - b_{n\mu}) \ , \tag{2.16}$$

$$f_{2\mu} = (\tfrac{1}{2}\Lambda)^{1/2} \frac{(1-\Lambda^{-5})^{1/2}}{(1-\Lambda^{-2})} \sum_{n=0}^{\infty} [(1-\Lambda^{-3})\Lambda^{-5n/2} - (1-\Lambda^{-1})\Lambda^{-n/2}](a_{n\mu} + b_{n\mu}) \ . \tag{2.17}$$

A general rule is that the expression for f_n involves only the combination $(a_n + b_n)$ if n is even, and only the combination $(a_n - b_n)$ if n is odd.

In order to understand the structure of the hopping Hamiltonian (2.14), it is useful to think of the one-electron *wave functions* (to be denoted by kets) to which the various second quantized operators we have defined correspond. For this purpose assume that energy and momentum are proportional, and that $D \sim \epsilon_F$. In the discussion that follows, energies are measured from the Fermi level in units of D, and distances are measured from the impurity site, in units of $1/k_F$.

The wave functions $(|a_k\rangle)$ that correspond to the set of conduction-electron operators in Eq. (2.4) are all s waves, with energies spacings of order v_F/R, where v_F is the Fermi velocity and R the typical size of the metal. They extend throughout the metal. (See Fig. 2.) The wave functions $|a_{np}\rangle$ and $|b_{np}\rangle$ that correspond to the operators defining the logarithmic discretization, on the other hand, are wave-packet states confined to their respective phase-space cells as depicted in Fig. 3. $|a_{np}\rangle$ has a mean energy $\sim\Lambda^{-n}$ ($|b_{np}\rangle$ has mean energy $-\Lambda^{-n}$), a spread in energy $\Lambda^{-n}(1-\Lambda^{-1})$, is peaked at a distance of $\Lambda^n p/(1-\Lambda^{-1})$ from the impurity site, and has a radial extent $\Lambda^n/(1-\Lambda^{-1})$. As n gets larger (i.e., as their energies get closer to the Fermi level), these wave-packet states resemble more and more the original s-wave states. The approximation of throwing away the $p \neq 0$ states corresponds to throwing away those states which are peaked away from the impurity site.

The states $(|f_n\rangle)$ contain equal amounts of positive and negative energy electron operators and hence have zero mean energies (i.e., their mean energy is at the Fermi level, or their mean wave number is

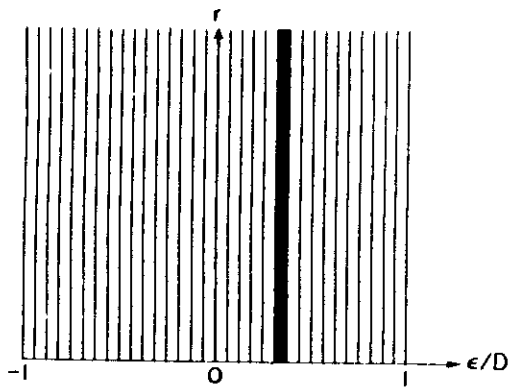

FIG. 2. Phase space for the states $|a_k\rangle$ shown in the $(\epsilon/D,r)$ space. Each state has a well-defined energy and extends throughout the volume of the system, as illustrated by the heavy bar.

$\sim k_F$), which is why there are no diagonal terms in Eq. (2.14). They are all peaked at the impurity site. $|f_n\rangle$ has a spread in energy $\sim\Lambda^{-n/2}$, which is the strength of its off-diagonal coupling in Eq. (2.14), and consequently an extent about the impurity of $\sim\Lambda^{n/2}$. $|f_0\rangle$ has the biggest spread in energy (-1), and is consequently the most localized (extent ~ 1 or $1/k_F$ in real units). (See Fig. 4.) The fact that c_d is coupled only to f_0 in Eq. (2.14) is a reflection of the fact that the impurity is localized. [Allowing ρ and V_d in Eq. (2.3) to be weakly energy dependent would couple c_d to some of the *first few* f_n's. See Sec. V D for more discussion.]

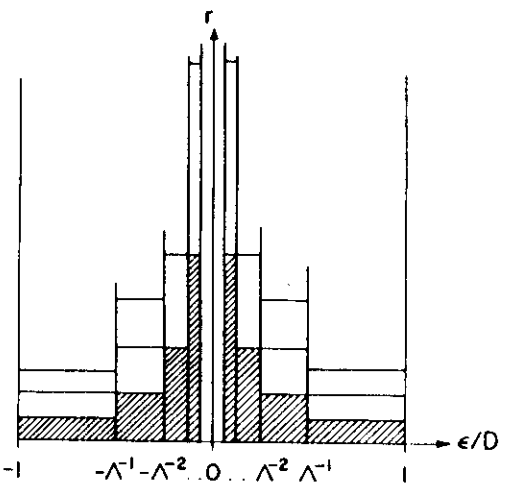

FIG. 3. Phase-space cell analysis for the $|a_{np}\rangle$ and $|b_{np}\rangle$ states [defined in Eq. (2.9)]. Shaded boxes constitute the phase spaces for the states $|a_{n0}\rangle$ and $|b_{n0}\rangle$; the open boxes next to them for $|a_{n1}\rangle$ and $|b_{n1}\rangle$; the next set for $|a_{n2}\rangle$ and $|b_{n2}\rangle$, etc.

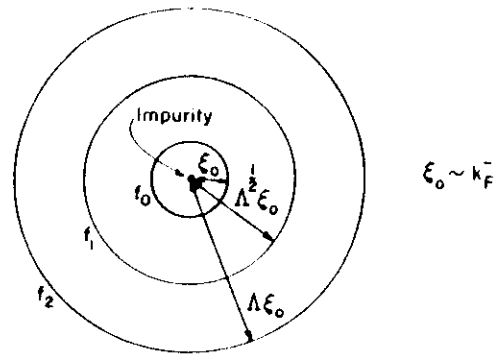

FIG. 4. Spherical shells in r space depicting the extents of the wave functions of f_n. Within their shells, every wave function has oscillations so that they are mutually orthogonal. Alternately one can show that, in the wave-vector space, neglecting a_{np} for $p>0$, $\sqrt{2}f_n = g_n(\Lambda)\int_{-1}^{1} dk\, P_n(k)a_k$, where $P_n(k)$ is the n-order Legendre polynomial and $g_n(\Lambda)$ a function of Λ which goes to $(2n+1)^{1/2}$ as $\Lambda\to 1$.

D. Iterative diagonalization

In order to solve the hopping Hamiltonian, one defines a sequence of Hamiltonians H_N as follows:

$$H_N \equiv \Lambda^{(N-1)/2}\Bigg[\sum_{n=0}^{N-1}\Lambda^{-n/2}\xi_n\left(f_{n\mu}^{\dagger}f_{n+1\mu}+f_{n+1\mu}^{\dagger}f_{n\mu}\right) + \tilde{\delta}_d c_{d\mu}^{\dagger}c_{d\mu}+\tilde{\Gamma}^{1/2}\left(f_{0\mu}^{\dagger}c_{d\mu}+c_{d\mu}^{\dagger}f_{0\mu}\right) + \tilde{U}\left(c_{d\mu}^{\dagger}c_{d\mu}-1\right)^2\Bigg] , \tag{2.18}$$

where we have defined, for convenience,

$$\tilde{\delta}_d \equiv \left(\frac{2}{1+\Lambda^{-1}}\right)\frac{1}{D}\left(\epsilon_d+\tfrac{1}{2}U\right) \equiv \tilde{\epsilon}_d+\tilde{U} , \tag{2.19}$$

$$\tilde{U} \equiv \left(\frac{2}{1+\Lambda^{-1}}\right)\frac{U}{2D} , \tag{2.20a}$$

$$\tilde{\Gamma} \equiv \left(\frac{2}{1+\Lambda^{-1}}\right)^2\frac{2\Gamma}{\pi D} = \left(\frac{2}{1+\Lambda^{-1}}\right)^2\frac{2\rho|V_d|^2}{D} . \tag{2.20b}$$

The full discrete approximation to $\mathcal{H}_A$ can now be recovered as the limit

$$\mathcal{H}_A = \lim_{N\to\infty}\tfrac{1}{2}(1+\Lambda^{-1})D\,\Lambda^{-(N-1)/2}H_N . \tag{2.21}$$

The scale factor $\Lambda^{(N-1)/2}$ in Eq. (2.18) has been introduced so as to make the lowest energy scale in H_N, which is coefficient of $(f_{N-1\mu}^{\dagger}f_{N\mu}+f_{N\mu}^{\dagger}f_{N-1\mu})$,

be of order 1. Roughly speaking, information about the many-electron energy-level structure of $\mathcal{H}_A$ at energies $\sim\Lambda^{-(N-1)/2}D$ is contained in the energy-level structure of H_N at energies ~ 1. (Energy levels of Hamiltonain are assumed to be measured relative to their ground-state energies throughout both papers.)

It is easy to see from Eq. (2.18) that the Hamiltonians (H_N) satisfy the following *recursion relation:*

$$H_{N+1}=\Lambda^{1/2}H_N+\xi_N(f^\dagger_{N\mu}f_{N+1\,\mu}+f^\dagger_{N+1\,\mu}f_{N\mu}) \quad . \tag{2.22}$$

This recursion relation is the central aspect of the formalism being discussed. The point of defining the sequence (H_N) is in fact that one can use Eq. (2.22) to set up *recursive* procedure (to be described below) for obtaining the many-particle eigenstates and energy levels of H_{N+1} given the same for H_N. The initial Hamiltonian H_0 (H_N for $N=0$) involves only the operators f_0 and $c_{\cdot\mu}$.

$$H_0=\Lambda^{-1/2}[\tilde{\delta}_d c^\dagger_{d\mu}c_{d\mu}+\tilde{\Gamma}^{1/2}(f^\dagger_{0\mu}c_{d\mu}+c^\dagger_{d\mu}f_{0\mu}) + \tilde{U}(c^\dagger_{d\mu}c_{d\mu}-1)^2] \quad . \tag{2.23}$$

It is straightforward to compute the eigenstates and energy levels of this Hamiltonian. Repeated use of the recursive procedure then enables one to solve the whole sequence of Hamiltonians (H_N).

The basic scheme of te recursive proccdure, briefly, is as follows. Let $|l,N\rangle (l=0,1,2,\ldots,L_N)$ denote the eigenstates of H_N, with $l=0$ corresponding to the ground state. H_N has $2(N+2)$ fermion operators: $c_{d\mu},f_{0\mu},\ldots,f_{N\mu}$. Since each fermion operator has a space of two states (empty and full), L_N will be given by $(2^{2(N+2)}-1)$. Suppose that one knows all the energy levels $E(l,N)$ and all the matrix elements $\langle l,N|f^\dagger_{n\mu}|l',N\rangle$. One now constructs from each of the states $|l,N\rangle$ the following four states:

$$\begin{aligned}
|1,l,N\rangle &= |l,N\rangle \quad ,\\
|2,l,N\rangle &= f^\dagger_{N+1\uparrow}|l,N\rangle \quad ,\\
|3,l,N\rangle &= f^\dagger_{N+1\downarrow}|l,N\rangle \quad ,\\
|4,l,N\rangle &= f^\dagger_{N+1\uparrow}f^\dagger_{N+1\downarrow}|l,N\rangle \quad .
\end{aligned} \tag{2.24}$$

It is clear that the $4(1+L_N)$ states that result provide an orthonormal basis that spans the space of H_{N+1}. One can now calculate the matrix elements of H_{N+1} in this basis by sandwiching Eq. (2.22) between $\langle i',l',N|$ and $|i,l,N\rangle$. All four states in Eq. (2.24) are eigenstates of H_N belonging to the eigenvalue $E(l,N)$. $f_{N+1\,\mu}$ or $f^\dagger_{N+1\,\mu}$ will connect only states with the same index l, and matrix elements such as $\langle i',l,N|f^\dagger_{N+1\,\mu}|i,l,N\rangle$ do not depend on what the index l is, and can be abbreviated as $\langle i'|f^\dagger_{N+1\,\mu}|i\rangle$ (for example, $\langle 2,l,N|f^\dagger_{N+1\uparrow}|1,l,N\rangle \equiv \langle 2|f^\dagger_{N+1\uparrow}|1\rangle = 1$). $f_{N\mu}$ or $f^\dagger_{N\mu}$ does not connect states with different values of i and i', and $\langle i,l',N|f_{N\mu}|i,l,N\rangle = \langle l',N|f_{N\mu}|l,N\rangle$. Therefore we have

$$\begin{aligned}
\langle i',l',N|H_{N+1}|i,l,N\rangle &= \Lambda^{1/2}E(l,N)\delta_{ii'}\delta_{ll'}\\
&\quad+\xi_N(\langle l',N|f^\dagger_{N\mu}|l,N\rangle\langle i'|f_{N+1\,\mu}|i\rangle\\
&\quad+\langle i'|f^\dagger_{N+1\,\mu}|i\rangle\langle l',N|f^\dagger_{N\mu}|l,N\rangle) \quad .
\end{aligned} \tag{2.25}$$

Knowledge of $E(l,N)$ and $\langle l',N|f^\dagger_{N\mu}|l,N\rangle$ is thus sufficient to evaluate the matrix for H_{N+1}. Diagonalizing this matrix yields the new eigenstates $|l,N+1\rangle (l=0,1,\ldots,L_{N+1})$ of H_{N+1} and the energies $E(l,N+1)$ and also allows one to calculate $\langle l,N+1|f^\dagger_{N+1\,\mu}|l',N+1\rangle$. One can then use this knowledge and the above procedure to solve H_{N+2}, and so on.

As is well known the symmetries of a Hamiltonian, leading to conserved quantum numbers, considerably reduce the labor involved in diagonalizing that Hamiltonian. All the Hamiltonians we have been considering conserve spin and electron number. The spin operator appropriate to H_N is

$$\vec{S}_N=\tfrac{1}{2}\sum_{n=0}^{N}f^\dagger_{n\mu}\vec{\sigma}_{\mu\nu}f_{n\nu}+\tfrac{1}{2}c^\dagger_{d\mu}\vec{\sigma}_{\mu\nu}c_{d\nu} \quad , \tag{2.26}$$

where $\vec{\sigma}(\sigma_x,\sigma_y,\sigma_z)$ are the Pauli matrices. Instead of the electron-number operator, it is more convenient to define a "charge" operator appropriate to H_N:

$$Q_N=\sum_{n=0}^{N}(f^\dagger_{n\mu}f_{n\mu}-1)+(c^\dagger_{d\mu}c_{d\mu}-1) \quad . \tag{2.27}$$

It is easy to verify that both operators commute with H_N. The eigenstates of H_N can hence be chosen to be also the eigenstates of Q_N, $(\vec{S}_N)^2$, and S_{Nz}, and can be labeled by the corresponding quantum numbers Q, S, and m_S. The point is that when the states in Eq. (2.24) are constructed, they can be classified according to their values of Q, S, and m_S. H_{N+1} will not have matrix elements between states that have different (Q,S,m_S) values, and its diagonalization can be carried out independently in each (Q,S,m_S) subspace. In fact, energy eigenvalues will be independent of m_S, and one can avoid having to keep track of m_S by using Clebsh-Gordon coefficients and working entirely in terms of the *reduced matrix elements* $\langle Q,S\|f^\dagger_N\|Q',S'\rangle$ instead of using $\langle Q,S,m_S|f^\dagger_{N\mu}|Q',S',m_S'\rangle$. All this results in a considerable reduction in the size of matrices that have to be diagonalized. For details see Appendix B.

For the symmetric case $(\epsilon_d=-\frac{1}{2}U)$ it was remarked earlier that $\mathcal{H}_A$ had particle-hole symmetry. In terms of the operators $(f_{n\mu})$ and $(c_{d\mu})$, the symmetry operation is: $f_{n\mu}\leftrightarrow(-1)^n f^\dagger_{n\mu}$ and $c_{d\mu}\leftrightarrow -c^\dagger_{d\mu}$. It is easy to verify that this leaves every H_N invari-

ant, since δ_d is zero when $\epsilon_d = -\frac{1}{2}U$ [cf. Eqs. (2.18) and (2.19)]. This symmetry operation takes Q_N to $-Q_N$ (which, in fact, is the reason for calling Q_N the charge), which means that the state (Q,S) has the same energy as the state $(-Q,S)$. For the symmetric case, it is hence necessary to carry out the diagonalization only for states with $Q \geq 0$.

As a practical matter, however, calculating *all* the states of H_N for large N is completely out of the question because the number of states of H_N grows exponentially with $N(\sim 2^{2(N+2)})$, and the numerical diagonalization of the large-sized matrices that result becomes prohibitively expensive. We will see in Sec. II E that for calculating low-temperature properties of $\mathcal{H}_A$, one is mainly interested in the low-lying states of H_N. So in practice one selects and keeps only a small number of low-lying states after each step in the iterative process described earlier. In order that the discretized approximation be fairly representatiave of the continuum limit, one would like Λ to be close to 1. But, for a given number of selected states, the accumulation (with increasing N) of errors due to the truncation gets worse as $\Lambda \to 1$. One's choice of Λ and of the number of states one keeps is therefore determined by a trade-off between the accuracy one desires and the consideration of computing costs. The separation and the sequential consideration of the different energy scales is the crucial reason that permits the truncation of states to be a good approximation. For a more detailed discussion, see Sec. VIII, Ref. 6.

E. Calculation of impurity properties and the connection between N and the temperature

The calculation of the temperature-dependent properties of $\mathcal{H}_A$ involves the operator $\exp(-\beta\mathcal{H}_A)$ where $\beta \equiv 1/(k_B T)$ as usual. In view of Eq. (2.21), it seems reasonable to assume that, in the thermodynamic limit, it is correct first to calculate *an equivalent property* for H_M using the operator

$$\exp -\beta[\tfrac{1}{2}(1+\Lambda^{-1})]D\Lambda^{-(M-1)/2}H_M = \exp -\bar{\beta}_M H_M \ , \tag{2.28}$$

where we have written

$$\bar{\beta}_M = \beta[\tfrac{1}{2}(1+\Lambda^{-1})]D\Lambda^{-(M-1)/2} = \tfrac{1}{2}(1+\Lambda^{-1})\Lambda^{-(M-1)/2}\left(\frac{k_B T}{D}\right)^{-1} \ , \tag{2.29}$$

and *then* take the limit $M \to \infty$. M rather than N is used as the index here in order to avoid confusion in the discussion to follow. It is important to note that every property must be calculated as an impurity contribution, i.e., one must always subtract out the value of the property when no impurity is present. In this paper only the initial (zero-field) magnetic susceptibility and the specified heat will be discussed. The definitions are, using Eq. (2.28)

$$\chi_{\rm imp}(T) = \frac{(g\mu_B)^2}{k_B T}\lim_{M\to\infty}\left[\frac{\mathrm{Tr}S_{Mz}^2 \exp -\bar{\beta}_M H_M}{\mathrm{Tr}\exp -\bar{\beta}_M H_M} - \frac{\mathrm{Tr}S_{Mz}^{0^2}\exp -\bar{\beta}_M H_M^0}{\mathrm{Tr}\exp -\bar{\beta}_M H_M^0}\right] \ , \tag{2.30}$$

$$F_{\rm imp}(T) \equiv -k_B T \lim_{M\to\infty}\left[\ln \mathrm{Tr}\exp -\bar{\beta}_M H_M - \ln \mathrm{Tr}\exp -\bar{\beta}_M H_M^0\right] \ , \tag{2.31}$$

$$C_{\rm imp}(T) = -T\frac{\partial^2}{\partial T^2}F_{\rm imp}(T) \ . \tag{2.32}$$

μ_B is the Bohr magneton; g, the electronic g factor, ($=2$) has been assumed to be the same for both the impurity and the conduction electrons. $\vec{S}_M$ was defined earlier in Eq. (2.26). $F_{\rm imp}$ is essentially the impurity contribution to the free energy (except for contributions due to ground-state energies, which do not affect $C_{\rm imp}$ anyway). The superscript "0" refers to the situation when no impurity is present:

$$H_M^0 \equiv \Lambda^{(M-1)/2}\left[\sum_{n=0}^{M-1}\Lambda^{-n/2}\xi_n(f_{n\mu}^\dagger f_{n+1\mu} + f_{n+1\mu}^\dagger f_{n\mu})\right] \ , \tag{2.33}$$

$$\vec{S}_M^0 \equiv \tfrac{1}{2}\sum_{n=0}^{M} f_{n\mu}^\dagger \vec{\sigma}_{\mu\nu} f_{n\nu} \ . \tag{2.34}$$

For notational convenience, the label "imp" and the factor $(g\mu_B)^2$ will often be omitted hereafter.

Since the lowest-energy scale in H_M is ~ 1, the $M \to \infty$ limit above basically means that one must consider values of M large enough to make $\bar{\beta}_M \ll 1$. A more precise statement of this idea is that the error one makes by evaluating Eqs. (2.30) and (2.31) at a finite value "N" of M instead of taking the limit $M \to \infty$ is only $0(\bar{\beta}_N/\Lambda)$. The proof of this result for the case of the susceptibility proceeds as follows. Consider some large $M > N$, and split H_M and H_M^0 by separating the operators $(c_d, f_0, \ldots, f_N)$ from $(f_{N+1}, \ldots, f_M)$. Starting from the definitions of H_M and H_M^0, it is easy to verify that one can write

$$\bar{\beta}_M H_M = \bar{\beta}_N H_N + \bar{\beta}_N H_I + \bar{\beta}_M R_{M,N+1} \ , \tag{2.35}$$

$$\bar{\beta}_M H_M^0 = \bar{\beta}_N H_N^0 + \bar{\beta}_N H_I + \bar{\beta}_M R_{M,N+1} \ ; \tag{2.36}$$

where $R_{M,N+1}$ contains only the operators $(f_{N+1}, \ldots, f_M)$, and H_I is a term coupling f_N to f_{N+1}:

$$R_{M,N+1} \equiv \Lambda^{(M-1)/2}\left[\sum_{n=N+1}^{M-1} \Lambda^{-n/2}\xi_n(\ldots) f_{n+1\mu} + f^\dagger_{n+1\mu} f_{n\mu})\right] , \quad (2.37)$$

$$H_I \equiv \Lambda^{-1/2}(f^\dagger_{N\mu} f_{N+1\mu} + f^\dagger_{N+1\mu} f_{N\mu}) . \quad (2.38)$$

One can similarly split $\vec{S}_M$ and $\vec{S}^0_M$

$$\vec{S}_M = \vec{S}_N + \vec{S}_{M,N+1}; \quad \vec{S}^0_M = \vec{S}^0_N + \vec{S}_{M,N+1} , \quad (2.39)$$

$$\vec{S}_{M,N+1} \equiv \frac{1}{2}\sum_{n=N+1}^{M} f^\dagger_{n\mu}\,\vec{\sigma}_{\mu\nu} f_{n\nu} . \quad (2.40)$$

The point is that, if H_I, which couples f_N to f_{N+1}, is ignored, the separated parts are *completely independent* of each other, and substitution into Eq. (2.30) results in a complete cancellation of the terms involving the operators $(f_{N+1}, \ldots, f_M)$. For details see Sec. IX, Ref. 6. Therefore, if one makes the separation as above for an arbitrarily large $M(>N)$ and evaluates Eq. (2.30) treating H_I as a perturbation the zero-order term will just be Eq. (2.30) evaluated for $M = N$. The contribution due to treating H_I to first order can be shown to vanish; and the contribution due to treating H_I to second order can be shown to be $O(\bar{\beta}_N/\Lambda)$. See Appendix F.

The result cited in the preceding paragraph is the key to the following important connection between the sequence of Hamiltonians $\{H_N\}$ and the physics of the original Hamiltonian $\mathcal{H}_A$. Suppose that one is interested in evaluating $\chi(T)$ and $F(T)$ at some low temperature T, to some preassigned degree of accuracy. All that one has to do is to pick an appropriately small, fixed number $\bar{\beta}$, then choose an N such that $\bar{\beta}_N = \bar{\beta}$, and finally evaluate Eqs. (2.30) and (2.31) at the finite value N of M. In other words, the Hamiltonians H_N enable one to compute χ and F, to an accuracy $O(\bar{\beta}/\Lambda)$, at a whole sequence of temperatures T_N determined by the condition that $\bar{\beta}_N = \bar{\beta}$, i.e.,

$$T_N = \frac{D}{k_B}\frac{1}{2}(1+\Lambda^{-1})\Lambda^{-(N-1)/2}/\bar{\beta} . \quad (2.41)$$

The expressions that one uses for this purpose are

$$k_B T_N \chi(T_N) \cong \frac{\mathrm{Tr} S^2_{N_z} \exp -\bar{\beta}H_N}{\mathrm{Tr}\exp -\bar{\beta}H_N} - \frac{\mathrm{Tr} S^{0\,2}_{N_z} \exp -\bar{\beta}H^0_N}{\mathrm{Tr}\exp -\bar{\beta}H^0_N} , \quad (2.42)$$

$$F(T_N) \cong -k_B T_N [\ln \mathrm{Tr}\exp -\bar{\beta}H_N - \ln \mathrm{Tr}\exp -\bar{\beta}H^0_N] . \quad (2.43)$$

The index N thus defines a logarithmic temperature scale T_N as given by Eq. (2.41). Large values of N clearly correspond to temperatures T_N that are small compared to the bandwidth.

The evaluation of Eqs (2.42) and (2.43) can in principle be done if all the energy levels of H_N are known. In accordance with the discussion of Sec. II D, let the states of H_N be denoted $|k,S,m_S,N)$, where k takes care of all labels (charge, etc.) other than the spin labels S and m_S. The energies do not depend on m_S and can be denoted $E_N(k,S)$. One now has the results

$$\mathrm{Tr}\exp -\bar{\beta}H_N = \sum_{k,S}(2S+1)\exp -\bar{\beta}E_N(k,S) , \quad (2.44)$$

$$\mathrm{Tr} S^2_{N_z}\exp -\bar{\beta}H_N = \sum_{k,S}\frac{1}{12}(2S+1)[(2S+1)^2-1] \times \exp -\bar{\beta}E_N(k,S) , \quad (2.45)$$

where the spin factors result from summing over m_S. One can write down similar expressions for H^0_N in terms of its energies E^0_N. In fact H^0_N, being a quadratic Hamiltonian, can be diagonalized exactly into a set of single-particle levels whence the evaluation of the above traces becomes rather trivial, as we will see later.

Now consider the *practical* aspects of evaluating the sums (2.44) and (2.45) using the numerical results for the energy levels of H_N. It is at once obvious that one cannot really choose $\bar{\beta}$ to be very small because an accurate evaluation of the above sum requires energy levels up to an energy somewhat bigger than $1/\bar{\beta}$ and highly excited states of H_N are *not* calculated numerically. In other words, there is a trade-off between the small $\bar{\beta}$ one needs in order to make the calculation at a finite value N of M representative of the $M \to \infty$ limit and the large number of states whose energies one needs to know to compute Eqs. (2.44) and (2.45) accurately. The compromise adopted in practice is to choose $\bar{\beta}$ to be only slightly smaller than 1 so that the high-energy states ($E_N > 10$ say) of H_N that are ignored do not contribute appreciably to Eqs. (2.44) and (2.45); and to correct for the effects of $\bar{\beta}$ not being very small by actually calculating the $O(\bar{\beta}/\Lambda)$ correction alluded to earlier. (See Appendix F.)

However, we will see later that there are *ranges of* N where the energy levels of H_N can be obtained analytically by doing perturbation theory using various *effective Hamiltonians*. Then one can indeed use values of $\bar{\beta}$ small enough that one can neglect the $O(\bar{\beta}/\Lambda)$ corrections. For corresponding ranges of temperature [related to the ranges of N by Eq. (2.41)] one can obtain analytical expressions for $\chi_{\mathrm{imp}}(T)$ and $C_{\mathrm{imp}}(T)$. These calculations are presented in Sec. V.

This completes our brief discussion of the basic

TABLE I. States and energies of the initial Hamiltonian H_0 Eq. (2.23) for the symmetric ($\tilde{\delta}_d = 0$) Anderson model.

Charge Q	Spin S	Index r	Energy/$\Lambda^{1/2}$	State
-2	0	1	$\frac{1}{2}(\tilde{U}^2+16\tilde{\Gamma})^{1/2}+\frac{1}{2}\tilde{U}$	$\|\Omega\rangle$
-1	$\frac{1}{2}$	1	$\frac{1}{2}(\tilde{U}^2+16\tilde{\Gamma})^{1/2}-\frac{1}{2}(\tilde{U}^2+4\tilde{\Gamma})^{1/2}$	Different linear combinations of $f_0^\dagger\|\Omega\rangle$ and $c_d^\dagger\|\Omega\rangle$
		2	$\frac{1}{2}(\tilde{U}^2+16\tilde{\Gamma})^{1/2}+\frac{1}{2}(\tilde{U}^2+4\tilde{\Gamma})^{1/2}$	
0	0	1	0	Different linear combinations of $f_{0\uparrow}^\dagger f_{0\downarrow}^\dagger\|\Omega\rangle$, $c_{d\uparrow}^\dagger c_{d\downarrow}^\dagger\|\Omega\rangle$ and $(f_0^\dagger c_d^\dagger)_s\|\Omega\rangle$
		2	$\frac{1}{2}(\tilde{U}^2+16\tilde{\Gamma})^{1/2}+\frac{1}{2}\tilde{U}$	
		3	$\frac{1}{2}(\tilde{U}^2+16\tilde{\Gamma})^{1/2}$	
	1	1	$\frac{1}{2}(\tilde{U}^2+16\tilde{\Gamma})^{1/2}-\frac{1}{2}\tilde{U}$	$(f_0^\dagger c_d^\dagger)_t\|\Omega\rangle$
1	$\frac{1}{2}$	1	$\frac{1}{2}(\tilde{U}^2+16\tilde{\Gamma})^{1/2}-\frac{1}{2}(\tilde{U}^2+4\tilde{\Gamma})^{1/2}$	Different linear combinations of $f_0^\dagger(c_{d\uparrow}^\dagger c_{d\downarrow}^\dagger\|\Omega\rangle)$ and $c_d^\dagger(f_{0\uparrow}^\dagger f_{0\downarrow}^\dagger)\|\Omega\rangle$
		2	$\frac{1}{2}(\tilde{U}^2+16\tilde{\Gamma})^{1/2}+\frac{1}{2}(\tilde{U}^2+4\tilde{\Gamma})^{1/2}$	
2	0	1	$\frac{1}{2}(\tilde{U}^2+16\tilde{\Gamma})^{1/2}+\frac{1}{2}\tilde{U}$	$f_{0\uparrow}^\dagger f_{0\downarrow}^\dagger c_{d\uparrow}^\dagger c_{d\downarrow}^\dagger\|\Omega\rangle$

techniques. The rest of this paper will consist of a detailed discussion of the results obtained by the application of these techniques to the symmetric case defined by the condition $\epsilon_d = -\frac{1}{2}U$. In this case the parameters that have to be specified are the two dimensionless numbers Γ/D and U/D. One then computes the energy levels and the invariant matrix elements of f_0 between the eigenstates of the initial Hamiltonian H_0 [cf. Eq. (2.23)] with $\tilde{\delta}_d = 0$. The energy levels are listed in Table I. Use of the iterative diagonalization procedure discussed in Sec. II D then enables one to solve the whole sequence of Hamiltonians H_N. From the energy levels of H_N one can calculate the susceptibility at temperature T_N determined by Eq. (2.39) using the procedure discussed in Sec. II E.

The numerical calculations that will be presented in this paper were performed on a CDC 7600 computer, Λ was chosen to be 2.5, and a maximum of 611 states was kept. Susceptibility calculations were carried out using $\bar{\beta}$ values 0.460, 0.578, and 0.727. Note that the values of $\bar{\beta}$ were chosen so that T_N for $\bar{\beta} = 0.727$ is equal to T_{N+1} for $\bar{\beta} = 0.46$. [This follows from Eq. (2.39), and the result that $0.727 = (0.460)(2.5)^{1/2}$.] The difference between the susceptibility calculated from H_N for $\bar{\beta} = 0.727$ and that calculated from H_{N+1} for $\bar{\beta} = 0.460$, which is a *rough* measure of the accuracy of the numerical results for the susceptibility, indicated an absolute error of around 0.004 in $k_B T\chi/(g\mu_B)^2$.

III. PRELIMINARY LOOK AT THE NUMERICAL RESULTS

In this section numerical results for the energy levels of $\{H_N\}$ and for $\chi_{\text{imp}}(T)$ for the symmetric Anderson model will be presented for several typical values of Γ/D and U/D. The important characteristic of these results will be that they can be understood in terms of H_N crossing over (as N increases) between various fixed points of the transformation (2.22) which is an example of a renormalization-group transformation. Therefore, prior to the actual presentation of the results, the stage will be set for their interpretation by discussing these fixed points.

A. Renormalization group and fixed points; the free-electron Hamiltonian

Consider the transformation (2.22) relating H_N to H_{N+1} for large N. Since ξ_N is 1 for large N [cf. Eq. (2.15)] and since the Hamiltonians H_N are supposed to be defined with their ground-state energies sub-

tracted, the transformation for large N can be written more precisely as

$$H_{N+1} = \Lambda^{1/2} H_N + (f^\dagger_{N\mu} f_{N+1\mu} + f^\dagger_{N+1\mu} f_{N\mu}) - E_{G,N+1} \ , \tag{3.1}$$

where $E_{G,N+1}$ is chosen so as to make the ground-state energy of H_{N+1} zero. Equation (3.1) is an example of a renormalization-group transformation.[6,7] One can write this symbolically as $H_{N+1} = \mathcal{T}[H_N]$, and think of the transformation $\mathcal{T}$ as producing, from an input list of the eigenvalues and the matrix elements of f_N between the eigenstates of H_N, an output list of the eigenvalues and the matrix elements of f_{N+1} between the eigenstates of H_{N+1} according to the prescription for iterative diagonalization outlined in Sec. II D.

A fixed point H^* of the transformation $\mathcal{T}$ is a Hamiltonian that remains invariant under $\mathcal{T}$: $\mathcal{T}[H^*] = H^*$. Actually $\mathcal{T}$ itself does not have any fixed points; but $\mathcal{T}^2$ ($\mathcal{T}$ operating twice), which takes H_N to H_{N+2} and is also a renormaliztion-group transformation, does have fixed points. The numerical characterization of a fixed point of $\mathcal{T}^2$ is a set of (many-particle) energy levels and matrix elements (of f_N) that repeat themselves when one performs the iterative diagonalization twice. The point is that a Hamiltonian changes very little under a renormalization-group transformation if it is close to a fixed point of that transformation: if H_N is close to H^* where $\mathcal{T}^2[H^*] = H^*$, by continuity $\mathcal{T}^2[H_N]$ is close to H^* and is therefore close to H_N. This is indeed the way one recognizes fixed points from the numerical results: one sees a set of energy levels that change very little from iteration N to iteration $(N+2)$.

The fixed points of $\mathcal{T}^2$ that are of interest in case of the symmetric Anderson model can all be written down easily once one understands the structure of the free-electron Hamiltonian H_N^0 defined in Eq. (2.31)

$$H_N^0 = \sum_{n=0}^{N-1} \Lambda^{(N-1-n)/2} \xi_n (f^\dagger_{n\mu} f_{n+1\mu} + f^\dagger_{n+1\mu} f_{n\mu}) \ . \tag{3.2}$$

For large N, H_N^0 clearly satisfies the recursion relation (3.1) (assuming that one subtracts its ground-state energy). What is more, being a quadratic form it can be diagonalized *exactly* into $(N+1)$ *single-particle levels* by making a unitary transformation on the set of operators $(f_0, f_1, \ldots, f_N)$. The single-particle energies are just the eigenvalues of the $(N+1)\times(N+1)$ matrix $\mathcal{K}_N^0$ whose *only* nonvanishing matrix elements are

$$(\mathcal{K}_N^0)_{n,n+1} = (\mathcal{K}_N^0)_{n+1,n} = \Lambda^{(N-1-n)/2} \xi_n \ ; \quad n = 0, 1, 2, \ldots, N-1 \ . \tag{3.3}$$

This follows from the fact that H_N^0 can be written as the scalar product $f^\dagger \mathcal{K}_N^0 f$ where f stands for the "vector" $(f_0, f_1, \ldots, f_N)$; so that if the real orthogonal matrix $\mathfrak{M}$ diagonalizes $\mathcal{K}_N^0$, the operators forming the vector $\mathfrak{M}f$ are just the single-particle operators that diagonalize H_N^0. For details, see Sec. VIII, Ref. 6.

The eigenvalues of the matrix $\mathcal{K}_N^0$ can be obtained by diagonalizing it numerically. The particle-hole symmetry of H_N^0 leads to the result that if η is an eigenvalue of $\mathcal{K}_N^0$, so is $-\eta$ [this can also be deduced directly from Eq. (3.3)]. This has the consequence that when $(N+1)$ is even there are $\frac{1}{2}(N+1)$ *positive* eigenvalues which will be denoted $\eta_j(N)$, $j = 1, 2, \ldots, \frac{1}{2}(N+1)$, and the other $\frac{1}{2}(N+1)$ eigenvalues are just their negatives; when $(N+1)$ is odd, there is one *zero* eigenvalue denoted $\hat{\eta}_0$, there are $(\frac{1}{2}N)$ positive eigenvalues which will be denoted $\hat{\eta}_j(N)$, $j = 1, 2, \ldots, \frac{1}{2}N$, and the other $\frac{1}{2}N$ eigenvalues are just their negatives.

The negative-energy single-particle levels will all be fully occupied (with two electrons each) in the ground state of H_N^0. [For odd $(N+1)$ the ground state of H_N^0 is quadruply degenerate because of the zero-energy single-particle level $\hat{\eta}_0$.] The subtraction of the ground-state energy from H_N^0 can be accomplished by the standard trick of introducing hole operators conjugate to the negative-energy electron operators into H_N^0 and normal ordering them. Electrons and holes then have the same set of positive single-particle energies. [For odd $(N+1)$ there is a lone zero-energy electron level.] Further, holes have a negative charge relative to the electrons and a hole-creation operator with an "up"-spin index actually creates a spin-down hole. All this is summarized in Table II, where we have denoted the electron and hole operators that diagonalize H_N^0 by $g_{j\mu}$ and $h_{j\mu}$, respectively. For $(N+1)$ odd there is an extra electron operator $g_{0\mu}$ (associated with $\hat{\eta}_0$).

What one finds on evaluating $\eta_j(N)$ and $\hat{\eta}_j(N)$ numerically for a given Λ is that, as N increases, they rapidly approach a limiting set of values which will be denoted η_j^* and $\hat{\eta}_j^*$, respectively. For $j \gg 1$ these limiting values are: $\eta_j^* = \Lambda^{j-1}$; $\hat{\eta}_j^* = \Lambda^{j-1/2}$; for small j the Λ dependence of η_j^* and $\hat{\eta}_j^*$ is not so simple. For example, at $\Lambda = 2.5$ one has, accurate to six decimal places,

$$\eta_j^*: \ 0.746\,856, \ 2.493\,206, \ 6.249\,995, \ (2.5)^3, \ (2.5)^4, \ \ldots, (2.5)^{j-1}, \ \ldots, (N+1) \text{ even} \ ; \tag{3.4}$$

$$\hat{\eta}_j^*: \ 1.520\,483, \ 3.952\,550, \ 9.882\,118, \ (2.5)^{7/2}, \ (2.5)^{9/2}, \ \ldots, (2.5)^{j-1/2}, \ \ldots, (N+1) \text{ odd} \ ; \tag{3.5}$$

TABLE II. Information about free-electron Hamiltonian H_N^0 (cf. Sec. III A). Note in particular the values of α_{0j} and α_{1j} and, for large j, η_j, $\hat{\eta}_j$, etc.

$(N+1)$ even	$(N+1)$ odd
$H_N^0 = \sum_{j=1}^{(N+1)/2} \eta_j (g_{j\mu}^\dagger g_{j\mu} + h_{j\mu}^\dagger h_{j\mu})$	$H_N^0 = \hat{\eta}_0 g_{0\mu}^\dagger g_{0\mu} + \sum_{j=1}^{N/2} \hat{\eta}_j (g_{j\mu}^\dagger g_{j\mu} + h_{j\mu}^\dagger h_{j\mu})$
$Q_N^0 = \sum_{j=1}^{(N+1)/2} (g_{j\mu}^\dagger g_{j\mu} - h_{j\mu}^\dagger h_{j\mu})$	$Q_N^0 = (g_{0\mu}^\dagger g_{0\mu} - 1) + \sum_{j=1}^{N/2} (g_{j\mu}^\dagger g_{j\mu} - h_{j\mu}^\dagger h_{j\mu})$
$\vec{S}_N^0 = \sum_{j=1}^{(N+1)/2} \frac{1}{2} [g_{j\mu}^\dagger \vec{\sigma}_{\mu\nu} g_{j\nu} + h_{j\mu} \vec{\sigma}_{\mu\nu} h_{j\nu}^\dagger]$	$\vec{S}_N^0 = \frac{1}{2} g_{0\mu}^\dagger \vec{\sigma}_{\mu\nu} g_{0\nu} + \sum_{j=1}^{N/2} \frac{1}{2} [g_{j\mu}^\dagger \vec{\sigma}_{\mu\nu} g_{j\nu} + h_{j\mu} \vec{\sigma}_{\mu\nu} h_{j\nu}^\dagger]$
$f_{0\mu} = \Lambda^{-[(N-1)/4]} \left(\sum_{j=1}^{(N+1)/2} \alpha_{0j} (g_{j\mu} + h_{j\mu}^\dagger) \right)$	$f_{0\mu} = \Lambda^{-[(N-1)/4]} \left(\hat{\alpha}_{00} g_{0\mu} + \sum_{j=1}^{N/2} \hat{\alpha}_{0j} (g_{j\mu} + h_{j\mu}^\dagger) \right)$
$f_{1\mu} = \Lambda^{-3[(N-1)/4]} \left(\sum_{j=1}^{(N+1)/2} \alpha_{1j} (g_{j\mu} - h_{j\mu}^\dagger) \right)$	$f_{1\mu} = \Lambda^{-3[(N-1)/4]} \left(\sum_{j=1}^{N/2} \hat{\alpha}_{1j} (g_{j\mu} - h_{j\mu}^\dagger) \right)$

where, for large N and for $j \gg 1$, we have

$\eta_j = \Lambda^{j-1}$	$\alpha_0 = [\frac{1}{2}(1-\Lambda^{-1})]^{1/2}$	$\hat{\eta}_j = \Lambda^{(j-1/2)}$
$\alpha_{0j} = \alpha_0 \Lambda^{(j-1)/2}$		$\hat{\alpha}_{0j} = \alpha_0 \Lambda^{(j-1/2)/2}$
$\alpha_{1j} = \alpha_1 \Lambda^{3[(j-1)/2]}$	$\alpha_1 = [\frac{1}{2}(1-\Lambda^{-3})]^{1/2}$	$\hat{\alpha}_{1j} = \alpha_1 \Lambda^{3[(j-1/2)/2]}$

and one finds that all the eigenvalues η_j(15) and $\hat{\eta}_j$(16) are already indistinguishable from the above values to six decimal places.

The limiting, *infinite*, set of single-particle levels $\{\eta_j^*\}$ and $\{\hat{\eta}_j^*\}$ and their associated electron and hole operators clearly define two distinct fixed-point Hamiltonians of $\mathcal{T}^2$. The fixed point associated with η_j^* will be referred to as the "even" fixed point H^*. The fixed point associates with $\hat{\eta}_j^*$ will be called the "odd" point $\hat{H}^*$. The result one has is that as $N \to \infty$, H_N^0 goes to H^* if $(N+1)$ is even, and to $\hat{H}^*$ if $(N+1)$ is odd.

An important property of the fixed points which will be useful later is *their insensitivity to the specific values assumed by the coefficients ξ_n for small n.* This property is verified numerically as follows. Suppose that one defines a Hamiltonian $H_N^{0\prime}$ by replacing the coefficients ξ_n in Eq. (3.2) by another set of coefficients ξ_n' but making sure that ξ_n' continues to be 1 for large n so that $H_N^{0\prime}$ also satisfies the renormalization-group transformation (3.1) for large N. The single-particle levels of $H_N^{0\prime}$ can be determined numerically by diagonalizing the matrix $H_N^{0\prime}$ obtained by replacing ξ_n in Eq. (3.3) by ξ_n'. One again finds the results that as $N \to \infty$, $H_N^{0\prime}$ goes to H^* if $(N+1)$ is even and to $\hat{H}^*$ if $(N+1)$ is odd. The only difference is that the approach to H^* or to $\hat{H}^*$ of $H_N^{0\prime}$ is slower than that of H_N^0 and is nonuniform: the jth single-particle level of $H_N^{0\prime}$ is close to the jth single-particle level of the fixed point only for $N \gg j$.

For later reference, also recorded in Table II are the expansions for f_0 and f_1 in terms of the electron and hole operators that diagonalize H_N^0. Note should be taken of the N-dependent factors in front and of the values of the N-independent coefficients α_{0j}, α_{1j}, etc., for $j \gg 1$. The expansions for the operators f_2, f_3, etc., have very similar structures. f_2, for instance, has a piece proportional to f_0 and a piece going as $\Lambda^{-5(N-1)/4}$; f_3 has a price proportional to f_1 and a piece going as $\Lambda^{-7(N-1)/4}$; and so on. These expansions will have a crucial role to play when we come to discuss the "stability" of fixed-point Hamiltonians in Sec. IV.

One can also obtain expansions for f_0, f_1, etc., in terms of the electron and hole operators that diagonalize $H_N^{0\prime}$ (defined above). What one finds is that

the new expansions differ from the corresponding expansions for H_N^0 only by overall proportionality factors. The precise values of these factors will depend on the values of ξ_n' for small n. (Recall that $\xi_n' = 1$ for large n.)

The following viewpoint makes the various features of H_N^0 appear rather obvious. The point is that H_N^0 was essentially obtained by the truncation and rescaling of an original set of single-particle levels that scaled as Λ^{-n}. If the truncation were inconsequential, the single-particle levels of H_N^0 would be given by $\Lambda^{(N-1)/2}\Lambda^{-n}$, where n takes values 0, 1, 2, etc., up to $\frac{1}{2}(N-1)$ if $(N+1)$ is even, up to $\frac{1}{2}(N-2)$ if $(N+1)$ is odd. On reindexing the levels, one hence expects that $\eta_j = \Lambda^{j-1}$ and $\hat{\eta}_j = \Lambda^{j-1/2}$, as is indeed the case for large N and for $j \gg 1$. In fact, one can claim that, for large N and for $j \gg 1$, *the operators g_j and $h_j^\dagger$ must be essentially the same as the operators a_n and b_n of the same energy:* $g_j = a_n$ and $h_j^\dagger = b_n$ where n equals $[\frac{1}{2}(N-1) - (j-1)]$ for even $(N+1)$ and $[\frac{1}{2}(N-1) - (j-\frac{1}{2})]$ for odd $(N+1)$. This result plus the expressions for f_0, f_1, etc., in terms of the operators (a_n, b_n) immediately give the correct coefficients for expanding f_0, f_1, etc., in terms of the operators $(g_j, h_j^\dagger)$. For example, according to Eq. (2.13) f_0 has an expansion in $(a_n + b_n)$ with a coefficient $[\frac{1}{2}(1-\Lambda^{-1})]^{1/2}\Lambda^{-n/2}$. By the above prescription this translates to an expansion in $(g_j + h_j^\dagger)$ with a coefficient $[\frac{1}{2}(1-\Lambda^{-1})]^{1/2}\Lambda^{-(N-1)/4+(j-1)/2}$ for even $(N+1)$. This is precisely the result quoted in Table II (for large N and for $j \gg 1$). All other expansions can be similarly obtained.

B. Fixed points for the symmetric Anderson model

There are several interesting fixed points for the symmetric Anderson Hamiltonian, which has the following sequence of Hamiltonians H_N [obtained by setting $\tilde{\delta}_d = 0$ in Eq. (2.18)]:

$$H_N = \Lambda^{(N-1)/2}\left\{\sum_{n=0}^{N-1}\Lambda^{-n/2}\xi_n(f_{n\mu}^\dagger f_{n+1\mu} + f_{n+1\mu}^\dagger f_{n\mu}) + \tilde{\Gamma}^{1/2}(f_{0\mu}^\dagger c_{d\mu} + c_{d\mu}^\dagger f_{0\mu}) + \tilde{U}(c_{d\mu}^\dagger c_{d\mu} - 1)^2\right\} . \tag{3.6}$$

The important point is that all these fixed points can be obtained by choosing special values for $\tilde{\Gamma}$ and $\tilde{U}$, and comparing the resulting H_N (in the limit $N \to \infty$) with the free-electron Hamiltonian discussed earlier.

1. Free-orbital fixed points: H_{FO}^* and $\hat{H}_{FO}^*$

Suppose that $\tilde{\Gamma}$ and $\tilde{U}$ are both set equal to zero in Eq. (3.6). The resulting Hamiltonian, which will be denoted $H_{N,FO}^*$, is clearly just the free-electron Hamiltonian H_N^0 *plus* a free-impurity orbital of zero energy. Since H_N^0 goes rapidly to its fixed points as $N \to \infty$, one gets two new fixed points of $\mathcal{T}^2$, to be denoted H_{FO}^* and $\hat{H}_{FO}^*$. H_{FO}^* ($\hat{H}_{FO}^*$) is just H^* ($\hat{H}^*$) *plus* a free-impurity orbital of zero energy at the origin. Starting from every many-electron state of H^* ($\hat{H}^*$) one can construct four degenerate states of H_{FO}^* ($\hat{H}_{FO}^*$) by combining that state with each of the four states of the impurity orbital (empty, with ↑ electron, with ↓ electron, and with ↑↓ electrons). As $N \to \infty$, $H_{N,FO}^*$ goes to H_{FO}^* for even $(N+1)$ and to $\hat{H}_{FO}^*$ for odd $(N+1)$.

2. Local-moment fixed points: H_{LM}^* and $\hat{H}_{LM}^*$

Now suppose that, keeping $\tilde{\Gamma}$ fixed, one lets U become much larger than the energies of interest in Eq. (3.6). Consider how this affects the energy levels and the states of H_0 listed in Table I. Neglecting states which have energies $\tilde{U}$ above the ground state, and calculating the energies of the other states only to $O(\tilde{\Gamma}/\tilde{U})$, one gets the much simpler Table III. Note that only the singly occupied states of the impurity orbital, i.e., the states $c_{d\uparrow}^\dagger|\Omega\rangle$ and $c_{d\downarrow}^\dagger|\Omega\rangle$ where $|\Omega\rangle$ is the "vacuum" state, appear in this table. These two states can clearly be used to define a spin-$\frac{1}{2}$ variable, with an associated Pauli operator $\vec{\tau}$, say. It is straightforward to show that the states and the energies in Table III are precisely the ones that one would construct had H_0 been the Hamiltonian

$$H_0 = \Lambda^{-1/2}\left(\frac{\tilde{\Gamma}}{\tilde{U}}\right)(f_{0\mu}\vec{\sigma}_{\mu\nu}f_{0\nu})\cdot\vec{\tau} . \tag{3.7}$$

This means that for any N, if one neglects states that have energies $\sim\tilde{U}\Lambda^{(N-1)/2}$, then to $O(\tilde{\Gamma}/\tilde{U})$ one is

TABLE III. States and energies of the initial Hamiltonian H_0 Eq. (2.23) in the limit $\Gamma \ll U$. Compare with Table I.

Charge Q	Spin S	Index r	Energy/$\Lambda^{1/2}$	State
-1	$\frac{1}{2}$	1	$3\left(\frac{\tilde{\Gamma}}{\tilde{U}}\right)$	$c_d^\dagger\|\Omega\rangle = \|\tau\rangle$
0	0	1	0	$(f_0^\dagger c_d^\dagger)_s\|\Omega\rangle = (f_0^\dagger\|\tau\rangle)_s$
	1	1	$4\left(\frac{\tilde{\Gamma}}{\tilde{U}}\right)$	$(f_0^\dagger c_d^\dagger)_t\|\Omega\rangle = (f_0^\dagger\|\tau\rangle)_t$
+1	$\frac{1}{2}$	1	$3\left(\frac{\tilde{\Gamma}}{\tilde{U}}\right)$	$(f_{0\uparrow}^\dagger f_{0\downarrow}^\dagger)c_d^\dagger\|\Omega\rangle = f_{0\uparrow}^\dagger f_{0\downarrow}^\dagger\|\tau\rangle$

(ii) when N is even

$$\frac{Z_B}{Z_I} \cong \prod_{l=1}^{(M-N)/2} \frac{(1+e^{-\beta\epsilon_l})^4}{(1+e^{-\bar{\beta}\Lambda^{-l+1/2}})^4} \left\{ \prod_{l'=1}^{N/2} (1+e^{-\bar{\beta}\Lambda^{l'-1/2}})^{-4} \right\}^{\frac{1}{4}} , \tag{F49}$$

$$X_B - X_I \cong \sum_{l=1}^{(M-N)/2} \left[\frac{e^{-\bar{\beta}\epsilon_l}}{(1+e^{-\bar{\beta}\epsilon_l})^2} - \frac{e^{-\bar{\beta}\Lambda^{-l+1/2}}}{(1+e^{-\bar{\beta}\Lambda^{-l+1/2}})^2} \right] - \sum_{l'=1}^{N/2} \frac{e^{-\bar{\beta}\Lambda^{l'-1/2}}}{(1+e^{-\bar{\beta}\Lambda^{l'-1/2}})^2} - \frac{1}{8} . \tag{F50}$$

In writing down the above expressions for (Z_B/Z_I), we have taken out the ground-state-energy terms. We note that the quantities (Z_B/Z_I), $(X_B - X_I)$ and the sums, u_1, u_2, and u_3 defined in Eqs. (F39) - (F41) have well-defined limits as $M \to \infty$. They are even independent of N for large N, and need be numerically evaluated only once for all the iterations.

---

*Permanent address: Indian Institute of Science, Bangalore-560012, India.

[1]P. W. Anderson, Phys. Rev. 124, 41 (1961).
[2]H. R. Krishna-murthy, K. G. Wilson, and J. W. Wilkins, Phys. Rev. Lett. 35, 1101 (1975).
[3]H. R. Krishna-murthy, K. G. Wilson, and J. W. Wilkins, in *Valence Instabilities and Related Narrow-Band Phenomena*, edited by R. D. Parks (Plenum, New York, 1977), p. 177.
[4]*Magnetism*, edited by G. T. Rado and H. Suhl (Academic New York, 1973), Vol. V.
[5]D. J. Scalapino, Phys. Rev. Lett. 16, 937 (1966).
[6]K. G. Wilson, Rev. Mod. Phys. 47, 773 (1975). A brief discussion of the calculations can be found in *Nobel Symposia—Medicine and Natural Sciences* (Academic, New York, 1974), Vol. 24, p. 68.
[7]K. G. Wilson and Kogut, Phys. Rep. C, 12, 75 (1974).
[8]F. Wegner, Phys. Rev. B 5, 4529 (1972).
[9]These results can be obtained, for example, after some algebra starting from the results given in Ref. 5, above.
[10]J. R. Schrieffer and P. A. Wolff, Phys. Rev. 149, 491 (1966).
[11]F. D. M. Haldane, J. Phys. C 11, 5015 (1978).
[12]L. Oliveira and J. W. Wilkins (private communication).
[13]K. Yamada, Progr. Theor. Phys. 53, 970 (1975); 54, 316 (1975); K. Yosida and K. Yamada, Progr. Theor. Phys. 53, 1286 (1975).
[14]M. L. Mills, M. T. Beal-Monod, and P. Lederer, in Ref. 4, p. 89. This model is also called the Wolff model: P. A. Wolff, Phys. Rev. 124, 59 (1961).
[15]J. Mathews and R. L. Walker, *Mathematical Methods of Physics* (Benjamin, California, 1973), p. 73.

Low-Temperature Properties of the Two-Impurity Kondo Hamiltonian

B. A. Jones,[1],[a] C. M. Varma,[2] and J. W. Wilkins[1],[b]

[1]*Laboratory of Atomic and Solid State Physics, Clark Hall, Cornell University, Ithaca, New York 14853*

[2]*AT&T Bell Laboratories, Murray Hill, New Jersey 07974*

(Received 22 December 1987)

For the two-impurity Kondo system, the low-temperature properties—impurity spin-spin correlation function, susceptibilities, specific heat, and Wilson ratio—are strongly nonuniversal functions of the ratio I_0/T_K of the Ruderman-Kittel-Kasuya-Yosida coupling to the single-impurity Kondo temperature. In particular, there is a new unstable fixed point for an antiferromagnetic coupling with $I_0/T_K \simeq -2.2$. The calculations utilize a newly found symmetry of Kondo Hamiltonians, axial charge.

PACS numbers: 75.20.Hr, 75.30.Hx, 75.30.Mb

The understanding of correlations in heavy-fermion systems is far from complete.[1] The behavior of a pair of spin-$\frac{1}{2}$ impurities is a start for our understanding of a lattice of localized moments.[2] The low-temperature behavior for antiferromagnetic correlations is especially complex, since the interimpurity Ruderman-Kittel-Kasuya-Yosida (RKKY) interaction and Kondo effects compete directly in a way that has been addressed by only a few previous theories.[3] Recently two of us discussed the specific application of Wilson's numerical renormalization-group method to the two-impurity Kondo Hamiltonian and presented results primarily for fairly small ferromagnetic initial RKKY couplings.[4]

Here we present ground-state (low-temperature) properties for a full range of initial interactions and develop a two-parameter Fermi-liquid Hamiltonian for a slightly simplified case of the antiferromagnetic regime. For antiferromagnetic RKKY couplings $I_0 \sim -2T_K$ (where T_K is the single-impurity Kondo temperature) we find a new unstable fixed point characterized by diverging staggered susceptibility and coefficient of specific heat. At this new fixed point, both the ratio I_0/T_K and the impurity spin-spin correlation function $\langle \mathbf{S}_1 \cdot \mathbf{S}_2 \rangle$ are remarkably constant with T_K varying over 2 orders of magnitude. The Wilson ratio reaches a minimum value of much less than unity.

Our Hamiltonian is a natural extension of the original Kondo model to two spin-$\frac{1}{2}$ impurities $\mathbf{S}_1$ and $\mathbf{S}_2$, separated by a distance r, each impurity spin interacting with the spins $\mathbf{s}_c(\mathbf{r}_i)$ of the conduction electrons at the sites i.[4] The interaction term is

$$H_{\rm int} = J[\mathbf{s}_c(\mathbf{r}_1)\cdot\mathbf{S}_1 + \mathbf{s}_c(\mathbf{r}_2)\cdot\mathbf{S}_2]. \quad (1)$$

This Hamiltonian introduces a new scale—the initial (high-temperature) RKKY coupling $I_0 \propto (\rho J)^2$ where ρ is the density of conduction-electron states. (In general I_0 is a function of the impurity separation r, oscillating between the ferromagnetic and antiferromagnetic values.) The other important scale is the single-impurity Kondo temperature $T_K \propto (|\rho J|)^{1/2}\exp(1/\rho J)$.

There are three regimes of low-temperature behavior, depending on the ratio of the initial RKKY interaction to the single-impurity Kondo temperature. (a) When zero $I_0/T_K > -2.2$, that is, for all ferromagnetic interactions and medium to small initial antiferromagnetic interactions, the ground state is that of impurity spins completely quenched by the Kondo effect,[2] with nonzero interimpurity spin correlations. (b) When $I_0/T_K < -2.2$, for large antiferromagnetic initial interactions, *no* Kondo effect occurs.[2] The ground state is an uncompensated singlet with strong spin correlations. (c) When $I_0/T_K \approx -2.2$, at moderate antiferromagnetic initial couplings, there occurs an unstable fixed point of complex nature, completely unlike those of the single-impurity system. Its properties are discussed in subsequent sections.

These ground states are summarized in Fig. 1 by the impurity spin-spin correlation function $\langle \mathbf{S}_1 \cdot \mathbf{S}_2 \rangle$ at zero temperature as a function of I_0/T_K.[5] Note that $\langle \mathbf{S}_1 \cdot \mathbf{S}_2 \rangle$ is a continuous function through the unstable fixed point (marked by a symbol). For I_0/T_K larger than the critical value the moments are quenched by a Kondo effect while for smaller values no Kondo effect occurs. Note that the critical value of the antiferromagnetic coupling is far larger than commonly thought would allow a Kondo effect. The ground state is a singlet for all values except $\langle \mathbf{S}_1 \cdot \mathbf{S}_2 \rangle = 0.25$.

The most remarkable fact is the near constancy of the ratio I_0/T_K for the unstable fixed point, especially since T_K varies 2 orders of magnitude between $|\rho J| = 0.15$ and $|\rho J| = 0.35$. Unlike other fixed points of the one- and two-impurity problems, this fixed point apparently cannot be obtained by the scaling of variables of the original Hamiltonian to special values such as infinity, since T_K arises from a many-body low-temperature effect, and does not appear as a parameter in the original Hamiltonian (1). Also remarkable is the near coincidence of the curves, especially for the two smaller $|J|$'s, for antiferromagnetic couplings up to even moderate sizes. For ferromagnetic couplings we find no such scaling of the correlation function.

At low temperatures we can quantitatively express the deviations from the fixed point in regions (a) and (b) above in terms of a Fermi-liquid–like effective Hamil-

tonian[4] with six parameters:

$$\Delta H_{12}^{\mathrm{fl}} = -\sum_{p=e,o} t_p (f_{0p\mu}^{\dagger} f_{1p\mu} + \mathrm{H.c.}) + \sum_{p=e,o} U_p (n_{0p}-1)^2 + U_{eo} 4\mathbf{j}_{0e}\cdot\mathbf{j}_{0o} - J_{eo} 4\mathbf{s}_{0e}\cdot\mathbf{s}_{0o}. \quad (2)$$

The subscripts $p=e,o$ refer to states that are even and odd combinations of the state about the origin between the two impurities. Here, as in Ref. 4, f_0 and f_1 are momentum-shell operators for the conduction electrons, with f_0 localized about the impurity center and f_1 orthogonal to f_0 and slightly less localized. The number and spin of the f_0 electrons are $n_{0p} \equiv f_{0p\downarrow}^{\dagger} f_{0p\downarrow} + f_{0p\uparrow}^{\dagger} f_{0p\uparrow}$, and $\mathbf{s}_{0p} \equiv f_{0p\mu}^{\dagger} \frac{1}{2} \sigma_{\mu\mu'} f_{0p\mu'}$, respectively. Finally, the axial charge, $\mathbf{j}_{0p}$, is a (newly found) conserved vector quantity whose components[6] commute like those of angular momentum and which is a result of particle-hole symmetry in Hamiltonian (1). Axial charge is also conserved in the single-impurity Kondo and Anderson Hamiltonians. The z component of $\mathbf{j}_{0p}$ is one-half the charge as defined by Wilson[7] and Krishna-murthy, Wilkins, and Wilson[8]: $j_{0e}^{z} \equiv \frac{1}{2}(n_{0e}-1)$, for example.

The coefficients t_p, U_p, U_{eo}, and J_{eo} are deduced from the energy levels generated from the numerical renormalization-group approach. We can then treat the effective Hamiltonian as a perturbation on the fixed-point energy levels and analytically calculate thermodynamic quantities such as the susceptibility, uniform and staggered, and the coefficient of specific heat. Figure 2[9] shows low-temperature impurity contributions to χ, χ_s(staggered) $\propto \beta\langle(S_1^z - S_2^z)^2\rangle$, and $\gamma \equiv C/T$. The new unstable fixed point (marked by a bar on the I_0/T_K axis) is characterized by diverging values of staggered susceptibility and specific-heat constant while the uniform susceptibility remains fairly small.

Even the stable fixed points are surprising. In the strong antiferromagnetic limit, in which of course there is no Kondo effect, the loss of degrees of freedom suggests a ground-state singlet, but $\langle \mathbf{S}_1 \cdot \mathbf{S}_2 \rangle$ never achieves the singlet value of $-\frac{3}{4}$. In fact, as Fig. 1 indicates, over the range of ρJ examined, $\langle \mathbf{S}_1 \cdot \mathbf{S}_2 \rangle$ never drops below -0.66. For large antiferromagnetic couplings all thermodynamic quantities tend toward zero, as expected for nearly free electrons. For zero initial RKKY interaction $\chi = \chi_s \approx 2\gamma$. As ferromagnetic interactions increase, the three thermodynamic quantities diverge, with $\chi \approx 2\gamma \approx 2\chi_s$.

Figure 3 shows the dependence of the Wilson ratio

$$R = \tfrac{1}{3}\pi^2 (k_B/\mu_B)^2 \chi/\gamma \quad (3)$$

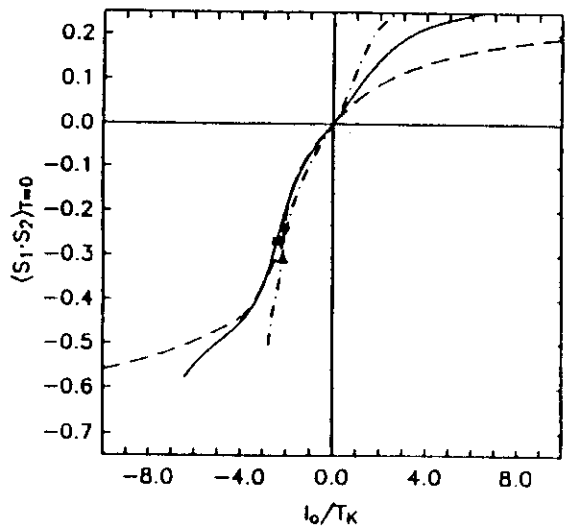

FIG. 1. Zero-temperature impurity spin-spin correlation function as a function of the ratio of the initial RKKY coupling I_0 to the Kondo temperature T_K for three values of $\rho J = -0.15$ (dashed line), -0.25 (solid line), and -0.35 (dash-dotted line). The unstable fixed points—indicated for decreasing ρJ by the circle, square, and triangle, respectively—are remarkably close even though T_K varies over 2 orders of magnitude. Note there is a limiting value of the antiferromagnetic correlation that can be achieved without explicitly adding to Eq. (1) an $\mathbf{S}_1 \cdot \mathbf{S}_2$ term.

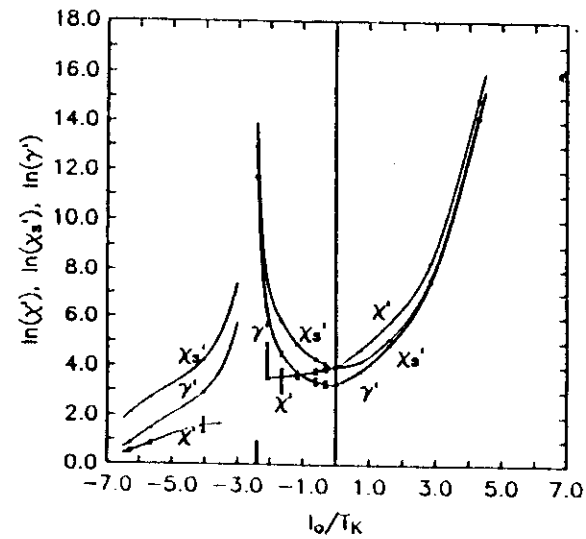

FIG. 2. Logarithms of impurity contributions to susceptibilities (uniform and staggered) scaled by $1/4\rho\mu_B^2$, and to specific-heat coefficient scaled by $3/4\rho\pi^2 k_B^2$, as functions of the scaled RKKY coupling I_0/T_K with $\rho J = -0.25$. (The dimensionless thermodynamic quantities are denoted by primes. Since these plots are for a single value of J, the scaling of I_0 is merely for comparison with Fig. 1.) Approaching the (hitherto unmentioned) stable ferromagnetic fixed point occurring at $r=0$ (for $I_0/T_K = 6.42$) $\chi_s' \approx \gamma'$ and $\chi' \approx 2\chi_s'$ diverge sharply. In the antiferromagnetic regime, χ_s and γ diverge at the unstable fixed point, which occurs at $I_0/T_K \approx -2.3$, as bracketed by the vertical lines. χ appears to be decreasing, but large error bars make the unstable fixed-point value uncertain. For large antiferromagnetic couplings, all properties tend toward zero, with $\chi' \approx \gamma'$ (i.e., Wilson ratio $R = 1$.)

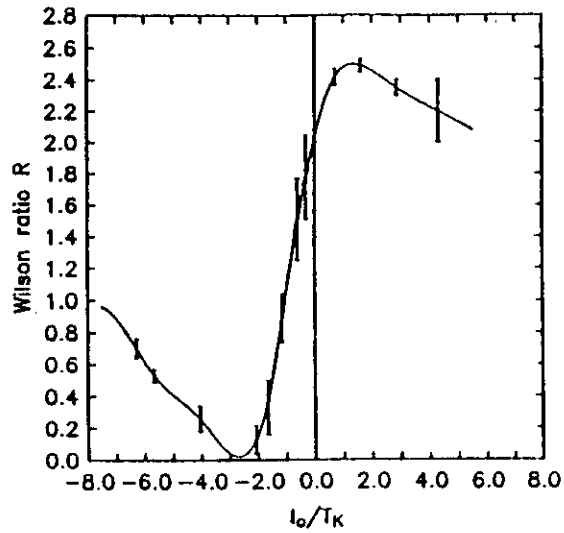

FIG. 3. Wilson ratio R [Eq. (3)] vs scaled initial RKKY coupling (for $\rho J = -0.25$). For reference, $R = 1$ for free-electron and strong antiferromagnetic limits; $R = 2$ for single-impurity (Kondo) limit and, perhaps, also for the strong ferromagnetic limit. At the unstable fixed point ($I_0/T_K \sim -2.3$) R is quite small. The behavior for $\rho J = -0.35$ is indistinguishable from that of $\rho J = -0.25$ for small antiferromagnetic couplings.

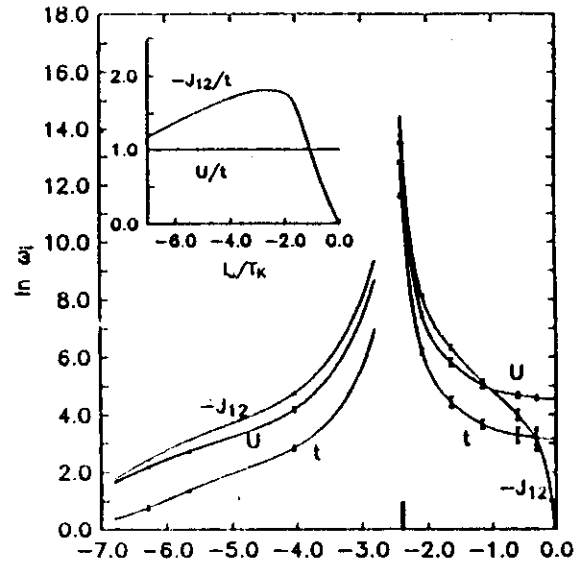

FIG. 4. Logarithms of coupling constants of the simplified effective Hamiltonian (4) vs scaled antiferromagnetic initial RKKY. For the single-impurity problem, U/t is independent of ρJ. For the two-impurity problem, the extra coupling constant $-J_{12}$, while zero for independent impurities, rapidly grows antiferromagnetically to diverge with U and t at the unstable fixed point. For large initial antiferromagnetic couplings all three coupling constants tend toward the noninteracting quasiparticles value of zero. Inset: Schematic plot of scaled ratios (see text) U/t and $-J_{12}/t$ such that the Wilson ratio is $R = 1 + (U + J_{12})/t$ in these units. (Error bars have been suppressed for clarity.) As for the single-impurity problem, we find the ratio U/t to be unity. J_{12}, however, varies widely, giving the nonuniversal Wilson ratio shown in Fig. 3. The unstable fixed point is characterized by a maximum in the ratio $-J_{12}/t$.

on the ratio of I_0/T_K for $\rho J = -0.25$. Note the very dynamic range of R about the (universal) single-impurity value $R = 2$, quantitatively confirming its nonuniversal nature for the two-impurity Kondo problem.[4] In particular, at the new unstable fixed point R reaches a minimum value much less than 1; indeed within our numerical accuracy it is zero.

It is possible to characterize the Wilson ratio in terms of a simple Fermi-liquid model. The complex interactions in the antiferromagnetic regime near the unstable fixed point are not dependent on any asymmetry between the strengths of the even- and odd-parity interactions, and so we set them equal for simplicity. The effective Hamiltonian (2) in this case, written in terms of operators at sites $i = 1$ and 2, is[10]

$$\Delta H^{\text{eff}}_{(\text{AFM})} = -t \sum_{i=1,2} (f^{\dagger}_{0i\mu} f_{1i\mu} + \text{H.c.}) + U \sum_{i=1,2} (n_{0i} - 1)^2 + U_{12} 4\mathbf{j}_1 \cdot \mathbf{j}_2 - J_{12} 4\mathbf{s}_1 \cdot \mathbf{s}_2. \tag{4}$$

U_{12} does not appear in either the susceptibility or the specific heat, and numerically it is zero.[11] Figure 4[9] displays the other three coefficients U, $-J_{12}$, and t as functions of scaled antiferromagnetic RKKY interaction. For independent impurities ($I_0 = 0$) $J_{12} = 0$, and ΔH^{eff} reduces to the same two terms as found for the single-impurity problem. As the initial RKKY interaction is increased, the high-temperature interactions between the moments are mirrored at low temperatures by increased (antiferromagnetic) interactions between the quasiparticles: $-J_{12}$ increases sharply. All three terms diverge rapidly (note the logarithmic scale) at the unstable fixed point. In the limit of strong antiferromagnetic initial couplings the deviations from the free-electron fixed point tend toward zero.

In terms of the Hamiltonian (4), the Wilson ratio can be rewritten

$$R = 1 + (U/t + J_{12}/t) C(\Lambda). \tag{5}$$

Here $C(\Lambda)$ is a constant of order unity which depends on details of the renormalization procedure.[12] In the inset of Fig. 4 the ratios U/t and $-J_{12}/t$ scaled by C are plotted versus I_0/T_K. We find that U/t takes the universal value one,[13] so that all the deviations from the single-impurity value $R = 2$ are governed by the behavior of J_{12}. The unstable fixed point is thus characterized by a maximum in antiferromagnetic quasiparticle spin interactions.

In summary, we find complex behavior in the antifer-

romagnetic regime of the two-impurity Kondo problem, including an unstable fixed point at moderate initial RKKY couplings. Many heavy fermions appear to have antiferromagnetic correlation or are close to a magnetic instability,[14] which raises the interesting question as to how close they may be to the antiferromagnetic instability found in the two-impurity problem. Although one would expect that a direct application of the two-impurity results here would have to be renormalized for a lattice, we nonetheless note the intriguing correlation between the uniformly small values of the Wilson ratio found experimentally[1,15] in heavy-fermion superconductors, and the very low values we find in the vicinity of the unstable fixed point.

This work was supported in part by the U.S. Department of Energy, Office of Basic Energy Sciences, Division of Materials Research. We thank G. Aeppli, A. J. Millis, E. Abrahams, P. A. Lee, N. Read, and G. Kotliar for helpful discussions, and C. Myers who did many of the computer runs.

---

[a]Present address: Lyman Laboratory of Physics, Harvard University, Cambridge, MA 02138.

[b]Present address: Physics Department, The Ohio State University, Columbus, OH 43210.

[1]P. A. Lee, T. M. Rice, J. W. Serene, L. J. Sham, and J. W. Wilkins, Comments Condens. Matter Phys. **12**, 99 (1986).

[2]Thermodynamic scaling results for the cases $|I_0| \gg T_K$ were derived by C. Jayaprakash, H. R. Krishna-murthy, and J. W. Wilkins Phys. Rev. Lett. **47**, 737 (1981); L. Chandran, H. R. Kirshnamurthy, and C. Jayaprakash, in *Theoretical and Experimental Aspects of Valence Fluctuations and Heavy Fermions*, edited by L. C. Gupta, S. K. Malic, and R. Vijayaraghavan (Plenum, New York, 1987), p. 531.

[3]See, however, important results for two (Anderson) impurities in R. M. Fye, J. E. Hirsch, and D. J. Scalapino, Phys. Rev. B **35**, 4901 (1987), and P. Coleman, Phys. Rev. B **35**, 5072 (1987).

[4]B. A. Jones and C. M. Varma, Phys. Rev. Lett. **58**, 843 (1987). Note that $2J_0$ in that paper is replaced in this Letter by J and K_0 by I_0.

[5]$\langle \mathbf{S}_1 \cdot \mathbf{S}_2 \rangle$ is calculated numerically as an expectation value for each eigenstate, based on the ratios of singlet and triplet impurity spin that existed at high temperature. At low enough temperatures $\langle \mathbf{S}_1 \cdot \mathbf{S}_2 \rangle$ takes the same value for all states, and it is this value we plot in Fig. 1.

[6]In terms of the $f_0, f_1, \ldots$ operators of Eq. (2), $j_p^+ \equiv \sum_n (-1)^n f_{np\uparrow}^\dagger f_{np\downarrow}^\dagger$; $j_p^- \equiv (j_p^+)^\dagger$; and $j_p^z \equiv \frac{1}{2} \sum_n (n_{np} - 1)$.

[7]K. G. Wilson, Rev. Mod. Phys. **47**, 773 (1975).

[8]H. R. Krishna-murthy, J. W. Wilkins, and K. G. Wilson, Phys. Rev. B **21**, 1003 (1980).

[9]Calculations for small antiferromagnetic couplings have appeared in C. M. Varma and B. A. Jones, in *Theoretical and Experimental Aspects of Valence Fluctuations and Heavy Fermions*, edited by L. C. Gupta, S. K. Malic, and R. Vijayaraghava (Plenum, New York, 1987), and B. A. Jones and C. M. Varma, Jpn. J. Appl. Phys. **26**, Suppl. 3, 1875 (1987).

[10]The coefficients of the unsymmetrized effective Hamiltonian (4) are related to those of even-odd parity H^{eff}, (2), by $t = \frac{1}{2}(t_e + t_o)$; $U = \frac{1}{4}(U_e + U_o + 3U_{eo} + 3J_{eo})$; $U_{12} = \frac{1}{4}(U_e + U_o + U_{eo} - 3J_{eo})$; $J_{12} = \frac{1}{4}(U_e + U_o - 3U_{eo} + J_{eo})$.

[11]$U_{12} = 0$ is expected. With no asymmetry between the even and odd interactions the Hamiltonian (4) now conserves charge at each site. Since, for example, $j_1^+ j_2^- + j_1^- j_2^+$ does not commute with n_1 (or n_2), the term involving U_{12} must be absent from (4).

[12]$C(\Lambda) = (1 - \Lambda^{-1})^{3/2}/(1 - \Lambda^{-3})^{1/2} 2 \ln \Lambda$. For the results presented here we chose $\Lambda = 3$.

[13]This current ratio between U and t is expected based on Nozières's "weak universality" argument, as noted in Ref. 4. See P. Nozières, J. Low Temp. Phys. **17**, 31 (1974); P. Nozières and A. Blandin, J. Phys. (Paris) **41**, 193 (1980).

[14]G. Aeppli, private communication. See, also, for example, G. Aeppli *et al.*, Phys. Rev. Lett. **57**, 122 (1986) [$CeCu_6$]; G. Aeppli *et al.*, Phys. Rev. Lett. **58**, 808 (1987) [UPt_3]; C. Broholm *et al.*, Phys. Rev. Lett. **58**, 917 (1987) [U_2Zn_{17}]; F. Steglich, in *Theory of Heavy Fermions and Valence Fluctuations*, edited by T. Kasuya and T. Saso, Springer Series in Solid State Sciences Vol. 62 (Springer-Verlag, New York, 1985), p. 23.

[15]G. R. Stewart, Rev. Mod. Phys. **56**, 755 (1984).

3774 (1988).

2637 (1978).

E. Fradkin, S. Kivelson and

B. A. Jones
Lyman Laboratory of Physics
Harvard University
Cambridge, MA 02138

Antiferromagnetic Phase Instability in the Two-Impurity Kondo Problem

Field theories in condensed matter physics/Zlatko Tesanovic
[editor].
p. cm.
Includes index.
1. Condensed matter. 2. Statistical physics. 3. Field theory
(Physics) I. Tesanovic, Zlatko.
QC173.4.C65F54 1990 530.4'1—dc19 90-363
ISBN 0-201-50391-3

This book was prepared by the author, using the TEX typesetting language.

We examine a model of two spin-one-half local moments in a conduction electron sea using Wilson's methods of numerical renormalization group. The competition between correlations of the itinerant electrons with the local moments, and of the local moments with each other, gives rise to complex behavior. For antiferromagnetic inter-moment interactions there occurs an unstable fixed point at finite coupling. This fixed point cannot be expressed in terms of a free-electron based Fermi liquid, a conclusion based upon examination of the fixed-point energy levels and of other anomalous properties of the system near the critical point.

I. INTRODUCTION

The competition between Kondo effects and magnetic ordering in a lattice can give rise to a complex set of interactions, effects which will have bearing on the behavior of heavy fermion materials and also perhaps on that of some high-temperature superconductors. The full theoretical solution of lattice of localized moments is at this point still far from complete, however.

As a start towards understanding this problem, we have been analyzing the behavior of two spin-$\frac{1}{2}$ local moments ("impurities") in a sea of conduction elec-

trons, using Wilson's methods[1,2] of numerical renormalization group. A review of previous studies[3] of the two-impurity system appears in Ref. 4. The two pertinent energy scales are the single-impurity Kondo temperature T_K and the inter-impurity RKKY coupling I_o. T_K is that temperature scale that would govern the quenching of the local moment spins in the absence of any interactions between them, $I_o = 0$. The RKKY interaction is generated indirectly by spin-flip scattering of a conduction electron off of one impurity site to the other, and can be of either sign depending on inter-impurity separation.

The behavior of the system for ferromagnetic RKKY interactions between the local moments is described in Refs. 5 and 6. In this paper we wish to focus on the case of antiferromagnetic interactions, and in particular on an unstable fixed point which occurs at finite coupling, between two stable regimes. At the unstable point the staggered susceptibility and the linear coefficient of specific heat diverge, and a simple explanation in terms of Fermi liquid theory breaks down.

We will describe how the preceding analysis is based upon examination of the fixed-point levels, and in the process illustrate the complexity of the unstable state. The paper is organized as follows The second section describes the transformations of the original Hamiltonian into an iterative form appropriate for the numerical renormalization group procedure. The Hamiltonian is first linearized, and then expressed in terms of operators on a logarithmically discretized space. The third section describes the stable fixed points for the antiferromagnetic regime, and their classification in terms of one-particle Hamiltonians of a set of N free electrons. We then present the lowest energy levels of the unstable fixed point, and discuss the contradictions inherent in trying to reproduce them by filling a set of single-particle levels. In the fourth section we briefly describe how finite-iteration deviations of the energy levels from their fixed-point values can be quantitatively parameterized by a Fermi-liquid-like effective Hamiltonian. The variation of the "Fermi-liquid" parameters as a function of initial energy scales, as well as the thermodynamic quantities which can be calculated from the effective Hamiltonian, give additional characterization of the unstable state. We end with a summary and directions of future research.

II. DISCRETIZATION OF THE HAMILTONIAN

The Hamiltonian is an extension of the original Kondo model to two spin-$\frac{1}{2}$ impurities $\vec{S}_1$ and $\vec{S}_2$, separated by a distance r. Direct interactions, of strength J, are only with those conduction electrons $\left(\text{also of spin } \frac{1}{2}\right)$ at each site:

$$H = \int d^3k \epsilon_k a^\dagger_{k\mu} a_{k\mu} + J[\vec{s}_c(\mathbf{r}_1)\cdot\vec{S}_1 + \vec{s}_c(\mathbf{r}_2)\cdot\vec{S}_2] \tag{1}$$

where

$$\vec{s}_c(\mathbf{r}_i) = \frac{\Omega_o}{8\pi^3}\int d^3k' \int d^3k\, e^{i(\mathbf{k}'-\mathbf{k})\cdot\mathbf{r}_i} a^\dagger_{k\mu} \frac{1}{2}\vec{\sigma}_{\mu\mu'} a_{k'\mu'}.$$

Here Ω_o is the volume and $J > 0$.

To apply the Wilson procedure, we assign to the conduction electrons a linear dispersion, a constant density of states ρ, and a band from $-D$ to D. The Hamiltonian (1) can then be linearized and all conduction electron states assigned a parity even (e) or odd (o) with respect to exchange of the two sites. As a last approximation, we take the resulting energy-dependent coupling coefficients to be constants just depending on the impurity separation, which enforces particle-hole symmetry on the interactions. (Note that this is not equivalent to evaluating all the coupling coefficients at a specific energy such as the Fermi energy, an approximation which would generate only ferromagnetic RKKY interactions.) The resulting Hamiltonian is

$$\frac{H}{D} = \int_{-1}^{1} d\epsilon\, \epsilon[a^\dagger_{e\epsilon\mu}a_{e\epsilon\mu} + a^\dagger_{o\epsilon\mu}a_{o\epsilon\mu}] + \frac{H_{int}}{D}, \tag{2}$$

$$\frac{H_{int}}{D} = \rho J_e \int_{-1}^{1} d\epsilon \int_{-1}^{1} d\epsilon' a^\dagger_{e\epsilon\mu}\frac{1}{2}\vec{\sigma}_{\mu\mu'}a_{e\epsilon'\mu'}\cdot(\vec{S}_1 + \vec{S}_2)$$

$$+ \rho J_o \int_{-1}^{1} d\epsilon \int_{-1}^{1} d\epsilon' a^\dagger_{o\epsilon\mu}\frac{1}{2}\vec{\sigma}_{\mu\mu'}a_{o\epsilon'\mu'}\cdot(\vec{S}_1 + \vec{S}_2) \tag{3}$$

$$+ \rho J_m \int_{-1}^{1} d\epsilon \int_{-1}^{1} d\epsilon' \left[a^\dagger_{e\epsilon\mu}\frac{1}{2}\vec{\sigma}_{\mu\mu'}a_{o\epsilon'\mu'} + a^\dagger_{o\epsilon\mu}\frac{1}{2}\vec{\sigma}_{\mu\mu'}a_{e\epsilon'\mu'}\right]\cdot(\vec{S}_1 - \vec{S}_2).$$

There are three interactions: even and odd, which preserve the total spin of the moments; and mixed, which intermixes singlet and triplet impurity spin states, and even and odd parity conduction electrons.

Note that there are no direct interactions between the impurities themselves in this model. There are, however, indirect interactions generated to all orders by spin-flip scattering of the conduction electrons. The leading order interaction is of the form $I(r)\vec{S}_1\cdot\vec{S}_2$ and known as the Ruderman-Kittel-Kasuya-Yosida (RKKY) interaction. If the interactions ρJ between the impurity and conduction electrons are small, the RKKY interaction I can be calculated by second-order perturbation theory to give the well-known oscillatory shape. For small r the interaction is ferromagnetic, and then oscillates on a scale of k_F^{-1} as r is increased, with an envelope for large r of $1/r^3$. For the above model (2), (3) we have for small (initial) ρJ,

$$\frac{I_o}{D} = 2 \ln 2\rho^2(2J_m^2 - J_e^2 - J_o^2) \propto (\rho J)^2. \tag{4}$$

(Both sides of the equality are implicitly r-dependent.) For ρJ not small, we cannot calculate the inter-impurity interaction directly. Single-impurity Kondo effects tend to renormalize ρJ to larger values; the resulting breakdown of perturbation theories for both ρJ and I/D give rise to the complex competing energy scales that necessitate the use of Wilson's procedure for a full solution.

The final transformations of this Hamiltonian are particular to the Wilson method. Wilson's numerical renormalization group method is an exact, iterative procedure for obtaining temperature-dependent properties of a Hamiltonian. Refs. 1 and 2 describe the technique as applied to the single-impurity Kondo and Anderson models, and we will not go into details here. Briefly, energy space is logarithmically discretized, and a new set of orthonormal operators $\{f_{np\mu}\}_{p=e,o;\mu=\uparrow,\downarrow}$ are defined which are roughly local to a given region of energy space, and thus also of real space. Those with index $n = 0$ are most localized about the center of the two impurities and extend the full bandwidth in energy space. The f_1 are somewhat less localized, and correspond to energies closer to the Fermi level. Interactions of f_n for n very large involve energies very close to the Fermi energy. In terms of these operators, the Hamiltonian (2), (3) becomes

$$\frac{H}{D} = \frac{1}{2}(1 + \Lambda^{-1}) \sum_{\substack{n=0 \\ p=e,o \\ \mu=\pm 1/2}}^{*} \Lambda^{-n/2}\xi_n[f^{\dagger}_{np\mu}f_{(n+1)p\mu} + f^{\dagger}_{(n+1)p\mu}f_{np\mu}] + 2\frac{\tilde{H}_{int}}{D}, \tag{5}$$

$$\begin{aligned}\frac{\tilde{H}_{int}}{D} = {} & \rho\left[J_e f^{\dagger}_{0e\mu}\frac{1}{2}\tilde{\sigma}_{\mu\mu'}f_{0e\mu'} + J_o f^{\dagger}_{0o\mu}\frac{1}{2}\tilde{\sigma}_{\mu\mu'}f_{0o\mu'}\right]\cdot(\tilde{S}_1 + \tilde{S}_2) \\ & + \rho J_m\left[f^{\dagger}_{0e\mu}\frac{1}{2}\tilde{\sigma}_{\mu\mu'}f_{0o\mu'} + f^{\dagger}_{0o\mu}\frac{1}{2}\tilde{\sigma}_{\mu\mu'}f_{0e\mu'}\right]\cdot(\tilde{S}_1 - \tilde{S}_2),\end{aligned} \tag{6}$$

with

$$\xi_n = \frac{(1 - \Lambda^{-(n+1)})}{[(1 - \Lambda^{-(2n+1)})(1 - \Lambda^{-(2n+3)})]^{1/2}}. \tag{7}$$

Λ is the discretization parameter, which we take to be 3.0. The point is that now the Hamiltonian can be expressed in an iterative form:

$$H/D \equiv \lim_{N\to\infty}\frac{1}{2}(1 + \Lambda^{-1})\Lambda^{-(N-1)/2}H_N \tag{8}$$

with

$$H_{N+1} = \Lambda^{1/2}H_N + \xi_N(f^{\dagger}_{Np\mu}f_{N+1p\mu} + f^{\dagger}_{N+1p\mu}f_{Np\mu}) \tag{9}$$

and

$$H_0 = \frac{4}{(1 + \Lambda^{-1})}\Lambda^{-1/2}\frac{\tilde{H}_{int}}{D}.$$

(Repeated indices p, μ are to be summed over.) The scaling by $\Lambda^{-(N-1)/2}$ insures that energy scales will be of order one for all iterations.

The input parameters are then ρJ_e, ρJ_o, and ρJ_m, subject to the sum rule $J_e^2 + J_o^2 + 2J_m^2 = J^2$, and such that the initial RKKY interaction (4) corresponds to a given spacing. The ground state energies are subtracted out. H_0 can be diagonalized by hand, and the rest of the H_N are formed and diagonalized by computer (Cray XMP). After a certain number of iterations the number of states $4^{(2N+3)}$ gets unwieldy even for a Cray, and the energy spectrum is truncated, keeping only the lowest energy several (many) hundred states. (Wilson[1] has studied this truncation as an approximation and found it to give a surprisingly accurate description of the low-energy states, provided of course that the number retained at each iteration is not too small.)

The output of such a procedure is, at each iteration, a set of energy eigenvalues and eigenvectors, with their corresponding symmetry labels. The Hamiltonian (2), (3) preserves three quantities:

a) total (impurities + electron) spin
b) total (impurities + electron) parity
c) a three-vector $\vec{j}$ which we call axial charge, a property of the electrons only.

The components of axial charge are[6]

$$j^{+} = \sum_{\substack{n=0 \\ p=e,o}}^{*}(-1)^n f^{\dagger}_{np\uparrow}f_{np\downarrow},$$

$$j^{-} = \sum_{\substack{n=0 \\ p=e,o}}^{*}(-1)^n f^{\dagger}_{np\downarrow}f_{np\uparrow} \tag{10}$$

$$j^{z} = \frac{1}{2}\sum_{\substack{n=0 \\ p=e,o}}^{*}(f^{\dagger}_{np\uparrow}f_{np\uparrow} + f^{\dagger}_{np\downarrow}f_{np\downarrow} - 1).$$

Component j^z is one half the charge q. The operators j^+, j^-, and j^z have the commutation relations of an angular momentum and all three components commute with the Hamiltonian. Hence j^z and j^2 are good quantum numbers and energy

eigenvalues are independent of j^z value. Note that particle-hole symmetry alone would require that states of $\pm q$ ($\pm j^z$) be degenerate, but conservation of axial charge further requires that all values of q: $-2j$, $-2j+2$, . . . , $2j-2$, $2j$ be degenerate.

We will label states by three quantum numbers in the form $(2j, 2S, p)$. Here $2j$ and $2S$ are twice the total axial charge and total spin, respectively, and p is parity: 0 = even, 1 = odd. All three indices are hence integers, and each such state has degeneracy $d = (2j+1)(2S+1)$.

III. LOW-TEMPERATURE FIXED POINTS

As the number of iterations increases, eventually the energy levels flow to one or the other of two stable fixed points. (For $\Lambda = 3$, typically 40 iterations were sufficient.) Since large iteration numbers correspond to low temperatures, these fixed points represent the two possible (stable) ground states. The relevant parameter separating the two stable regimes is the ratio of two initial energy scales, the RKKY interaction I_o (Eq. (4)) and the single-impurity Kondo temperature $T_K \approx D\sqrt{\rho J}e^{-1/\rho J}$. A summary of results[6] is as follows.

The ground state is a singlet for all nonzero impurity separations.

i) $I_o/T_K \lesssim 2.2$ For all ferromagnetic interactions ($I_o < 0$) and moderately small antiferromagnetic ones, the ground state is that of impurity spins completely quenched by the Kondo effect, with nonzero inter-impurity spin correlations.

ii) $I_o/T_K \gtrsim 2.2$ For large antiferromagnetic initial interactions, no Kondo effect occurs. The ground state is an uncompensated singlet with strong spin correlations.

iii) $I_o/T_K \approx 2.2$ For moderate antiferromagnetic initial coupling, we flow near an unstable fixed point of complex nature. This fixed point has quite unusual properties which will be detailed below.

Even though the nature of the ground state (Kondo or not) shows an abrupt transition at finite value of the coupling, the impurity spin-spin correlation $\langle \vec{S}_1 \cdot \vec{S}_2 \rangle$ is a *continuous* and monotonically decreasing function of I_o/T_K, even through the unstable point. In particular, it is zero only for the case of initially independent impurities, and reaches its limiting antiferromagnetic value of $-3/4$ in the ground state only in the limit of infinite I_o. At the transition through the unstable fixed point the value of $\langle \vec{S}_1 \cdot \vec{S}_2 \rangle$ is near $-1/4$, and there is at most a divergence in the derivative. Both the ratio I_o/T_K at which the transition occurs, $2.2 \pm .2$, and the value of the impurity spin-spin correlation function at that point, $\sim -1/4$, are remarkably constant through variations of T_K of over two orders of magnitude.

In the following we will briefly review the analysis[1,2] of a set of fixed point energy levels, a process which will highlight the unusual properties of the unstable state. Typically, the determination of an effective Hamiltonian for a fixed point

is a matter of educated guesswork. The point is to try to find a Hamiltonian which preserves all the symmetries of the original Hamiltonian, and which is exactly diagonalizable to give the same energies and eigenstates as are asymptotically approached in the numerical renormalizations. A good starting point is to assign some limiting values such as 0 or infinity to the parameters of the original Hamiltonian.

In this context, we examine the free-electron Hamiltonian, obtained by setting $J = 0$ (and hence $\tilde{H}_{mf} = 0$) in the Hamiltonian (9). With $\tilde{H}_{mf} = 0$ the Hamiltonian simply separates into independent even and odd channels, and we consider one such channel p:

$$H^{mr}_{N,p} \equiv \sum_{n=0}^{N-1} \Lambda^{(N-1-n)/2}\xi_n (f^\dagger_{np\mu} f_{n+1p\mu} + f^\dagger_{n+1p\mu} f_{np\mu}), \qquad p = e \text{ or } o. \tag{11}$$

Coefficient ξ_n is defined in Eq. (7) and is of order unity for large n. The $\Lambda^{-n/2}\xi_n$ factor is necessary in order for $H^{mr}_{N,p}$ to be a hopping (kinetic energy) in logarithmically discretized space. Hamiltonian (11) can be diagonalized exactly into $N+1$ single particle levels (per spin) by noting that $H^{mr}_{N,p} = f^\dagger \mathcal{H}^{eo}_N f$, where

$$(\mathcal{H}^{eo}_N)_{lm} = (\mathcal{H}^{eo}_N)_{ml} = \Lambda^{(N-1-m)/2}\xi_m \delta_{l,m+1}, \qquad l, m = 0, 1, 2, \ldots N \tag{12}$$

and "f" $= (f_0, f_1, \ldots f_N)$. The eigenvalues $\{\eta_i\}$ of $\mathcal{H}^{eo}_N$ are symmetric in energy space about $\eta = 0$, due to particle-hole symmetry. For N large, a limiting set of values is reached, which depend only on whether N is even or odd. For N even there is a zero eigenvalue $\eta_i = 0$ at $i = N/2$, while for N odd there is not.

The eigenstates of the free-electron Hamiltonian $H^{mr}_{N,p}$ are then obtained by variably occupying the single-particle levels. The ground state of $H^{mr}_{N,p}$ consists of fully occupying (two electrons each) all negative energy single-particle levels. Hence for N odd the ground state is nondegenerate, while for N even there is a four-fold ground state degeneracy corresponding to the variable occupancy of the $\eta_i = 0$ level. To subtract out the ground state energy one simply introduces hole operators conjugate to the negative-energy electron operators and normal orders in the usual way. Particles and holes then have the same set of positive (or zero) single-particle energies, and we may write the Hamiltonian as

$$H^{mr}_{N,p} = \sum_{i=1}^{N/2} \tilde{\eta}_i(N)(g^\dagger_{ip\mu} g_{ip\mu} + h^\dagger_{ip\mu} h_{ip\mu}) \qquad N \text{ even}$$

$$\tilde{\eta}_1^* = 1.70;\ \tilde{\eta}_2^* = 5.20; \ldots$$

(Complete set of operators includes $g_{0p\mu}$ of zero energy) (13)

TABLE 1 Listing of the first few energies and eigenstates of the free-electron Hamiltonian (11) in the limit of large particle number N and Λ = 3.0. The states below are those of $H_{N,e}^{free}$. The bars over the parity labels indicate those states that have odd parity for the case of $H_{N,o}^{free}$. (Recall the labeling: (2 × total axial charge, 2 × total spin, parity with even 0 and odd 1).) The degeneracy d of each level is also marked.

$H_{N,e}^{free}$		
$N \to \infty$, *even*		
$E = 0$:	$(100), (01\bar{0})$	$d = 4$
$E \simeq 1.70$:	$(100), (120), (21\bar{0}), (01\bar{0})$	$d = 16$
$N \to \infty$, *odd*		
$E = 0$:	(000)	$d = 1$
$E \simeq .80$:	$(11\bar{0})$	$d = 4$
$E \simeq 1.6$:	(200), (020)	$d = 6$

$$\sum_{j=1}^{(N+1)/2} \eta_j(N)(g_{jp\mu}^{\dagger} g_{jp\mu} + h_{jp\mu}^{\dagger} h_{jp\mu}) \qquad N \text{ odd}$$

$$\eta_1^* \simeq 0.80;\ \eta_2^* \simeq 3.00;\ \eta_3^* \simeq 9.00;\ \ldots .$$

Here $\eta_j^* = \lim_{N\to\infty}\eta_j(N)$. (Likewise for $\dot{\eta}_j$.) The numerical values given above for the η are for $\Lambda = 3.0$. Operator $g^{\dagger}$ creates a particle, and $h_{jp\mu}^{\dagger}$ creates a hole of parity p and spin $-\mu$. The first few eigenlevels of the large-iteration-N free-electron Hamiltonian for a single parity channel are accordingly as in Table 1.

We now return to the full interacting Hamiltonian with $J \neq 0$. Like the above eigenstates of a "chain" of free electrons, which depend on whether there is an even or an odd number of sites, the output of the computer diagonalization of the Hamiltonian (9) also alternates according to even or odd iteration number. In Figure 1 we show the energy flows as a function of odd iteration number for a typical value of strong antiferromagnetic RKKY coupling, $I_o/T_K \simeq 4.0$. Only the first few levels are shown. In the limit of large iterations, the energies reach plateaus, indicative of a stable fixed point. Comparison of the energy levels and eigenstates with those of the N = odd free-electron Hamiltonians above reveals that all states are identical (including higher energy states not shown in the figure) to those of the sum $H_{N,e}^{free} + H_{N,o}^{free}$ (N odd). (To verify, recall that both axial charge

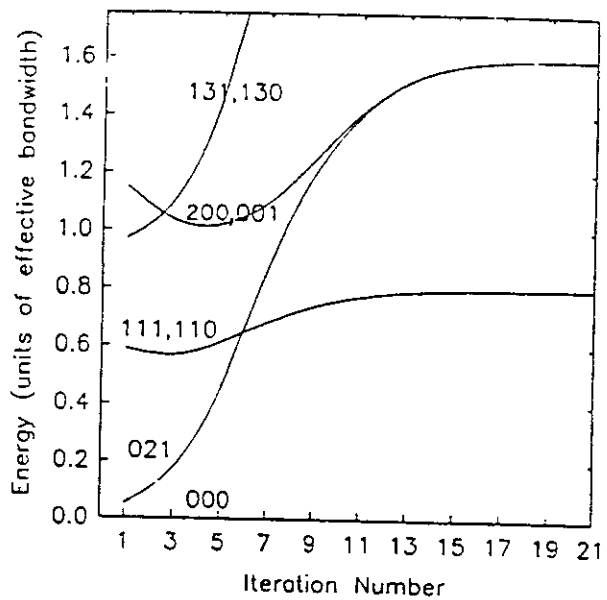

FIGURE 1 Energies (first few levels) vs. odd iteration number for strong antiferromagnetic coupling $I_o/T_K \simeq 4.0$. [At energy ≈1.6 there are a number of levels that are not illustrated for clarity. Besides (021), (200) and (001), there are also (201), (221), (020)(twice), and a second (200).] The stable fixed point, reached at around $N \simeq 15$, is that of free electrons, no impurities. For this figure and also Figures 2 and 3, $\rho J = 0.25$, $\Lambda = 3.0$.

and spin must be added as vectors; e.g. (110) + (111) = (001), (021), (201), (221).) Likewise even iteration eigenvalues, not shown, are identical to those of $H_{N,e}^{free} + H_{N,o}^{free}$ with $N \to \infty$, even.

We conclude that the fixed point for $I_o/T_K = 4.0$ is that of a set of free even and free odd electrons, with no remaining impurity degrees of freedom. That is, as far as the low-temperature excitations are concerned, the renormalized impurity is in a singlet ground state. One may further define asymptotic scattering states from the one-particle levels. Since the number of levels needed to describe the interacting (low-temperature) result is the same for both even and odd channels as the noninteracting case, the phase shifts for both even and odd channels are zero from the Friedel sum rule.

The flows for a typical Kondo-type fixed point are shown in Figure 2, for $I_o/T_K \simeq 0.31$, odd iterations. As in Fig. 1, only the first few levels are shown. However, one can as above get an exact match to energies and eigenstates, if one uses those of $H_{N,e}^{free} + H_{N,o}^{free}$ for *even* N. The conclusion is that the fixed point Hamiltonian is again that of a set of free even- and odd-parity electrons, but with the important difference that the number of one-electron levels needed to describe

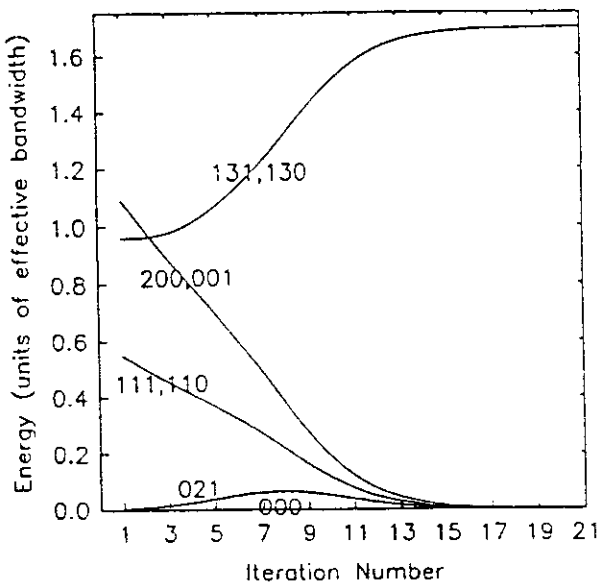

FIGURE 2 Energies (first few levels) vs. odd iteration number for weak antiferromagnetic RKKY $I_o/T_K \simeq 0.31$. The degeneracy at energy $\simeq 1.7$ is 128 and only a representative pair of levels is shown. The stable fixed point is reached at iteration $N \simeq 15$, and is characterized by a shift of the levels by one iteration from that of free electrons, Fig. 1. (That is, if we had plotted even iterations rather than odd in Fig. 1, the asymptotic levels would look exactly like those of Fig. 2.) This "capture" of one electron each in the even and in the odd parity channels to quench the impurity moments indicates a Kondo effect.

the interacting results are one less for both the even and the odd channels than would describe the noninteracting state. By Friedel's sum rule we obtain a phase shift of $\pi/2$ for both the even and the odd channels. Note that the results of Fig. 2 could not be described by a phase shift of less than $\pi/2$ in one channel and more than $\pi/2$ in the other, since this would produce energies which differed from the free-electron values of Table 1, and pairwise sums would not be able to replicate the unshifted totals of Fig. 2. Again the impurity degrees of freedom have disappeared from the problem, but at the expense of a phase shift at the Fermi level. This is just a rephrasing of the Kondo effect, and hence our classification of all such flows as Kondo-type fixed points.

All energy levels eventually flow to one or the other of the two fixed points that we have illustrated above. The choice of final fixed point and also the rate of approach to that fixed point are determined by I_o/T_K. For I_o/T_K arbitrarily close to a critical value ($\simeq 2.2 \pm .2$), however, the energies can be made to flow arbitrarily near an unstable fixed point which we illustrate in Figure 3. In Fig. 3

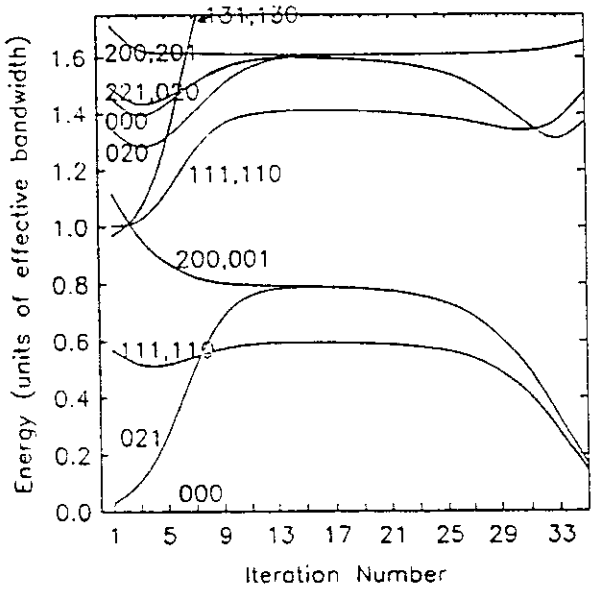

FIGURE 3 Iterations ~9 to ~29 illustrate the unstable fixed point, energy flows vs. iteration number. All levels at $E = 0$, ~.8, and ~1.6 are shown. (The states (131) and (130) are flowing to higher energy and do not belong in this grouping.) $I_o/T_K \simeq 2.4$. Odd iterations only are plotted, but during iterations 9–29, even iterations are virtually identical. The levels cannot be fit by any single-particle free-electron Hamiltonian as can those of Figs. 1 and 2.

a value of $I_o/T_K \simeq 2.4$ gives virtually constant energy levels from iterations ~9 to ~29. Around iteration 29 the flows in Fig. 3 happen to tend toward the Kondo fixed point: since the unstable fixed point occurs for a finite (probably irrational) value of the coupling parameters, it is in practice only possible to choose initial parameters such that the flows are asymptotically close to the unstable fixed point. We show only odd iterations, but during iterations 9 to 29 the energy levels and states of even iterations are virtually identical. All levels at energies 0, $\simeq .8$, and $\simeq 1.6$ are shown.

Note that the pattern of degeneracies cannot be explained by a set of free electron single particle levels, even with perhaps one or more associated zero-energy impurity degrees of freedom. The ground state is nondegenerate, and so any impurity degrees of freedom must be of finite energy. The next energy level up, at $E \simeq .8$, is 15-fold degenerate, and the next, at $E \simeq 1.6$, has degeneracy 30. (The deviations of (111), (110) from the other levels may be due to the presence of a marginal operator and may not be significant. If one considers the levels to have degeneracies 7, 8, and 8, 22, the following argument still holds.) These degeneracies can not be represented by single occupancy of a set of levels

$\{g_1^\uparrow; h_1^\downarrow; g_2^\uparrow; h_2^\downarrow; \ldots\}$, say, because of particle-hole and spin symmetry; for every particle operator there must be a hole operator, and for every up there must be a down. Hence even for a single parity channel the number of states at the single-particle level must be a multiple of 4. It must also be true that the fixed point is not a simple sum of even parity plus odd parity fixed points, as all the other fixed points are, since the one-channel Kondo Hamiltonian has no fixed points which do not show alternation between even and odd iterations. In short, the fixed point is quite complex in structure.

Because we cannot map the interacting case of the unstable state onto a set of free particles, there is no way to define phase shifts for this state, nor can we easily describe the renormalized state of the impurities. What is desired in an effective Hamiltonian a) which is expressed in terms of the original set of degrees of freedom, i.e., the "chain" operators f_0, f_1, . . . , b) which preserves all the symmetries of the original Hamiltonian; c) which reproduces all the energy levels and quantum labels; and d) shows repetition at every iteration, not every other. Scaling the parameters of the original Hamiltonian to special values to produce free-electron operators obviously does not work, and the question remains what, if any, effective Hamiltonian to use.

It is of interest to compare the above behavior with that of another Kondo system[7,8] already known to show a fixed point at finite value of coupling constants. The system is that of an n-channel single-impurity spin S Kondo problem with $n > 2S$. At its simplest level one considers the Hamiltonian

$$H' = H_{\text{K.E.}} + J_1 \vec{s}_{c,1} \cdot \vec{S} + J_2 \vec{s}_{c,2} \cdot \vec{S} \tag{14}$$

with $\vec{s}_{c,1}$, $\vec{s}_{c,2}$ and $\vec{S}$ all of spin $\frac{1}{2}$. Nozières and Blandin[7] and Cragg, Lloyd, and Nozières[8] have studied this problem both analytically and via Wilson numerical renormalization group techniques, with the following results. For $J_1 = J_2 = J$ there is an attractive fixed point at finite $J \approx 2$. That is, both $J = 0$ and $J = \infty$ are unstable, and flows are toward the fixed point that is attained most rapidly for initial $J \approx 2$. For $J_1 < J_2$ the fixed point becomes unstable, and behavior is dominated by J_2. The salient feature of these results is that the fixed point at $J \approx 2$ also does not show any even-odd alteration, and hence does not correspond to the filling of any asymptotic one-particle levels of free electrons. No effective (single-particle) Hamiltonian can be used to fit all of the levels, and correspondingly no phase shifts can be assigned to the channels, either.

However, the structure of the dressed impurity at the finite J fixed point can be determined by analysis[7,8] of the instabilities at $J = 0$ and $J = \infty$. At each stage of the iterations, the renormalized impurity is made up of an inner spin-$\frac{1}{2}$ object, bound antiferromagnetically to one electron from each channel, forming a new spin-$\frac{1}{2}$ center. This structure, duplicated at every iteration, extends outwards to the size of the system. Because of the logarithmic discretization of the Wilson procedure, the distance of each layer of electron pairs from the original spin center increases geometrically, with binding energy inversely proportional to the radius. The infinite size of the dressed impurity necessarily implies both the impossibility of defining asymptotic scattering states with respect to it and the lack of an odd-even iterations effect. [As a final note, the N-channel single-impurity Kondo problem was solved exactly via Bethe Ansatz by Tsvelick and Wiegmann[9] and Andrei and Destri,[10] who determined the scaling behavior at low temperatures and calculated critical exponents. These calculations did not modify the picture of the stable-J fixed point described above.]

Unfortunately for analysis of the anomalous fixed point of the two-impurity Kondo problem, it is not clear that there are many useful paralle. between the two Hamiltonians (3) and (14). In particular, the Hamiltonian (3) does not display the imbalance between number of scattering channels and size of impurity spin characteristic of the Cragg, Lloyd, and Nozières case above. This imbalance made both $J = 0$ and $J = \infty$ fixed points unstable and implied a stable fixed point between them. In our case, we have $n = 2S = 2$, and there are two strong coupling fixed points which are both stable. Unlike the case above, in which deviations from the well-characterized unstable points could be used to describe the structure of the stable point to which they flowed, we have the reverse case: two known stable points, with an unknown unstable point "between" them. One parallel may remain, however, and that is the lack of an odd-even effect, implying interactions which involve all the degrees of freedom of the system, and not just those closest to the impurity center. This may indicate interesting long-range (antiferromagnetic) correlations, an implication further supported by the facts of the next section.

IV. QUANTIZING FINITE-ITERATION DEVIATIONS FROM THE STABLE FIXED POINTS

Once one has an effective Hamiltonian describing a ($N = \infty$, $T = 0$) fixed point, one can calculate deviations about the fixed point to leading order in temperature. The result is a type of Fermi liquid which enables us to calculate thermodynamic properties of the system at low temperatures. We will not go into the details of the derivation here. It turns out that there are six operators to leading order for the Kondo-type and antiferromagnetic fixed points which preserve the symmetries (parity, spin, and axial charge) of the original Hamiltonian. (If just particle-hole symmetry is considered, there are seven.) The full expansion is presented in Refs. 5 and 6. For the simplified case of $J_z = J_\perp$ (in Hamiltonian (3)), the unstable fixed point is still displayed, and the effective Hamiltonian reduces to just three parameters:

$$H^{\text{eff}}_{(\Delta FM)} = H_c^{\text{free}} + H_\sigma^{\text{free}} + \Delta H^{\text{eff}} \Lambda^{(N-1)/2} + O(\Lambda^{-(N-1)}) \tag{15}$$

$$\Delta H^{eff} = -t \sum_{i=1,2} (f^{\dagger}_{0i\mu} f_{1i\mu} + f^{\dagger}_{1i\mu} f_{0i\mu}) + U \sum_{i=1,2} (n_{0i} - 1)^2 + 4J_{12}\vec{s}_1 \cdot \vec{s}_2. \quad (16)$$

Here $n_{0i} \equiv f^{\dagger}_{0i\uparrow} f_{0i\uparrow} + f^{\dagger}_{0i\downarrow} f_{0i\downarrow}$ and $\vec{s}_i = f^{\dagger}_{0i\mu} \frac{1}{2} \vec{\sigma}_{\mu\mu'} f_{0i\mu'}$. For clarity we have reexpressed the operators f in terms of impurity sites 1 and 2, rather than even and odd: $f_{i=1} \equiv \frac{1}{\sqrt{2}}(f_e + f_o); f_{i=2} \equiv \frac{1}{\sqrt{2}}(f_e - f_o)$. When the operators f_o, f_1 are expanded in terms of the free-electron operators g and h which diagonalize H^{free} (cf. Eq. (13) and also Ref. 2), the terms in ΔH^{eff} are all of order $\Lambda^{-(N-1)}$, revealing the leading correction to $H^{eff}_{(AFM)}$ to be of order $\Lambda^{-(N-1)/2}$, an irrelevant operator. The fixed point is thus stable.

The t term represents a hopping and can be considered a kinetic energy. One-fourth of $(n_{0i} - 1)^2$ is the square of the charge, making the U term a Coulomb repulsion. Both the U and t terms are of the type used to describe the single-impurity Kondo problem. The interaction J_{12} between the spins of the quasiparticles at sites 1 and 2 is specific to the two-impurity Hamiltonian. For the case of antiferromagnetic RKKY, t, U, and J_{12} are all positive.

The coefficient J_{12} is zero for independent impurities, $I_o = 0$. As the ratio I_o/T_K is increased, t, U, and J_{12} all increase rapidly, and ultimately diverge at the unstable fixed point. For larger I_o/T_K, the antiferromagnet regime, all three parameters of the effective Hamiltonian decrease, approaching zero in the limit of $I_o/T_K = \infty$. At this limiting point ($I_o = \infty$) the impurities completely disappear from the problem even at finite iterations, and the effective Hamiltonian is solely that of a set of free electrons with no residual interactions, consistent with the limiting value, $-3/4$, of the impurity spin-spin correlation function.

The single-impurity Kondo problem exhibits universal behavior with a single temperature scale T_K.[1] In the effective Hamiltonian, universality is displayed by a fixed ratio for U/t, independent of ρJ. For the two-impurity problem, U/t also has the same fixed value, a fact which may be derived using Nozières' "weak universality" argument.[5] However, the ratio J_{12}/t varies from zero at $I_o = 0$, to a maximum of $2U/t$ at the unstable fixed point, to U/t in the limit of large I_o/T_K. The two-impurity Kondo problem thus does not display universal behavior, and the unstable fixed point can be seen as a maximum in antiferromagnetic quasiparticle spin interactions. Returning to even-odd space, we note that a value of $2U$ for J_{12} at the unstable fixed point means that the coefficient J_{eo} of the operator $\vec{s}_e \cdot \vec{s}_o$ becomes identically zero at the critical point. Therefore not only is the total spin $\vec{s}_e + \vec{s}_o$ conserved, but we also have an additional symmetry induced at the unstable point: the spins of even-parity and odd-parity quasiparticles $\vec{s}_e$ and $\vec{s}_o$ are conserved separately.

Using the ΔH^{eff} term in (15) as a perturbation to the free-electron effective Hamiltonian $H^{free}_e + H^{free}_o$, one can calculate thermodynamics: uniform and staggered susceptibility, and specific heat. In particular, we calculate the difference of these thermodynamic quantities from their free-electron values to get the contribution of the impurities. To leading order at low temperatures, the susceptibilities χ and χ_s are independent of temperature, and the specific heat is linear $C = \gamma T$. A full presentation of these quantities as a function of I_o/T_K is given in Ref. 6. Specifically for the case of antiferromagnetic I_o, we find that the uniform susceptibility decreases apparently monotonically as I_o/T_K is increased. There may be a discontinuity at the unstable fixed point (the error bars on χ grow too large to tell), but no divergence. In contrast, the coefficient of specific heat γ and the staggered susceptibility χ_s increase as I_o/T_K increases, and both diverge sharply at the unstable fixed point. The divergence as a function of I_o/T_K follows a power law, $\chi_s, \gamma \sim [(I_o/T_K)_c - (I_o/T_K)]^{-2}$. The error bars on the exponent are around 10%, and $(I_o/T_K)_c$ is the previously quoted value $2.2 \pm .2$. Unfortunately, accuracy considerations currently prohibit the calculation of exponents for the divergence as a function of temperature for fixed I_o/T_K. Past the unstable point, for large I_o/T_K the total thermodynamic quantities approach those of a set of noninteracting free electrons, and hence the differences χ, χ_s, and γ asymptotically approach zero.

V. CONCLUSIONS

We have summarized those properties of the two-impurity Kondo Hamiltonian that have been obtained using techniques of the numerical renormalization group, for the case of antiferromagnetic RKKY coupling between the moments. The salient feature of these results is an unstable fixed point at finite value of the ratio I_o/T_K, where I_o is the initial (high temperature) value of the RKKY coupling (Eq. (4)), and T_K is the single-impurity Kondo temperature. Of note is the fact that neither I_o nor T_K are parameters of the original Hamiltonian (2), (3), and moreover that T_K is a many-body interaction energy describing low-temperature properties of the independent-impurity system.

By examining the energy levels of the unstable fixed point, one determines that they cannot be fit by a model of filled single-particle levels. The lack of an odd-even iterations alteration of the levels means that one cannot define asymptotic scattering states and thus phase shifts for the unstable state, which in turn implies long-range correlations about the impurity center. This concept of many degrees of freedom being involved in the unstable state is further supported by the calculation of a diverging specific heat. That the correlations are strongly antiferromagnetic is indicated by a diverging staggered susceptibility and by an effective Hamiltonian whose coefficient of inter-impurity quasiparticle spin interactions has a relative maximum. The value of the maximum means that an additional symmetry is induced at the unstable point: that of separate conservation of the spins of even and of odd parity quasiparticles.

Added to these facts is the impurity spin-spin correlation function, which is approximately $-1/4$ at the unstable point, corresponding to equal weighting of singlet and triplet of the impurity. It is as if the unstable state is a linear combination of two singlets: one a Kondo-compensated impurity triplet and the other

an impurity singlet. Unfortunately this picture violates charge conservation. The alternate picture, that of a simple linear combination of impurity spin triplet and spin singlet states to form a sort of Nèel state, violates conservation of spin.

It seems clear that the structure of the unstable state is quite complex and that a full explanation will require consideration of the many-body manifold of all the conduction electron states. What is not completely clear at this point is the role of various symmetries in the formation of the instability. A preliminary study[11] of a related model using a different technique revealed a phase transition but no divergences. This model in particular did not have particle-hole symmetry. Preventing a strict comparison, however, are other differences. The calculation, an auxiliary boson, large-N expansion, was done in the limit of infinite conduction electron and impurity spin, rather than spin-$\frac{1}{2}$. Fluctuations about the mean-field solution could give a variation in the critical behavior, as could the existence of a critical spin size greater than two.

Further characterization of the unstable fixed point would be provided by knowing the temperature-related critical exponents, for example, as well as by calculating various impurity-conduction electron correlation functions, and we are currently working on these projects. Several heavy fermion materials appear to be near an antiferromagnetic instability,[12] and it could be interesting to compare properties, such as neutron-scattering derived correlation functions, to those obtained from an analysis of a pair of impurities.

ACKNOWLEDGEMENTS

The author wishes to thank A. J. Millis, G. Kotliar, A. Auerbach, and particularly C. M. Varma and J. W. Wilkins, for helpful discussions. Support was provided by an IBM postdoctoral fellowship, and by the National Science Foundation through Grant No. DMR 85-14638 and the Harvard Materials Research Laboratory.

REFERENCES

1. K. G. Wilson, *Rev. Mod. Phys.* 47, 773 (1975).
2. H. R. Krishna-murthy, J. W. Wilkins, and K. G. Wilson, *Phys. Rev. B* 21, 1003 (1980).
3. Of note are the early thermodynamic scaling results of C. Jayaprakash, H. R. Krishna-murthy, and J. W. Wilkins, *Phys. Rev. Lett.* 47, 737 (1981), who studied the cases $|J_o| \gg T_K$. For Monte Carlo results for two Anderson impurities see J. E. Hirsch and R. M. Fye, *Phys. Rev. Lett.* 56, 2521 (1986); R. M. Fye, J. E. Hirsch, and D. J. Scalapino, *Phys. Rev. B* 35, 4901 (1987).

4. B. A Jones, Ph.D. Thesis, Cornell University, 1987.
5. B. A. Jones and C. M. Varma, *Phys. Rev. Lett.* 58, 843 (1987).
6. B. A. Jones, C. M. Varma, and J. W. Wilkins, *Phys. Rev. Lett.* 61, 125 (1988).
7. P. Nozières and A. Blandin, *J. Physique* 41, 193 (1980).
8. D. M. Cragg, P. Lloyd, and P. Nozières, *J. Phys. C* 13, 803 (1980).
9. A. M. Tsvelick and P. B. Wiegmann, *Z. Physik B* 54, 201 (1984).
10. N. Andrei and C. Destri, *Phys. Rev. Lett.* 52, 364 (1984).
11. B. A. Jones, G. Kotliar, and A. J. Millis, *Phys. Rev. B* 39, (1989) (Feb. 15 issue); See also A. J. Millis article in this workshop proceedings.
12. A recent neutron scattering study is, e.g., G. Aeppli, E. Bucher, C. Broholm, J. K. Kjems, J. Baumann, and J. Hufnagl, *Phys. Rev. Lett.* 60, 615 (1988).

Field theories in condensed matter physics/Zlatko Tesanovic [editor].
p. cm.
Includes index.
1. Condensed matter. 2. Statistical physics. 3. Field theory (Physics) I. Tesanovic, Zlatko.
QC173.4.C65F54 1990 530.4'1—dc19 90-363
ISBN 0-201-50391-3

This book was prepared by the author, using the TEX typesetting language.

A.J. Millis
AT&T Bell Laboratories
600 Mountain Avenue
Murray Hill, NJ 07974

B.G. Kotliar
Dept. of Physics, MIT
Cambridge, MA 02139

and

B.A. Jones
Dept. of Physics, Harvard University
Cambridge, MA 02138

The Two Kondo Impurity Problem: A Large *N* Biased Review

I. INTRODUCTION

The problem of two Anderson impurities coupled to a sea of conduction electrons has attracted a lot of attention as a first step towards understanding of the interactions between local magnetic moments in a metal and the formation of the heavy electron state. In this note we would like to review briefly some aspects of this problem with an emphasis on problems which are still open. The main breakthrough in this problem was provided by the numerical Renormalization group results of Jones and Varma.[1] Our results on the large N expansion appeared in Ref. (2). Other general references on the two impurities problem can be found in Ref. (7). The results of section 2 on symmetry considerations are new.

The Hamiltonian describing two Kondo impurities with a conduction electron band is given by:

$$H = H_0 + H_1 \tag{I-1a}$$

$$H_0 = -t \sum_{\eta} c^{\dagger}_{\eta} c_{\eta} \tag{I-1b}$$

$$H_1 = J_K[S_1 \cdot \sigma(-R) + S_2 \cdot \sigma(R)]. \tag{I-1c}$$

S_1 and S_2 are the impurity spin operators located at sites R and $-R$. $\sigma(R)$ is the

27

electron spin density at site R. $\sigma(R) = \sum_{kk'} e^{ik\cdot R} c^\dagger_{k\alpha}\sigma_{\alpha\beta}c_{k'\beta}$. $c^\dagger_{i\sigma}$ creates an electron with spin σ at site i and $c_k \equiv \frac{1}{\sqrt{N_s}}\sum_i e^{ik\cdot r_i}c_i$. N_s is the number of sites. In addition to (1) it is sometimes convenient to add a direct interaction between the impurities:

$$H_d = IS_1\cdot S_2. \tag{I-1d}$$

This problem has three energy scales. J_R the *RKKY* exchange energy, which reduces to I in the limit $I \gg T_k$. T_k is the Kondo binding energy, which reduces to J_k in the strong coupling limit $t \sim 0$. t is the conduction electron bandwidth. We wish to study the ground state and low temperature properties of the model. Since the interaction is purely local it seems natural to follow Nozieres and apply a Fermi liquid approach in which the low T properties are those of a Fermi gas of quasiparticles in the presence of some scattering potential. The ground state is just characterized in terms of the Fermi surface phase shifts of these quasiparticle excitations.

Two regimes can be easily identified. a) The *RKKY* regime, when $J \gg J_k$. Here the *RKKY* interaction locks the two impurities into a singlet and the conduction electrons are weakly scattered from a structureless potential. In this limit the phase shifts are close to zero. In the limit that $J \gg t \gg J_k$ this picture can be substantiated in perturbation theory in t noticing that the Kondo logarithms are explicitly cut off. b) The Kondo regime when $T_k \gg J_R$. Here the Kondo effect takes place in each individual site binding two conduction electrons and leaving behind a Fermi liquid with scattering phase shifts close to $\pi/2$ at the Fermi level.

Assuming that a local Fermi liquid picture is valid there are several important issues one can address: a) How to describe quantitatively the Kondo and the *RKKY* regimes? What is the behavior of the phase shifts, the density of states close to the Fermi level and the uniform and staggered susceptibility? b) How does the transition between the two regimes take place?

II. ROLE OF SYMMETRIES

One can often extract valuable information from symmetry considerations. In the spin 1/2 1 impurity Kondo problem, Nozieres[3] showed how many results, such as the value $\pi/2$ for the Fermi surface phase shift and the value 2 for the Wilson ratio, follow from particle-hole symmetry if a non-magnetic ground state is assumed. He and others[4] also showed how deviations from particle-hole symmetry either in the conduction band or in the Kondo coupling are irrelevant in the *RG* sense.

Here we attempt to apply similar considerations to the two impurity problem. Our new results are that if the model possesses particle-hole symmetry, then the only possible Fermi surface phase shifts are 0, $\pi/2$, or π. This result is important because it is clear on physical grounds that in the Kondo regime (for example, for widely separated impurities) the Fermi surface phase shifts must be close to $\pi/2$, while in the *RKKY* regime the phase shifts must be close to 0 or π. It then follows that for a particle-hole symmetric model there must be a nonanalyticality between the Kondo and *RKKY* regimes, rather than a smooth crossover. This argument does not determine the form of the nonanalyticity. As discussed in section III, the original numerical *RG* work of Jones, Varma and Wilkins shows that in the symmetric model the nonalalyticity has the character of a second order zero temperature phase transition.

An important question, then, is whether deviations from particle-hole symmetry are relevant or irrelevant. If the symmetry-breaking perturbations are relevant, then their effect on the transition must be determined. This issue is not yet resolved. In section IV we discuss some results of a large-N calculation which suggest that the particle hole symmetry breaking plays a very important role in the low energy behavior of the two impurity problem.

In the remainder of the section we define more precisely the particle-hole symmetry in which we are interested and show that it leads to the results we have stated for the phase shifts.

We are interested in $T = 0$ properties of the two impurity Kondo model. We assume that the ground state is nondegenerate and possesses a length, L, such that conduction electron wave packets which vanish at distances $d < L$ from the impurities evolve according to the non-interacting Hamiltonian Eq. (1-1b). In these circumstances one can learn about the phase shift by studying the conduction electron Green function, defined in imaginary time via

$$G(p, p'\tau - \tau') = -\langle T c_p(\tau)c^\dagger_{p'}(\tau')\rangle. \tag{II-1}$$

The T-matrix $T_{pp'}(w)$ in this problem is defined as

$$G(p, p') = G_0(p, w)\delta pp' + G(p, w)Tp, p'(w)G_0(p', w) \tag{II-2a}$$

As in any scattering problem, the phase shift δ_λ are defined in terms of the eigenstates of the scattering matrix λ via the expansion of the diagonal part t-matrix $T_{pp}(w)$[5]

$$T_{pp}(w \to \xi_p + i\delta) = -\sum_\lambda A^{(p)}_\lambda e^{i\delta_\lambda}\sin\delta_\lambda. \tag{II-2b}$$

Here p is momentum, ξ_p is the energy of the electron state with momentum p (in the absence of the electron-impurity interaction) and $A^{(p)}_\lambda$ is a real number depending on the density of states and the overlap between the plane-wave state $|p>$ and the eigenstate $|\lambda>$. Parity (more precisely, reflection symmetry in the plane perpendicular to and bisecting the line between the two impurities) is also a symmetry of the two impurity Kondo problem. It has been shown by Jones[6]

that for fixed parity only one channel of conduction electrons couples to the two impurities. Therefore the asymptotically low energy excitations affected by the impurities are conduction electron scattering states, characterized by a phase shift which depends on energy and parity but not on spin or any other quantum number. Hence in the present case, the index λ in II-1 runs over the values e and o, and refers to parity only.

In problems involving electrons in metals it is sometimes convenient to work only with positive energy excitations, of which at $T = 0$ there are two sorts: adding a particle at momentum $p > p_F$ or removing a particle at momentum $p < p_F$ (p_F is the Fermi momentum). Thus it is convenient to define particle operator $p_k^\dagger k \geq k_F$ and hole creation operators $h_k^\dagger$ for $k \leq p_F$ by

$$p_{k\sigma}^\dagger = c_{k\sigma}^\dagger (k > p_F)$$

$$h_{k\sigma}^\dagger = c_{-k\bar{\sigma}}(-1)^{n_\sigma} (k < p_F).$$

Here σ is a spin index, $\bar{\sigma} = -\sigma$ and $\eta_\sigma = 1$ for spin up and -1 for spin down. One must then consider two sorts of Green functions, a particle Green function defined by

$$G_p(k, k', \tau - \tau') = -\langle T_\tau p_k(\tau) p_{k'}^\dagger(\tau') \rangle \tag{II-3}$$

and hole Green function G_h, defined by

$$G_h(k, k', \tau - \tau') = -\langle T_\tau h_k(\tau) h_{k'}^\dagger(\tau') \rangle \tag{II-4}$$

if $|k|, k' < k_F$. Using the above definitions it is easy to see that

$$G_p^R(p, p', \omega) = G^R(p, p', \omega)\ p, p' > p_F \tag{II-5a}$$

$$G_h^R(k, k', \omega) = -G^A(-k', -k, -\omega)\ k, k' < p_F. \tag{II-5b}$$

Similar statements hold for the self energies. The superscript A, R denotes advanced and retarded and ω is a real frequency.

We may obtain the T-matrix referring to the even parity state only by studying the self energies of the even (odd) conduction electron Greens functions:

$$Ge_0(|p|, |p'|, \tau - \tau') = -\langle T_\tau (c_p^{(\tau)} \pm c_{-p}^{(\tau)})(c_{p'}^\dagger(\tau') \pm c_{-p'}^\dagger(\tau')) \rangle. \tag{II-6}$$

Clearly (II-5a) and (II-5b) hold separately for the even and odd Green's functions. The $\lambda = e, o$ terms in Eq. (II-2) are proportional to the diagonal part of the self energy of the even and odd Green's functions defined in Eq. (II-6).

In a theory with particle-hole symmetry the Hamiltonian must be invariant under the interchange of p_k and h_q operators, with $\xi_q = -\xi_k$. In the square lattice this correspondence is realized by $k = -(q + G)$ with $G = (\pi, \pi)$. Therefore

$$G_p^R(q, q', \xi_q) = G_h^R(k', k, -\xi_k) \tag{II-7}$$

Combining the statement of particle hole symmetry in Eq. (II-7) with the mathematical identity of Eq. (II-5) we have

$$G^K(q, q'\xi_q) = -G^R(-k', -k, \xi_k)^*. \tag{II-8}$$

Statement (II-8) obviously holds for the even and odd Green functions separately. The corresponding statement for the T matrix gives

$$\mathbf{T}^R(|q|, \xi_q)e_0 = -\mathbf{T}^K(|k|, -\xi_k)^* e_0. \tag{II-9}$$

As $q \to p_F$, one must have $k \to p_F$, $\xi_q \to 0$, $\xi_k \to 0$ and indeed $h_k^\dagger$ and $p_q^\dagger$ must create the same state. Then the discussion following Eq. (II-2) shows that the even and odd phase shifts at the Fermi surface must be 0, $\pi/2$, or π.

We note that this entire argument is only correct asymptotically as $q \to k_F$, for it tacitly assumes that one incident particle scatters to one outgoing particle of the same energy, and not to e.g. one outgoing particle hole plus a particle pair.

We stress that the argument depends on having overall particle-hole symmetry which is a condition on the conduction electron Hamiltonian Eq. (I-1b) *and* on the exchange Hamiltonian Eq. (I-1c).

III. THE WILSON *RG* APPROACH

In a very important development Jones and Varma and Jones, Varma, and Wilkins have obtained an exact numerical solution of a model Hamiltonian closely related to Eq. (1). Their work was the first to show that a phase transition was possible in the two impurity model. Their solution was carried out at the particle hole symmetric point. They found that the phase shifts in the Kondo phase were identically $\pi/2$, and in the $RKKY$ phase they are 0 or π[8] in agreement with the general arguments developed in the previous section. The transition between the two regimes was found to be second order. As the coupling was varied through the critical value x_c, the specific heat coefficient and staggered susceptibility diverged approximately as $(x - x_c)^{-\alpha}$.

IV. THE LARGE *N* APPROACH

We have generalized the model of Eq. (I-1) to 2 $SU(N)$ impurities and solved it exactly in a large N limit using the slave boson technique. This approach provides an analytic realization of the local Fermi liquid picture and allows an explicit

calculation of the Fermi liquid parameters in the large N limit where a mean field theory becomes exact.

As in the slave-boson treatment of the one impurity model, the mean field theory in the two impurity problem may be thought of as a resonant model. The spins are represented by localized Fermionic states which are coupled to each other by a term coming from the direct interaction Eq. (I-1d) and hybridize with the conduction electrons by a term coming from the Kondo couping, Eq. (I-1c). The physical parameters are determined by solving mean-field equations, which depend upon two dimensionless parameters. One is T_k/J_R where T_k is essentially the single-impurity Kondo temperature derived from J_k and J_R reduces to I in the large N limit. For $(T_k/J_R) < (T_k/J_R)_c \sim .5$, the coupling between the conduction electrons and the localized level vanishes. We interpret this as the non-Kondo regime. For $(T_k/J_R) > (T_k/J_R)_c$ the hybridization is non-zero; we interpret this as the regime in which the Kondo effect occurs. We interpret the transition between the two regimes as the large-N analogue of the transition found by Jones, Varma and Wilkins.

The other parameter on which our results depend, B, is defined by

$$B = \left| \sum_k \frac{\cos kr}{\epsilon_k} \right| \qquad \text{(IV-1)}$$

and is seen to depend on the conduction electron bandstructure and the inter-impurity separation r. For fixed ϵ_k, $B = 0$ only at special values of r. When $B = 0$, the mean-field theory has particle-hole symmetry in both even and odd channels, and the Fermi surface phase shifts are found to be 0 or π (in the non-Kondo regime) and $\pi/2$ (in the Kondo regime). When $B \neq 0$ the phase shifts differ from $\pi/2$ in the Kondo regime; however, the sum of the even channel and odd channel Fermi surface phase shifts remains π.

It is also interesting that the character of the transition between Kondo and non-Kondo regimes depends on B. For $B < 1/\pi$ the transition is first order; for $B > 1/\pi$ it is second order, with discontinuities only in derivatives of physical quantities such as the specific heat coefficient or the staggered susceptibility. It is interesting to speculate about the possible implications of these findings for the case $N = 2$. For the $B > 1/\pi$ regime experience with the one impurity problem suggests the transition becomes a *smooth crossover* for finite N. On the other hand the first order transition could in principle survive at finite N. There are however non perturbative effects in the form of instantons tunnelling between the Kondo and the *RKKY* minima which would not appear in a naive $1/N$ expansion and which could potentially convert the first order transition to a second order transition or a smooth crossover. We are currently investigating these possibilities.

V. OPEN PROBLEMS

The result of the large N expansion suggest that the presence and absence of particle hole symmetry. (i.e. the parameter B) is a potentially relevant perturbation *at the Kondo fixed point* and *at the transition with $B = 0$ fixed point.*

It has been suggested[9] that the equality of the phase shifts in the Kondo regime is a fundamental property of the two impurity problem being an "ultimate form of confinement." If this view is correct the parameter B should renormalize to zero at the Kondo fixed point.

The large N approach suggests a very different scenario. Here the phase shifts are generically unequal in the absence of particle hole symmetry. Their splitting is the first signature of the formation of a heavy Fermion band in the two impurity problem. We note that in the large N calculation the effect of B on the phase shifts appears at very low energies (of the order of Tk) indicating that the splitting of the resonances is also a low energy effect, which would then not renormalize to zero, unlike particle-hole asymmetry in the 1-impurity problem.[4]

These two different scenarios could be clarified by a numerical *RG* in the Kondo phase of a two impurity problem lacking particle hole symmetry. If B is indeed not driven to zero at low energies it is important to understand whether it could have an effect on the nature of the phase transition.

If the solution of the two impurity problem is to yield some clue about the lattice problem, it will be by understanding how the resonance splitting is renormalized by many body effects. We are only beginning to address this point. Expansions about solvable limits will provide some further insight, but at present it seems to us that only a numerical *RG* study or an exact solution of a particle hole asymmetric model will definitively settle this issue.

VI. REFERENCES

1. B. A. Jones and C. M. Varma, *Phys. Rev. Lett.* 58, 843 (1987) and B. A. Jones. C. M. Varma and J. W. Wilkins, *Phys. Rev. Lett.* 61, 125 (1988).
2. B. A. Jones, B. G. Kotliar, and A. Millis, *Phys. Rev. B* (1988) in press.
3. P. Nozieres and A. Blandin, *J. Physique* 41, 193 (1980).
4. P. Lloyd and D. M. Cragg, *J. Phys. C* 12, 3290 (1979); D. M. Cragg and P. Lloyd, *J. Phys. C* 11, L597 (1978) and *J. Phys. C* 12, L215 (1979); D. M. Cragg, P. Lloyd, and P. Nozieres, *J. Phys. C* 13, 803 (1980).
5. G. D. Mahan, *Many Particle Physics*, section 4.1 (Plenum Press, New York) 1983.
6. B. A. Jones, unpublished Ph.D. Thesis, Cornell University, 1987.
7. P. Coleman, *Phys. Rev. B* 35, 5072 (1987); C. Jayaprakash, H. R. Krishnamurthy, and J. W. Wilkins, *Phys. Rev. Lett.* 47, 737 (1981); H. Ishii, *Progress of Theoretical Physics*, 50, 1777 (1973).

8. B. A. Jones in these proceedings.
9. C. M. Varma and B. A. Jones, "Theoretical Effects of Valence Fluctuations and Heavy Fermions," L. C. Gupta and S. K. Malik editors, Plenum, NY, 878 (1987); C. M. Varma, *Phys. Rev. Lett.* 55, 2723 (1985).

PHYSICAL REVIEW B VOLUME 39, NUMBER 5 15 FEBRUARY 1989-I

Mean-field analysis of two antiferromagnetically coupled Anderson impurities

B. A. Jones
Department of Physics, Harvard University, Cambridge, Massachusetts 02138

B. G. Kotliar
Department of Physics, Massachusetts Institute of Technology, Cambridge, Massachusetts 02139

A. J. Millis
AT&T Bell Laboratories, 600 Mountain Avenue, Murray Hill, New Jersey 07974
(Received 4 November 1988)

We have solved, near $T=0$, a model describing two magnetic impurities coupled to a band of itinerant electrons and also antiferromagnetically to each other, using an auxiliary-boson mean-field theory which is exact in a large-N limit. Depending upon parameters we find two possible ground states: one in which the Kondo effect occurs and one in which it does not. As the direct antiferromagnetic interaction is varied relative to the Kondo coupling at $T=0$, a phase transition occurs which may be of first or second order. We compute the low-temperature behavior of the specific heat and the uniform and staggered susceptibility. The nature of the Kondo phase and of the phase transition differ notably from the results found in a recent numerical renormalization-group calculation of a similar model with $N=2$.

The interplay, in a material with a high density of magnetic moments, between the Kondo effect (which involves quenching of a local moment via coupling to conduction electrons) and magnetic ordering of the moments is a long-standing problem. It is of particular current relevance to the study of heavy-fermion metals, for in the past several years many of these have been shown by neutron scattering[1] or NMR (Ref. 2) to exhibit interesting magnetic behavior. The issue also arises in the theoretical analysis of a class of models[3] intended to describe the high-T_c CuO_2-based superconductors; these models idealize the high-T_c materials as a set of localized spins, residing on the Cu sites, magnetically coupled to each other and to itinerant holes on the O sites.

The interplay between the Kondo effect and magnetic ordering in a lattice is an unsolved problem. As a first step, much attention has been devoted to the problem of two magnetic impurities in a normal metal host. There are two important energy scales: the single-impurity Kondo temperature, T_K, and the magnetic interaction I. In our conventions $I>0$ corresponds to antiferromagnetic coupling of the two spins. It is clear that for $I \gg T_K$ the Kondo effect will be inhibited because the magnetic interaction will tend to bind the spins into a singlet. Until recently it was believed[4] that the $T=0$ physical properties of the two-impurity problem would vary smoothly with I/T_K.

However, a recent numerical renormalization-group (RG) study of the two-impurity Kondo problem found different behavior.[5] As the ratio I/T_K was varied through a critical value $(I/T_K)_c \approx 2.2$, a surprising behavior was found. For $(I/T_K) < (I/T_K)_c$, the ground state was one in which a Kondo effect occurred, while for $(I/T_K) > (I/T_K)_c$ the Kondo effect did not occur. For (I/T_K) near the critical value, the zero temperature values of the staggered susceptibility χ_s and the specific-heat coefficient $\gamma = C/T$ diverged approximately as $|I/T_K - (I/T_K)_c|^{-2}$, while the uniform susceptibility χ did not diverge. The existence of the phase transition raises many questions, including the robustness of these results to effects not included in the idealized model studied numerically and also the generalization to higher spin and to more than two impurities.

As a step towards understanding the issues outlined above we have solved in mean-field theory a model describing two magnetic impurities coupled to a band of itinerant electrons and also antiferromagnetically to each other via an exchange interaction I. The model with $I=0$ has been discussed previously.[6] Our mean-field solution is exact in an $N \to \infty$ limit where N is the spin degeneracy of the impurity levels and the conduction band. The magnetic coupling I is to be thought of as being mediated by degrees of freedom not explicitly included in the model, for example as a superexchange via filled orbitals. Such a term would also be generated by performing poor-man scaling[4,7] on an Anderson model. The Ruderman-Kittel-Kasuya-Yosida (RKKY) interaction mediated by the explicitly included conduction electron degrees of freedom would only appear as fluctuation corrections to the mean-field theory. As is shown below and in Ref. 6, the mean-field theory contains some intersite effects due to multiple scattering of the conduction electrons, but these are not due to the RKKY interaction.

Our results are summarized in Figs. 1 and 2 and discussed in detail below. We find that for typical values of parameters the mean-field equations have several solutions, of which more than one may be locally stable. If we restrict attention to the global minimum of the free energy, then in qualitative agreement with the numerical study of the two-impurity Kondo problem we find at $T=0$ two possible regimes. For $(I/T_K) > (I/T_K)_c \sim 2$ we find a regime in which the Kondo effect does not occur; while

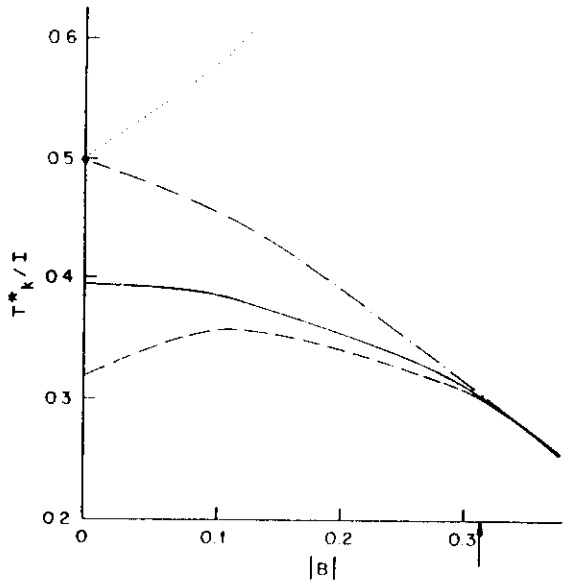

FIG. 1. Phase diagram for mean-field equations [Eqs. (3) in text]. The solid line is the boundary $(T_K^*/I)_c$ between the large (T_K^*/I) regime where the Kondo solution is the global energy minimum and the small T_K^*/I regime where the non-Kondo solution is the global minimum. The arrow marks the point $B=1/\pi$. For $B<1/\pi$ the transition is first order (light solid line); for $B>1/\pi$ the transition is continuous (thick solid line). Below the dashed line the non-Kondo solution is the only minimum, although an unstable solution of Eqs. (3) with $\mathrm{sgn}\delta=-\mathrm{sgn}B$ also exists. The non-Kondo solution is locally stable below the dash-dot line and locally unstable above. The dash and dot-dash lines merge with the solid boundary line for $B\geq 1/\pi$. Above the dotted line Eqs. (3) have only one solution, the Kondo solution described in the text. This solution evolves smoothly and without bifurcation as T_K^*/I is lowered at fixed B. Below the dotted line Eqs. (3) have other unphysical solutions with $\delta\neq\pi/2$.

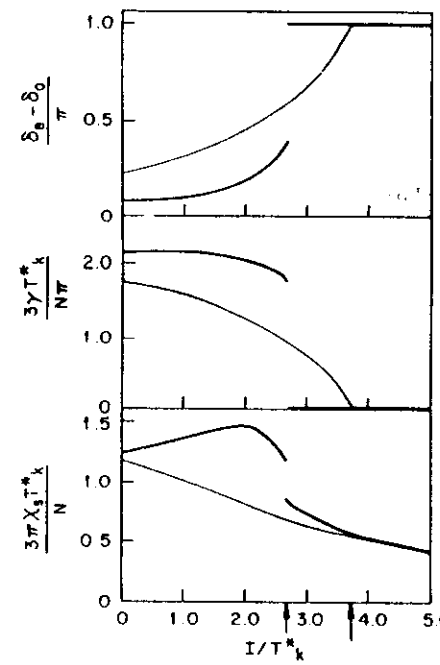

FIG. 2. Behavior of physical quantities as antiferromagnetic interaction I is varied at fixed T_K^*, for two representative values of $|B|$; $|B|=0.1$ (heavier curves), $|B|=0.4$ (lighter curves). The arrows indicate the values of I/T_K^* at which the transition from Kondo-like to non-Kondo-like solution occurs. The upper panel shows the difference of the even (δ_e) and odd (δ_o) channel phase shifts from $\pi/2$ (note $\delta_e+\delta_o=\pi$), the central panel shows the normalized specific-heat coefficient γ, and the lowest curve shows the normalized staggered susceptibility χ_s. For $B=0$ the curves would be independent of I for $I<(T_K^*)_c$.

for $(I/T_K)<(I/T_K)_c$ we find a regime in which the Kondo effect does occur. The Kondo regime may be thought of as a theory of two channels (even and odd parity) of electrons moving in scattering resonances with phase shifts δ_e and δ_o at the Fermi surface. In the numerical RG work, the result $\delta_e=\delta_o=\pi/2$ was found throughout the Kondo regime. In the mean-field theory we find that in general $\delta_e\neq\delta_o$, although $\delta_e+\delta_o=\pi$ as required by the Friedel sum rule. A further difference is that in the mean-field theory the transition between the Kondo and non-Kondo regime may be first or second order; in no case do any of the quantities γ, χ, and χ_s diverge at the transition. At present the reason for the difference between our results and the numerical RG results is not known. One possible explanation is that the RG calculation was performed for a model with $N=2$, while our calculation is valid in an $N\to\infty$ limit. At finite N, fluctuation corrections to the mean-field theory may become important. We discuss possible effects of such corrections at the end of this paper.

Our formal analysis proceeds from the standard auxiliary boson version of the two impurity $U=\infty$ Anderson model,[6] to which is added an antiferromagnetic interaction $I\mathbf{S}_1\cdot\mathbf{S}_2$ where $\mathbf{S}_{1,2}$ are the usual SU(N) spin operators and $I>0$.

The Hamiltonian is

$$H=\sum_{k,m}\varepsilon_k c^\dagger_{km}c_{km}+\sum_{\substack{a=1,2\\ m}}E_0 f^\dagger_{am}f_{am}+\frac{V}{\sqrt{N}}\sum_{\substack{a=1,2\\ m}}b^\dagger_a e^{ik\cdot r_a}c^\dagger_{km}f_{am}+\mathrm{H.c.}+\frac{I}{N}\sum_{m,m'}f^\dagger_{1m}f_{2m}f^\dagger_{2m'}f_{1m'}. \tag{1}$$

Here $a=1,2$ labels spin sites and we enforce the constraint $n_{fa}+n_{ba}=N/2$. Here n_{fi} and n_{bi} are the number of f electrons and auxiliary bosons on site a. In the previous heavy-fermion literature[6,8] a more general constraint $n_{fi}+n_{bi}=q_0N$ $(q_0\leq\frac{1}{2})$ was employed. We must choose $q_0=\frac{1}{2}$ to correctly represent the state where the two impurities are in a singlet.

We write the model as a functional integral, introducing Lagrange multipliers $i\lambda_i$ to enforce the constraints. We decouple the antiferromagnetic interaction via a Hubbard-Stratonovich transformation, introducing a link variable R,[9] integrate out the conduction and f electrons, and make a static approximation for R, $i\lambda_i$, and b_i. Because

there are two conservation laws (one for each site) there are two arbitrary phase degrees of freedom, which we choose so that the two auxiliary-boson (b_α) fields are real. The free energy per spin, F/N, may then be written

$$\frac{F}{N} = -\sum_{i,\omega_n} \mathrm{Tr} \ln \underline{M} + \sum_{\alpha=1,2} \left(\frac{\varepsilon_{f\alpha} - E_0}{\pi \rho V^2} \Delta_\alpha + \tfrac{1}{2} (\varepsilon_{f\alpha} - E_0) \right) + R^2/I . \tag{2}$$

Here $\varepsilon_{f\alpha} - E_0$ is the mean-field value of $i\lambda_\alpha$; $\Delta_\alpha = \pi \rho V^2 |b_\alpha|^2/N$, and now R and b_α denote mean-field values. ρ is the conduction-electron density of states at the Fermi level.

The 2×2 matrix $\underline{M}$ has components $M_{\alpha\alpha} = -i\omega_n + \varepsilon_{f\alpha} - i\Delta_\alpha \mathrm{sgn}\omega_n$,

$$M_{12} = R - (iA\,\mathrm{sgn}\omega_n + B)\sqrt{\Delta_1 \Delta_2} ,$$

$$M_{21} = R^* - (iA\,\mathrm{sgn}\omega_n + B)\sqrt{\Delta_1 \Delta_2} ,$$

and

$$\pi\rho(iA\,\mathrm{sgn}\omega_n + B) = \sum_k \frac{e^{ik\cdot r}}{-i\omega_n + \varepsilon_k} .$$

A and B are numbers of magnitude ≤ 1 determined by the conduction-electron band structure and the impurity separation r. As $r \to 0$, $A \to 1$. For $k_F^{-1} \ll r \ll L$ (where L is the Kondo length v_F/T_K) one finds $A \cong \sin k_F r/k_F r$ and $B \cong \cos k_F r/k_F r$.

The mean-field equations may be derived by varying the free energy with respect to Δ_α, $\varepsilon_{f\alpha}$, R, and R^*. The full mean-field equations are formidable; on the basis of the solution of the $I = 0$ case we have assumed $\Delta_1 = \Delta_2 = \Delta$ and $\varepsilon_{f1} = \varepsilon_{f2} = \varepsilon_f$ and we have checked the local stability of our results against static fluctuations in $\Delta_1 - \Delta_2$ and $\varepsilon_{f1} - \varepsilon_{f2}$.

The parameter R is complex; however, for $A < A_c(B)$ [with $A_c(B) \gtrsim 0.7$] we find that the physically relevant free-energy minima have $\mathrm{Im}R = 0$. For $A > A_c(B)$, solutions with both Δ and $\mathrm{Im}R \neq 0$ are favored. The case $A > A_c$ is briefly discussed below, and will be analyzed at length in a future paper.[10]

With the notation $E_1 = \varepsilon_f + B\Delta + R$, $E_2 = \varepsilon_f - (B\Delta + R)$, the mean-field equations are

$$\frac{1}{\pi} \tan^{-1} \frac{E_1}{\Delta(1-A)} + \frac{1}{\pi} \tan^{-1} \frac{E_2}{\Delta(1+A)} - 2\frac{\Delta}{\pi\rho V^2} = 0 , \tag{3a}$$

$$\frac{1}{\pi} \tan^{-1} \frac{E_1}{\Delta(1-A)} - \frac{1}{\pi} \tan^{-1} \frac{E_2}{\Delta(1+A)} - \frac{2R}{I} = 0 , \tag{3b}$$

$$\frac{2BR}{I} + \frac{1-A}{2\pi} \ln \frac{E_1^2 + \Delta^2(1-A)^2}{D^2} + \frac{1+A}{2\pi} \ln \frac{E_2^2 + \Delta^2(1+A)^2}{D^2} + \frac{2(\varepsilon_f - E_0)}{\pi\rho V^2} = 0 . \tag{3c}$$

In the Kondo limit, in which terms proportional to $\Delta/\rho V^2$ and $\varepsilon_f/\rho V^2$ are neglected, the three coupled nonlinear equations may be reduced to one,

$$\left(\frac{T_K^*}{I} \right) e^{B\delta} (\sin\delta - B\cos\delta) = \delta/\pi . \tag{4}$$

Here $T_K^* = De^{-1/\pi\rho J^*}$, where D is the conduction bandwidth and the modified Kondo coupling J^* is given by

$$(\rho J^*)^{-1} = -E_0/\rho V^2 + \frac{1}{\pi}[(1-A)\ln(1-A) + (1+A)\ln(1+A)] .$$

$-\pi/2 \leq \delta \leq \pi/2$ is an angle in terms of which the original variables are $\Delta = T_K^* e^{B\delta} \cos\delta$, $R + B\Delta = T_K^* e^{B\delta} \sin\delta$, and $\varepsilon_f = -A(B\Delta + R)$. Equation (4) may easily be solved by graphical or numerical techniques.

A and B express the intersite correlations. A gives the difference in widths of the two resonances in the Kondo limit and enters the theory in an essentially trivial way for $A < A_c(B)$. The parameter B gives the splitting of the resonances, and will be seen to play a more important role. Our results turn out to depend only on $|B|$. We note that J_{RKKY}, the RKKY interaction due to explicitly retained conduction electron degrees of freedom, goes for large $k_F r$ as

$$\cos(2k_f r)/(k_f r)^3 - (B^2 - 1^2)/k_f r .$$

Thus $|B|$, on which our results depend crucially, is not directly related to the magnitude or sign of J_{RKKY}.

Depending on the values of (T_K^*/I) and B, Eq. (4) may have 0, 1, 2, or 3 solutions. In addition, the solution $\Delta = 0$, $R = I/2$ is always a free-energy extremum. However, if we focus only on global minima of the free energy, then only two solutions are relevant. One is the non-Kondo solution $\Delta = 0$, $R = I/2$, which corresponds to decoupling the f electrons from the conduction band, but coupling them to each other, so that the even parity eigenfunctions are filled and lie $I/2$ below the chemical potential; the odd parity solutions are empty and $I/2$ above. This is the fermion representation of a spin singlet. The non-Kondo solution is the global minimum for $(T_K^*/I) < (T_K^*/I)_c$.

To construct the other, Kondo, solution, consider T_K^*/I large. For T_K^*/I sufficiently large, Eq. (4) has only one solution, with $\Delta = T_K^*/\sqrt{1+B^2}$ and $R = \alpha I\,\mathrm{sgn}B$. Here α is a number of order B. The Kondo solution evolves continuously as the ratio T_K^*/I is lowered until at $(T_K^*/I)_c$ the non-Kondo solution becomes favored. The Kondo solution is a theory of two channels of electrons moving in scattering resonances with phase shifts $\pi/2 \pm \delta$, where δ is the value of the relevant solution Eq. (4). We have found that for $B \neq 0$ it is not possible to find a stationary point which corresponds to two channels of electrons moving in Lorentzian scattering resonances with the same phase shift in each channel. Note also that the sign of R is found to be such as to *increase* the difference of the phase

shifts from $\pi/2$. The various regimes discussed above are shown in Fig. 1.

The specific-heat coefficient γ may be calculated in the standard way, by evaluating the Matsubara sum in Eq. (1) at nonzero temperature. The uniform (χ) staggered (χ_s) susceptibilities may be calculated by adding a term of the form $\sum_m (h/N) m (f^\dagger_{im} f_{im} \pm f^\dagger_{2m} f_{2m})$ to the initial Hamiltonian. We find

$$\gamma = \frac{N\pi}{3} \frac{2e^{-B\delta}\cos\delta}{(1-A^2)T_K^*} = \pi^2 \chi , \tag{5a}$$

$$\chi_s = \frac{N}{3\pi} \frac{e^{-B\delta}}{T_K^*} \frac{A \ln[(1+A)/(1-A)]\cos\delta + 2\delta\sin\delta}{\sin^2\delta + A^2\cos^2\delta} . \tag{5b}$$

The Wilson ratio $R=1$. The divergence of γ and χ_s for $|A| \to 1$ occurs because in that limit one of the resonances becomes arbitrarily narrow. The behavior of δ, γ, and χ_s as I is varied for fixed T_K^* is plotted in Fig. 2 for two representative values of B.

The above results have been obtained in the Kondo limit. Away from the Kondo limit the equations must be solved and the energies and stabilities checked numerically. We have verified that the two physically relevant solutions we have identified evolve smoothly as the ratio $\Delta/\rho V^2$ increases. We believe that the phase diagram remains essentially similar to what we have found in the Kondo limit.

In conclusion we speculate briefly upon the likely effect of including fluctuation corrections to the mean-field theory.

In mean-field theory we find a second-order phase transition for $B > 1/\pi$, with Δ vanishing and the physical quantities varying continuously through the transition. In this regime, for any finite N, fluctuation corrections will become comparable to the mean-field values sufficiently near the transition, leading to a breakdown of perturbation theory. We suspect that in this case the fluctuation effects will smooth out the transition, so that the model would exhibit only a smooth crossover as T_K^*/I is varied. In the single impurity Anderson model, an $N=\infty$ second-order phase transition with $\Delta \to 0$ at $T \sim T_K$ similarly becomes a crossover at any finite N. This argument suggests that in this model at finite N there is no order parameter characterizing the difference between the Kondo and non-Kondo regimes, because it is possible to go smoothly from the Kondo to the non-Kondo regimes by appropriately varying B and T_K^*/I.

For $B < 1/\pi$ the situation could be different. Because the transition is first order, a perturbation expansion in powers of $1/N$ would, we believe, converge at sufficiently large N, say $N > N_c$. Then, in the absence of nonperturbative effects arising for example from tunneling between the two minima, the transition would remain first order for $N > N_c$ so that the point $B = 1/\pi + O(1/N)$ would be a critical point, the end of a line of first-order phase transitions. For $N < N_c$ the transition could become a smooth crossover for all B or a second-order phase transition for some values of B. Nonperturbative effects could lead to $N_c = \infty$.

An important difference between our results and those of Ref. 5 is the value of the Fermi-surface phase shifts δ_e and δ_o. We note that the model of Ref. 5 has a special particle-hole symmetry in which even (odd) parity particles are mapped to even (odd) parity holes. When this symmetry is enforced in our model, $B=0$ implying $\delta_e = \delta_o = \pi/2$ in the Kondo phase. We are currently studying whether at finite N the symmetry is restored. It might be interesting to extend the analysis of Ref. 5 to a model that lacked the above symmetry.

The generalization of the results of this paper to the lattice is in principle straightforward;[10] however, the large variety of possible magnetic behavior (both ordered and resonating-valence-bond-like), will make the analysis much more involved.

We thank C. M. Varma for stimulating discussions. Portions of this work were performed at the Aspen Center for Physics. One of us (A.J.M.) acknowledges the hospitality of the physics departments at Harvard University and Massachusetts Institute of Technology. B.A.J. was supported by IBM and by the the National Science Foundation through the Harvard Materials Research Laboratory and Grant No. DMR-85-14638. B.G.K. was supported by the National Science Foundation through Grants No. DMR-85-21377 and DMR-86-57557.

[1]See, e.g., G. Aeppli, E. Bucher, C. Broholm, J. K. Kjems, J. Baumann, and J. Hufnagl, Phys. Rev. Lett. **60**, 615 (1988).

[2]See, e.g., F. Ohkawa *et al.*, J. Magn. Magn. Mater. (to be published).

[3]B. G. Kotliar, P. A. Lee, and N. Read, Physica B&C **153-154**, 538 (1988); C. Castellani and B. G. Kotliar, Phys. Rev. B **39**, 2876 (1989); P. Coleman and N. Andrei (unpublished).

[4]C. Jayaprakash, H. R. Krishna-murthy, and J. W. Wilkins, Phys. Rev. Lett. **47**, 737 (1981).

[5]B. A. Jones and C. M. Varma, Phys. Rev. Lett. **58**, 843 (1987); B. A. Jones, C. M. Varma, and J. W. Wilkins, *ibid.* **61**, 125 (1988).

[6]P. Coleman, Phys. Rev. B **35**, 5072 (1987); D. M. Newns and N. Read, Adv. Phys. **39**, 799 (1987).

[7]P. W. Anderson, J. Phys. C **3**, 2436 (1970).

[8]N. Read, D. M. Newns, and S. Donaich, Phys. Rev. B **30**, 3841 (1984); A. J. Millis and P. A. Lee, *ibid.* **35**, 3394 (1987); A. Auerbach and K. Levin, Phys. Rev. Lett. **57**, 877 (1986).

[9]I. Affleck and J. B. Marston, Phys. Rev. B **37**, 3774 (1988).

[10]B. A. Jones, B. G. Kotliar, and A. J. Millis (unpublished).

Physica B 171 (1991) 53–60
North-Holland

Pair correlation effects in heavy fermions

B.A. Jones
IBM Almaden Research Laboratory, 650 Harry Road, San Jose, CA 95120-6099, USA

Invited paper.

We summarize progress in studying a model of two Kondo impurities interacting directly with a conduction electron sea and indirectly with each other. In the presence of particle–hole symmetry, a critical point exists at finite ratio of (antiferromagnetic) RKKY coupling to Kondo temperature. For the more general case of no particle–hole symmetry, however, indications from both a $1/N$ (mean field) expansion and numerical renormalization group studies of potential scattering are that the transition is washed out. We discuss the implications of these findings on pair correlations in a real (lattice) system.

1. Introduction

Of interest in the study of strongly correlated materials is the question of the onset of coherence: when do the interacting spins see each other, and how? Heavy-fermion materials at high temperatures behave like a collection of individual local moments. At lower temperatures correlations set in. If a local moment is Kondo compensated, how can spin polarizations propagate to other local moments? If two moments are in a quantum singlet state, how can the Kondo effect occur? The simplest model incorporating both these competing aspects is the two-impurity Kondo model. In this paper we discuss a numerical renormalization group solution. Although no RKKY term is put in explicitly by hand, we find we need to invoke it anyway in order to describe the results.

The key to the questions raised above is in thinking not in terms of a spatial distribution of individual moments, but of scattering channels, even and odd. Ground states are coherent states of the system as a whole. Correlations build as the temperature is lowered, and we find the RKKY interaction to be a relevant operator. That is, both the Kondo coupling and the RKKY interaction grow as the temperature is lowered, and we need both to describe the ground state.

For the special case of particle–hole symmetry, one cannot go simply from one state to the other. The scattering phase shifts are $\frac{1}{2}\pi$ or 0, with no values in between. We know from the single-impurity problem that potential scattering, which breaks particle–hole symmetry, is an irrelevant operator – the net phase shift is still $\frac{1}{2}\pi$. Indeed, if one keeps the even and odd-channel scattering potentials V_e and V_o the same in the two-impurity problem, one also gets no net additional phase shifts. However, if $V_e \neq V_o$, then the phase transition is washed out. That is, $V_e - V_o$ is a relevant operator, and the magnitude of $|V_e - V_o|$ determines the smoothness of the phase shifts as a function of the ratio of RKKY coupling to Kondo temperature.

Some of the above features can also be predicted with an analytic $1/N$ mean-field approach, and we discuss the pros and cons of this method.

2. The model

The two-site Kondo problem describes the interactions of two spin-$\frac{1}{2}$ local moments in a

0921-4526/91/$03.50

Fermi sea,

$$H = \int d^3k\, \varepsilon_k a^\dagger_{k\mu} a_{k\mu} + J[s_c(-\tfrac{1}{2}R)\cdot S_1 + s_c(\tfrac{1}{2}R)\cdot S_2] \quad (1)$$

Here S_1 and S_2 are the two local moment spins and s_c is the conduction electron spin at that site. Coupling J is taken to be positive. Note that there is no explicit RKKY term added – all inter-spin interactions are via polarization of the conduction electron sea.

This Hamiltonian introduces two (bare) temperature scales: (i) the single-impurity Kondo temperature $T_K \propto \sqrt{\rho J}\exp(-1/\rho J)$; and (ii) the RKKY coupling $I_o \propto (\rho J)^2 f(R)$, where $f(R)$ oscillates with period $1/2k_f$ and envelope $\propto 1/R^3$ for large R. The latter description is a perturbative result good only for small ρJ. Restated in this context, the questions raised in the introduction are: how do T_K and I_o scale as the temperature is lowered? Does the Kondo effect occur? Are the local spins correlated?

Hamiltonian (1) conserves total spin, charge, and because of reflection symmetry, parity. Two sites imply two scattering channels, even and odd. We can hence define even and odd phase shifts δ_e and δ_o. We associate $\delta = \frac{1}{2}\pi$ with the 'Kondo' phase (characterized by a resonance at the Fermi level, strong spin scattering, etc.). Likewise the opposite extreme $\delta = 0$ can be considered an 'RKKY' phase for which there is no scattering.

3. Particle–hole symmetric case, numerical renormalization group solution

In order to explore the questions posed at the end of the previous section, we have examined Hamiltonian (1) with Wilson's method of numerical renormalization group (NRG). The advantage of this method is that one can successively calculate properties at exponentially smaller energy scales. The existence of stable fixed points means that we can obtain properties at $T = 0$ exactly.

Symmetrizing the conduction band and the energy dependence of the interactions produces a particle–hole symmetric model with which we start. The details of this section have been described elsewhere [1–3], and here we review the results.

We find three regimes of behavior, depending on the ratio of energy scales I_o/T_K (ratio of RKKY interaction at initial J and fixed R to Kondo temperature).

(i) $-2.2\ldots < I_o/T_K < +\infty$(FM), the ground state is that of a correlated Kondo effect, $\delta_e = \delta_o = \frac{1}{2}\pi$, ('Kondo');

(ii) $-\infty$(AFM) $< I_o/T_K < -2.2\ldots$, no Kondo effect occurs. The ground state is an uncompensated singlet with strong spin interactions ('RKKY') $\delta_e = 0 = \delta_o$. Both regimes (i) and (ii) above represent a Fermi-liquid ground state. In between the two, however, at $I_o/T_K \approx -2.2$, there occurs a third regime:

(iii) $I_o/T_K \approx -2.2$, an unstable fixed point of complex nature. This state is not a Fermi liquid, and represents a state with long-range antiferromagnetic correlations.

In fig. 1 we reprint from ref. [2] the thermodynamic properties of the system. We see that at the unstable point, the linear coefficient of specific heat $\gamma = C/T$ diverges as does the staggered susceptibility χ_s, indicating second-order critical behavior. The divergence goes as roughly $[I_o/T_K - (I_o/T_K)_c]^{-2}$, with $(I_o/T_K)_c \approx -2.2$. The uniform susceptibility remains finite with a possible discontinuity. Since the zero base line indicates properties of the pure free-electron gas, we can understand why γ, χ, and χ_s tend toward zero for large antiferromagnetic I_o: the local moments are locking into a singlet, and the system acts as if the local moments were not present. What is intriguing is that the system does not evolve smoothly from this free-electron state for large antiferromagnetic I_o to a pair of independent Kondo effects at $I_o = 0$, but rather displays critical behavior in between.

Likewise the phase shifts for the two scattering channels (δ_e, δ_o) are either exactly $(\frac{1}{2}\pi, \frac{1}{2}\pi)$ or $(0, 0)$, with finite discontinuity as a function of I_o/T_K at the critical point. That is, the ground states are either completely Kondo or no Kondo

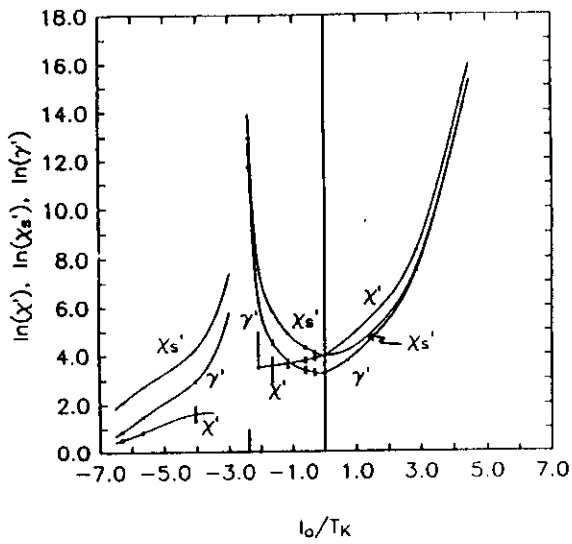

Fig. 1. Thermodynamic properties of the particle–hole symmetric model from NRG: uniform susceptibility χ, staggered susceptibility χ_s, and linear coefficient of specific heat $\gamma = C/T$. (Primes denote scaling by dimensioned constants so logs can be taken.) Plots are as a function of RKKY interaction divided by single-impurity Kondo temperature. Reprinted from ref. [2].

effect at all. It appears that one ingredient of the critical behavior observed may be the existence of this discontinuity.

In fact, one can argue [4] that as long as one can define a Fermi liquid, a model with parity-preserving particle–hole symmetry (i.e., even parity particles can be exchanged with even-parity holes, and same for odd) must have phase shifts of 0 or $\frac{1}{2}\pi$ (mod π) in each channel. Reference [3] gives another argument leading to the same result. A discontinuity and hence (possible) critical behavior thus seems almost predicated for the particle–hole symmetric case. The question is then what occurs when this symmetry is broken, which we discuss in the next section.

4. Potential scattering: breaking particle–hole symmetry (NRG study)

In order to generalize the model of the previous section, we add potential scattering terms in each parity channel to the symmetric Hamiltonian:

$$\Delta H = V_e \int\int d^3k\, d^3k'\, a^\dagger_{ek\mu} a_{ek'\mu} + V_o \int\int d^3k\, d^3k'\, a^\dagger_{ok\mu} a_{ok'\mu} . \quad (2)$$

The magnitude of V_e and V_o gives a measure of the (particle–hole) symmetry breaking.

In fig. 2 we show the phase shift as a function of (antiferromagnetic) I_o/T_K for the most extreme case, $V_e = -V_o = -V$. (One would expect this to be the most 'extreme' case for the following reason: one can represent the $V = 0$ result of equal even- and odd-parity phase shifts as resonances both centered at the Fermi level. A finite V would tend to move the resonances away from the Fermi level, and V's of opposite sign would move the resonances in opposite directions, away from each other.) For this case $\delta_e = -\delta_o$, and we only show δ_e. Since even otherwise free conduction electrons ($J = 0$) with added potential scattering develop a phase shift, in fig. 2 we have subtracted off this (trivial) phase shift to show the effects of finite J. We also show the case of $V = 0$ for comparison.

We see that for even small values (0.01 of bandwidth) of V, the discontinuity in δ is smoothed out, except for possibly a slope discontinuity at the single point $(I_o/T_K)_c$. For larger $V = 0.10$, all discontinuities are washed out al-

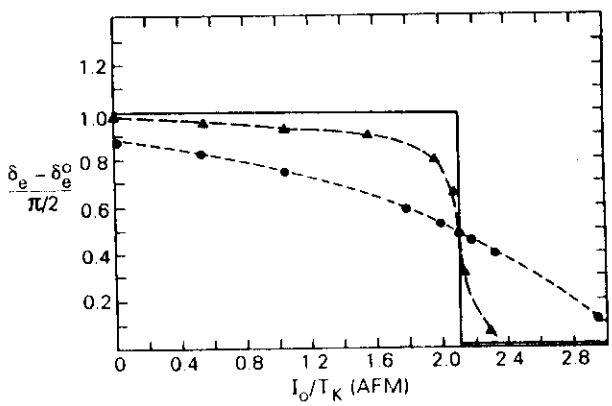

Fig. 2. Even parity phase shift as a function of RKKY to Kondo temperature for $V_e = -V_o = -V$; $V = 0$ (solid line), 0.01 (triangles), and 0.10 (dots).

together and we see a smooth evolution from δ nearly $\frac{1}{2}\pi$ at $I_o/T_K = 0$ to δ near 0 at I_o/T_K large.

We have also calculated the linear coefficient of specific heat (preliminary results) for this same range of antiferromagnetic I_o/T_K. Even with large error bars, it seems clear that the divergence seen for the particle–hole symmetric case turns into a peak for $V \neq 0$. By $V = 0.1$, the peak is hardly visible and the curve is almost monotonically decreasing. The smaller V, the sharper the maximum; work in progress is studying the crossover exponents. Thus it appears that any finite V of opposite sign in even and odd channels washes out the critical behavior to a greater or lesser degree. In fig. 3 we illustrate the general behavior with phase diagrams showing the low-temperature fixed points for two Kondo impurities. The arrows indicate the flow as temperature is lowered. Figure 3a shows the particle–hole symmetric case, $V = 0$, for which there

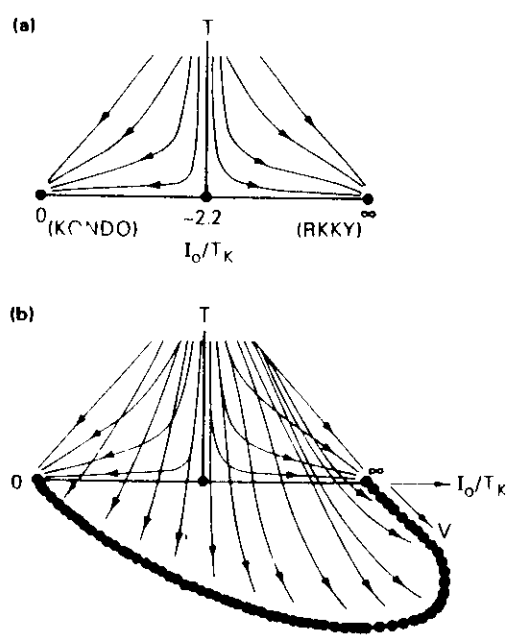

Fig. 3. Flow diagrams showing fixed points as temperature is lowered (direction of arrows). (a) Particle–hole symmetric case, $V = 0$. At low temperatures states flow to either 'Kondo' or 'RKKY' fixed points, depending on initial I_o/T_K. At antiferromagnetic $I_o \approx 2.2T_K$, there is an unstable fixed point. (b) Case of $V_e = -V_o$. There is a whole line of stable ground states, one for every V. 'Kondo' fixed point can be seen as 'RKKY' + ($V = \infty$).

are three low-temperature fixed points (two stable and one unstable). The Kondo state represents I_o/T_K scaling to zero, while the RKKY state can be thought of as I_o/T_K scaling to infinity.

Adding potential scattering V adds a third axis to these flow diagrams, see fig. 3b. With an extra dimension, the pure Kondo fixed point ($\delta = \frac{1}{2}\pi$) can be seen as the RKKY state ($\delta = 0$) plus an infinite potential scattering V. (Adding an infinite potential scattering to a set of free electrons results in a Fermi liquid with $\delta = \frac{1}{2}\pi$.) There is now a whole line of fixed points, one for every value of V, representing a continuum of possible ground states with δ from 0 to $\frac{1}{2}\pi$. The critical point only appears on the $V = 0$ plane.

5. Large degeneracy-N expansion

For comparison with the finite potential scattering results, we now discuss an analytic approach to the two-impurity Kondo problem, the results of a $1/N$ 'slave bosom' expansion [5]. The advantages of this method are: (i) it gives quantitatively correct answers for the single-impurity Kondo problem; (ii) it is non-numerical, i.e., analytic, and (iii) it provides a 'straightforward' extension to the lattice.

The model Hamiltonian is that of the $U = \infty$ Anderson model,

$$H = \sum_{km} \epsilon_k c^+_{km} c_{km} + \sum_{\substack{\alpha=1,2 \\ m}} E_0 f^+_{\alpha m} f_{\alpha m} + \frac{V}{\sqrt{N}} \sum_{\substack{\alpha=1,2 \\ m}} e^{ik\cdot r_\alpha} b^+_\alpha c^+_{km} f_{\alpha m} + \text{H.c.} + \frac{I}{N} \sum_{mm'} f^+_{1m} f_{2m} f^+_{2m'} f_{1m'} . \quad (3)$$

Here α is a site index and m takes on the values $-N, -N+1, \ldots, N-1, N$. The auxiliary boson constraint is imposed by $n_{f\alpha} + n_{b\alpha} = \frac{1}{2}N$. In the Kondo limit we take $n_{\beta\alpha} \ll N$ and $\epsilon_f \ll \rho V^2$. I is taken to be purely antiferromagnetic.

One aspect of this model to note is the explicitly added RKKY term I. This term is neces-

sary because without it, RKKY does not enter in until order $1/N^2$, a higher order than normally calculated. (Thus most previous $1/N$ studies of multiple impurities have been for the case of basically independent Kondo effects.) One might question whether the physics of two directly coupled moments is the same as of two moments indirectly coupled by intervening conduction electron spin polarization as in the previous sections. We have performed numerical (NRG) studies of a model of independent Kondo impurities with an added direct $S_1 \cdot S_2$ exchange, and found in fact that the results of the previous sections are entirely unchanged, actually a remarkable result, so that this added I term does not represent a crucial approximation.

In the Kondo limit, our Hamiltonian is then the large-N version of eq. (1) with an added $IS_1 \cdot S_2$ term. The method used is the usual one [6]: we write the model as a functional integral, with Lagrange multipliers (ε_f) to enforce the constraint that the number of f electrons per site be less than $\frac{1}{2}N$. The RKKY interaction can then be decoupled via a Hubbard–Stratonovich transformation, yielding another variable R. One integrates out the conduction and f electrons, and makes a mean-field approximation for R, ε_f, and the slave bosons b_i. The result is a free energy per spin, which is minimized with respect to the variables above to find the ground states.

We find the results depend on impurity separation and band structure via two parameters A and B, defined by

$$\pi\rho(iA\,\mathrm{sgn}(\omega_n) + B) \equiv \sum_k \frac{e^{ik\cdot R}}{-i\omega_n + \varepsilon_k} . \qquad (4)$$

In the limit of large R, $A \sim (\sin k_F R)/k_F R$ and $B \sim (\cos k_F R)/k_F R$. Parameter A just renormalizes the Kondo temperature $T_K \to T_K^*$. B, however, gives the splitting of the Kondo resonances and is related to the difference in phase shifts δ. In this formulation band non-symmetries are parameterized by the single variable B.

We now discuss the mean-field ($N \to \infty$) results. We find that there are two possible global minima, depending on the ratio I/T_K^*: one in which the Kondo effect occurs for $I/T_K^* < (I/T_K^*)_c$, and one in which it does not (and RKKY dominates), for $I/T_K^* > (I/T_K^*)_c$. We show a phase diagram in fig. 4a. As shown, these results depend strongly on B: the transition is first order for B small (and zero, the particle–hole symmetric case), and becomes second order for large enough B. Figure 4b shows the phase shifts for two characteristic values of B. The phase shifts are not $(\frac{1}{2}\pi, \frac{1}{2}\pi)$ unless $B = 0$.

The linear coefficient of specific heat is just proportional to δ_c, and ih fig. 4c we show the staggered susceptibility as a function of I/T_K^* for the same two characteristic values of B. The results summarized in fig. 4 suggest that B affects the character of the transition, and raises the question of whether B is relevant, in the renormalization group sense. In the next section we discuss this question and the above $1/N$

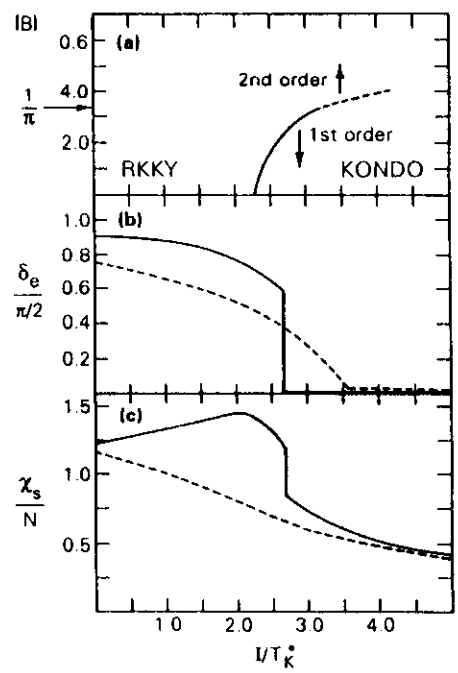

Fig. 4. Mean-field ($1/N$) results: (a) phase diagram, showing first-order (solid line) and second-order (dashed line) transitions between RKKY and Kondo fixed points for varying amounts of particle–hole asymmetry B; (b) plot of even-parity phase shift versus I/T_K^* for two representative values of B, $B = 0.1$ (first order, solid line) and $B = 0.4$ (second-order, dashed line); (c) staggered susceptibility for above two values of B, in units of $3\pi T_K^*$.

solution in the context of the NRG results of the previous sections.

6. Remaining ambiguities

There are still a number of questions that are raised by the NRG and $1/N$ solutions to the two-impurity problem. We discuss the NRG solution for the particle–hole symmetric case first.

One major area of uncertainty is the nature of the long-range correlations that develop in the unstable intermediate state. These correlations are certainly antiferromagnetic, but the precise nature of the ordering needs to be determined. As noted below, even if the critical point is washed out by potential scattering, there will be associated crossover exponents, and aspects of the unstable state could remain even reasonably far from the critical point.

Comparison work of note are the Monte Carlo studies of Fye, Hirsch and Scalapino on Anderson and Kondo two-impurity systems [7]. Even for the particle–hole symmetric case, they do not find evidence of critical behavior. There is qualitative agreement with NRG in some other respects, such as the growth of spin–spin correlations as the temperature is lowered. The correlations saturate at T_K, however. Probable resolutions of the disagreement with NRG results are that the Monte Carlo does not reach low enough temperatures. (The critical behavior occurs well below T_K.) Also, Fye and coworkers do not calculate the specific heat coefficient γ, only the staggered susceptibility χ_s, and for χ_s they use a different definition, one which may represent a quantity which does not diverge at criticality.

We now discuss the $1/N$ mean-field results of the previous section. The $1/N$ procedure does indeed find two stable ground states, one each of Kondo and RKKY character, in agreement with the NRG. However, the order of the transition for $B=0$, particle–hole symmetry, is wrong: first, rather than second order. The probable resolution of this disagreement is that fluctuations, if included properly, could wipe out the second-order (large-B part), and turn the first-order (small-B) regime to second order. Since a line of second-order points is unlikely. B_c (marking the end of the original first-order regime) probably also scales to zero (see fig. 5). An alternative explanation is that instanton effects (tunneling between the two minima) could kill the transition, and work is in progress on this idea.

Secondary problems with $1/N$ are that the Wilson ratio is always one, indicating that correlation effects are not being correctly included (a result that could change with the inclusion of fluctuations). Since the Wilson ratio involves thermodynamic quantities, this also raises the question of how they might change if the correct ratio were to be achived.

7. Extension to the lattice

There are several implications for the lattice that can be derived from the NRG results. The first is that, at least for two impurities, adding an explicit RKKY term to the model by hand gives qualitatively the *same* results as a model with an indirectly generated RKKY interaction. Hencc lattice models with explicit RKKY terms are probably fine, except that one has to be careful that the magnitude put in by hand has some physical basis.

When potential scattering is present, the splitting of the resonances could be a mechanism for the formation of a strongly correlated narrow band, with the distance between the resonances the width of the band. The results of the previous sections also provide a solution to problems posed by the Anderson compensation theorem (or Nozières exhaustion principle), namely the

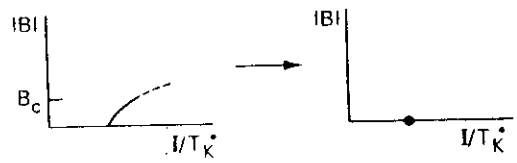

Fig. 5. Plausible effects of fluctuations to mean-field $1/N$ solution for phase diagram (fig. 4a) needed to make it consistent with symmetric NRG results. Single point at $B=0$ in 'final' diagram is second order.

lack of enough electrons within T_K of the Fermi level to compensate all the spins of the lattice. The result is that the spins compensate each other to some extent. The $1/N$ mean-field calculation for two impurities shows that the degree of inter-spin compensation can be arbitrary. (This fact was also pointed out by Millis [8] for the large-N solution to the lattice.)

The NRG, an exact technique, can of course not be used as a complete lattice solution since even two impurities use up most of the memory of current supercomputers. One is thus led to consider approximate methods. The success of the $1/N$ expansion for a single impurity makes it an obvious candidate for the lattice, with the RKKY terms put in by hand. However, the two-impurity $1/N$ results raise a problematic question: if one has to do so much 'interpretation' (cf. fig. 5) of the $1/N$ results to obtain the correct solution for just two impurities, what hope has one of getting transitions in the lattice right? New techniques are perhaps indicated here, as indeed discussed by several of the participants in the conference (e.g., Coleman [9], etc.).

In general, certainly any method for the lattice must include RKKY correlations. New methods should be checked to give *both* the correct two- and as well as one-impurity results.

8. Conclusions

We have shown that low-temperature spin–spin correlations are present between two Kondo impurities in a Fermi sea, even when the impurities are compensated by the Kondo effect, unless initial RKKY is identically zero. The local moments do not lock into a singlet or triplet unless the RKKY is infinite. Compensation of the moments is collective, through parity channels, rather than of individual moments. The ground state in all cases is a singlet Fermi liquid.

In the particle–hole symmetric case, a critical point occurs between two stable ground states, one in which the Kondo effect occurs and one dominated by RKKY. Potential scattering of opposite sign in even and odd parity channels washes out the critical point. However, depending on the crossover exponents, remnants of the critical behavior could persist to quite high values of asymmetry. (The divergence in γ and χ_s changes to a peak.)

Of interest is to what extent pair correlation effects appear in real materials. For example, most heavy fermions display a strong magnetic instability (for magnetic correlations see, e.g., [10]), to pressure or to doping, say. The decreased Wilson ratio, and enhanced linear specific heat and susceptibility all raise the intriguing possibility that heavy fermions are those materials with an RKKY to Kondo temperature ratio which is close to the critical value. Determination of the crossover exponents associated with potential scattering is still needed in order to say how realistic this picture is.

Finally, extension of these results to the lattice via a $1/N$, or any other, expansion needs to be done with care. Transitions thus obtained may be of the wrong order or in fact entirely spurious. The $1/N$ technique applied to two impurities does get essential physics correct, however: it finds two ground states of the right type, separated by a transition which is strongly affected by the amount of particle–hole symmetry. In that sense it does represent a solution to the problem, and may be an indication of its usefulness for the lattice. It is probable that getting a full picture of the lattice will involve input from several different techniques, including the pair correlation effects described here.

Acknowledgements

The author wishes to thank collaborators C.M. Varma, A.J. Millis and G. Kotliar for particularly helpful discussions.

References

[1] B.A. Jones and C.M. Varma, Phys. Rev. Lett. 58 (1987) 843;
B.A. Jones, in: Field Theoretic Methods in Condensed

Matter Physics, Zlatko Tesanovic, ed. (Addison-Wesley, Redwood City, 1990) p. 87.
[2] B.A. Jones, C.M. Varma and J.W. Wilkins, Phys. Rev. Lett. 61 (1988) 125.
[3] B.A. Jones and C.M. Varma, Phys. Rev. B 40 (1989) 324.
[4] A.J. Millis, B.G. Kotliar and B.A. Jones, in: Field Theoretic Methods in Condensed Matter Physics, Zlatko Tesanovic, ed. (Addison-Wesley, Redwood City, 1990) p. 159.
[5] B.A. Jones, B.G. Kotliar and A.J. Millis, Phys. Rev. B 39 (1989) 3415.
[6] P. Coleman, Phys. Rev. B 35 (1987) 5072;
D.M. Newns and N. Read, Adv. Phys. 39 (1987) 799.
[7] J.E. Hirsch and R.M. Fye, Phys. Rev. Lett. 56 (1986) 2521;
R.M. Fye, J.E. Hirsch and D.J. Scalapino, Phys. Rev. B 35 (1987) 4901,
R.M. Fye and J.E. Hirsch, Phys. Rev. B 40 (1989) 4780.
[8] A.J. Millis and P.A. Lee, Phys. Rev. B 35 (1987) 3394.
[9] P. Coleman, these proceedings.
[10] S.M. Shapiro, C. Stassis and G. Aeppli, Phys. Rev. Lett. 62 (1989) 94;
also contributions by Aeppli and others at this conference.

Study of the Two-Impurity, Two-Channel Kondo Hamiltonian

Kevin Ingersent,[1],[a] Barbara A. Jones,[2] and John W. Wilkins[1]
[1]*Department of Physics, The Ohio State University, Columbus, Ohio 43210*
[2]*IBM Research Division, Almaden Research Center, 650 Harry Road, San Jose, California 95120*
(Received 3 August 1992)

The two-channel Kondo Hamiltonian has recently been proposed as a description of several experimental systems. Our numerical renormalization-group treatment of a pair of magnetic impurities shows that at low temperatures, interimpurity interactions destabilize the "marginal-Fermi-liquid" behavior predicted by a single-impurity model. We find four stable zero-temperature regimes, three of which can be described by Fermi-liquid theory. The fourth possesses a complex many-body ground state and non-Fermi-liquid properties which are expected to be governed by nonuniversal critical exponents.

PACS numbers: 75.20.Hr, 75.30.Hx, 75.30.Mb

The single-impurity, two-channel Kondo Hamiltonian describes the exchange interaction between a localized spin-$\frac{1}{2}$ moment and *two* degenerate channels (or bands) of conduction electrons. This Hamiltonian is notable for possessing a nontrivial critical point at temperature $T=0$ which is responsible for non-Fermi-liquid behavior at low temperatures [1], including such remarkable properties [2–5] as (i) a specific-heat coefficient C/T and a static susceptibility which diverge logarithmically as $T\to 0$, (ii) a residual entropy of $\frac{1}{2}\ln 2$ per impurity, (iii) a dynamical susceptibility of the form proposed as the basis for "marginal-Fermi-liquid" phenomenology [6], and (iv) a spin-spin correlation length diverging as $1/T$.

Considerable attention has recently been focused on possible experimental realizations of two-channel Kondo behavior. It has been proposed that certain uranium-based heavy-fermion materials [3,5], the cuprate superconductors [5,7] and electron-assisted tunneling in metallic glasses [8] can in various ways be mapped onto the two-channel Kondo Hamiltonian. Experiments on the heavy-fermion system $Y_{1-x}U_xPd_3$ (for $0.1\lesssim x\lesssim 0.2$) find impurity contributions to the specific heat, the residual entropy, and the resistivity of the appropriate form [9,10], although the response of the specific heat to an applied magnetic field has been argued to be inconsistent with a purely single-impurity description [10]. Resistivity measurements on $Pb_{1-x}Ge_xTe$ [11], on heavily doped polyacetylene and polypyrrole [12], and on structurally disordered metallic nanorestrictions [13], provide evidence for two-channel Kondo behavior arising from electron-assisted tunneling.

This paper reports the first theoretical study of interimpurity interactions in a two-channel Kondo system. The $1/T$ divergence of the single-impurity spin correlation length [4,5] hints at the importance of such interactions at low temperatures. Here we consider just two impurities, the simplest model featuring competition between ordering of the impurities via the Ruderman-Kittel-Kasuya-Yosida (RKKY) interaction and formation of a critical state around each impurity through the two-channel Kondo effect. Our numerical renormalization-group (NRG) calculations indicate that the RKKY coupling destabilizes the single-impurity critical state and radically alters the low-energy physics. Three zero-temperature regimes exhibit Fermi-liquid behavior; a fourth is unlike any previously discovered in a Kondo system: We expect many of its properties to be described by nonuniversal critical exponents which depend on such parameters as the RKKY coupling strength and the shape of the conduction-band density of states.

Our formulation of the problem extends the treatment of the two-impurity, *one-channel* Kondo model by Jones *et al.* [14]. The interaction term in the Hamiltonian is

$$H_{\rm int}=J\{\mathbf{S}_l\cdot[\mathbf{s}_1(\mathbf{r}_l)+\mathbf{s}_2(\mathbf{r}_l)]+\mathbf{S}_r\cdot[\mathbf{s}_1(\mathbf{r}_r)+\mathbf{s}_2(\mathbf{r}_r)]\}\,, \quad (1)$$

where $\mathbf{S}_l$ and $\mathbf{S}_r$ are the "left" and "right" spin-$\frac{1}{2}$ impurity moments, residing at positions $\mathbf{r}_l$ and $\mathbf{r}_r$, respectively, and $\mathbf{s}_c(\mathbf{r})$ (for $c=1,2$) is the spin of the channel-c conduction electrons at position $\mathbf{r}$. The two conduction bands are assumed to have identical attributes, their electrons distinguished solely by the channel index c. The coupling J is positive in all cases of interest.

For simplicity, we take the conduction bands to be isotropic in momentum space, and to be symmetric in energy space about the Fermi level with a width $2D$. Real-space symmetries of $H_{\rm int}$ allow the impurities to couple to just four conduction states at each energy ε—states created by operators $a^\dagger_{\alpha cp\mu}$, where $\mu=\pm\frac{1}{2}$ is the spin and $p=e,o$ is the spatial parity under reflection in the plane midway between the impurities. Then Eq. (1) becomes

$$H_{\rm int}=\int d\varepsilon\int d\varepsilon'\sum_c\{(\mathbf{S}_l+\mathbf{S}_r)\cdot[\Gamma_e a^\dagger_{\alpha ce\mu}\boldsymbol{\sigma}_{\mu\mu'}a_{\varepsilon' ce\mu'}+\Gamma_o a^\dagger_{\alpha co\mu}\boldsymbol{\sigma}_{\mu\mu'}a_{\varepsilon' co\mu'}]+(\mathbf{S}_l-\mathbf{S}_r)\cdot[\Gamma_m a^\dagger_{\alpha ce\mu}\boldsymbol{\sigma}_{\mu\mu'}a_{\varepsilon' co\mu'}+\text{H.c.}]\}\,, \quad (2)$$

where $\Gamma_{e,o,m}=g_{+,-,+}(\varepsilon)g_{+,-,-}(\varepsilon')$, with $g^{\gamma}_{\pm}(\varepsilon)=(J/4)\rho(\varepsilon)[1\pm\sin k_\varepsilon R/k_\varepsilon R]$. Here $R\equiv|\mathbf{r}_l-\mathbf{r}_r|$ is the separation between the impurities, k_ε describes the electron dispersion, and $\rho(\varepsilon)$ is the conduction-band density of states.

Two energy scales emerge from Eq. (2): the single-impurity, two-channel Kondo temperature [15], $T_K \approx D\Gamma\exp(-1/\Gamma)$, where $\Gamma \equiv J\rho(0)$, and the RKKY coupling—the coefficient of the effective term $I(R)\mathbf{S}_I\cdot\mathbf{S}_r$ arising in $H_{\rm int}$ due to exchange of virtual electrons between the impurities.

We follow Ref. [14] in averaging Γ_e, Γ_o, and Γ_m over ε and ε' in such a way that the couplings are functions of R only. In the limit $\Gamma \ll 1$, these three couplings can be reexpressed in terms of a more intuitive set of dimensionless parameters, Γ, I/T_K, and $(\Gamma_e-\Gamma_o)/(\Gamma_e+\Gamma_o)$ which, respectively, measure the electron-impurity exchange coupling, the relative energy scales for interimpurity and intraimpurity effects, and the asymmetry between the coupling of even- and odd-parity conduction states to the net impurity spin.

Thus simplified, Eq. (2) can be solved via Wilson's NRG method [14,16], which allows one to follow the renormalization of the "bare" parameters Γ, I/T_K, and $(\Gamma_e-\Gamma_o)/(\Gamma_e+\Gamma_o)$ via many-body interactions as the temperature is reduced. The renormalized parameters eventually flow to a fixed point which describes the zero-temperature properties of the system.

Our calculations reveal a rich variety of behaviors, which are summarized in the phase diagram shown in Fig. 1. Table I lists the locations and properties of the NRG fixed points.

There are four types of *stable* fixed points, each with a spin-singlet ground state, and each determining the low-temperature behavior within a region of parameter space delineated by thick lines in Fig. 1 [17].

(a) Even-parity Kondo.—For $\Gamma_e > \Gamma_o$, and ferromagnetic or sufficiently weak antiferromagnetic RKKY interactions (i.e., bare parameters lying above, and to the right of all thick lines in Fig. 1), the impurity spins are completely quenched by condition electrons of the more strongly coupled parity. As the temperature is lowered, Γ_e diverges while the quantities Γ_o and I/T_K renormalize to zero. One even-parity electron from each channel effectively binds to the impurities to form a spin singlet. The remaining even-parity electrons form a Fermi liquid with a $\pi/2$ phase shift due to strong scattering from the impurities, whereas the odd-parity conduction states decouple and undergo no phase shift. Although the screening at each impurity site is reminiscent of one-channel Kondo behavior, the two Kondo effects are not independent; there are correlations between the impurity spins in the ground state unless the bare RKKY coupling is identically zero [18].

(b) Odd-parity Kondo.—Since the Hamiltonian (2) is invariant under exchange of parity labels, $e \leftrightarrow o$, the

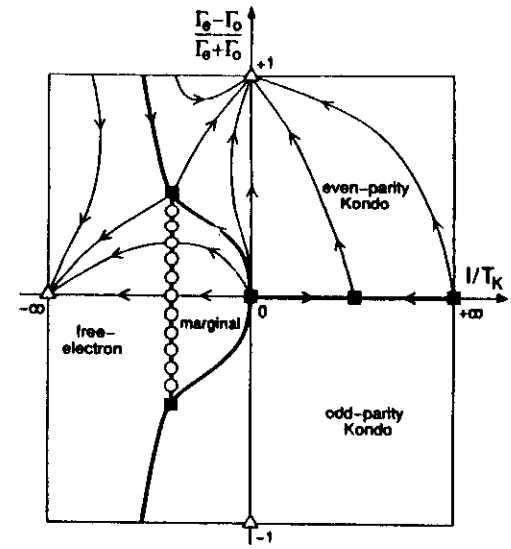

FIG. 1. Schematic renormalization-group (RG) phase diagram for the two-impurity, two-channel Kondo Hamiltonian, parametrized by I/T_K, the ratio of the interimpurity coupling to the single-impurity Kondo temperature, and $(\Gamma_e-\Gamma_o)/(\Gamma_e+\Gamma_o)$, the fractional difference between the coupling of the total impurity spin to even- and odd-parity conduction states [17]. Thin curves represent RG flows (drawn only in the upper half plane—the flows are mirror symmetric about the horizontal axis). Triangles, squares, and circles denote stable, unstable, and marginal fixed points, respectively. Thick lines demarcate four distinct regimes of low-temperature behavior. A continuous line of fixed points separates the marginal and free-electron regimes.

TABLE I. Renormalization-group fixed points of the two-impurity, two-channel Kondo Hamiltonian; see also Fig. 1. At fixed points exhibiting Fermi-liquid (FL) behavior, even- and odd-parity conduction states are scattered with phase shifts δ_e and δ_o, respectively. (Note that these shifts are independent of the channel index.)

Fixed point	I/T_K	$(\Gamma_e-\Gamma_o)/(\Gamma_e+\Gamma_o)$	Stability	Physical behavior
(a) Even-parity Kondo	0	+1	Stable	FL ($\delta_e=\pi/2,\delta_o=0$)
(b) Odd-parity Kondo	0	−1	Stable	FL ($\delta_e=0,\delta_o=\pi/2$)
(c) Free electron	$-\infty$	0	Stable	FL ($\delta_e=\delta_o=0$)
(d) Marginal line	$O(-1)$	~ -0.5 to $+0.5$	Marginal	Critical (nonuniversal)
(e) Even, odd antiferromagnetic	$O(-1)$	$\sim \pm 0.5$	Unstable	Critical
(f) Single impurity	0	0	Unstable	Critical
(g) Strong ferromagnetic	$+\infty$	0	Unstable	Critical
(h) Intermediate ferromagnetic	$O(+1)$	0	Unstable	Critical

NRG flows are mirror symmetric about the horizontal axis of Fig. 1. At the odd-parity Kondo fixed point, the counterpart of (a) for $\Gamma_o > \Gamma_e$, only odd-parity electrons quench the impurities.

(c) Free electron.—For strong antiferromagnetic RKKY interactions (i.e., bare parameters lying to the left of all thick lines in Fig. 1, or $I/T_K \lesssim -1$), there is no Kondo effect. The low-energy electrons completely decouple from the impurities; both even- and odd-parity electrons form Fermi liquids with zero phase shifts. Higher-energy electrons still play an important role in the formation of the spin-singlet ground state [18].

(d) Marginal.—The three preceding regions surround a fourth, characterized by weak antiferromagnetic RKKY couplings, within which the renormalized parameters flow towards a continuous line of fixed points which are only marginally stable (being stable to the right of the thick vertical line in Fig. 1, but unstable to the left). Each marginal fixed point exhibits a different non-Fermi-liquid spectrum: Certain energy splittings vary smoothly along the line, passing through zero precisely at $\Gamma_e = \Gamma_o$. As a consequence, we expect many of the low-temperature physical properties to be nonuniversal, governed by critical exponents that vary continuously with the bare parameters.

The bare parameters which select between the above regimes depend on the impurity separation R and the density of states $\rho(\varepsilon)$. For flat conduction bands, the bare parameters vary with increasing R in such a way that the low-temperature regime repeatedly cycles through the sequence: even-parity Kondo, marginal, odd-parity Kondo, marginal. For sufficiently small Γ, the bare parameters may also pass through the free-electron region. Thus, in principle, the regimes (a)–(d) are all accessible.

There are also five *unstable* fixed points in the problem, which in general affect the behavior only at high temperatures. Starting from the leftmost solid squares in Fig. 1, they are as follows:

(e) Even and odd antiferromagnetic.—At each end of the marginal line is an unstable fixed point, beyond which the energy splittings diverge and the NRG flows head towards either the Kondo or the free-electron fixed point.

(f) Single impurity.—A fixed point at $I/T_K = 0$ and $\Gamma_e = \Gamma_o$ corresponds to the limit of infinite separation between the impurities. The ground state, a product of single-impurity critical states, contains spin-singlet and -triplet components with equal weight. *A principal result of this work is the instability of this "single-impurity" fixed point with respect to any nonzero RKKY coupling or any difference between the coupling of the net impurity spin to even- and odd-parity conduction states.* For bare parameters lying close to the fixed point, a single-impurity approximation may be valid down to low energies. However, there must eventually be a crossover at some finite temperature to one of the stable regimes (a), (b), or (d).

(g) Strong ferromagnetic.—There exists a novel fixed point that can be reached only by starting with $\Gamma_e = \Gamma_o$ and $I = I_{\max}(\Gamma)$, where $I_{\max}(\Gamma)$ is the strongest possible ferromagnetic RKKY coupling that can be generated from Eq. (2), obtained by setting $\Gamma_m = 0$ [14]. We conjecture that this fixed point, which has a spin-triplet ground state and a non-Fermi-liquid excitation spectrum, is equivalent to the nontrivial fixed point of *four* channels of conduction electrons interacting equally with a *single, spin-one* impurity.

(h) Intermediate ferromagnetic.—For $\Gamma_e = \Gamma_o$ and $0 < I < I_{\max}(\Gamma)$ [see (g)], the NRG flows are towards another novel fixed point, which also possesses a spin-triplet ground state and a non-Fermi-liquid excitation spectrum. The slightest difference between Γ_e and Γ_o drives the NRG flows off to one or another of the Kondo fixed points. However, this intermediate fixed point would be stable if some additional symmetry were to maintain equality between the even- and odd-parity couplings. None of the realizations of the two-channel Kondo Hamiltonian proposed to date exhibits such a symmetry.

It is instructive to compare the above results with those from the NRG treatment of the two-impurity, *one-channel* Kondo model [14], most of which have recently been confirmed using conformal field theory [19]. Although Kondo and free-electron regimes figure prominently in both the one- and two-channel problems, there are significant differences between the two cases.

(i) In the one-channel model, any asymmetry between the even- and odd-parity couplings always renormalizes to zero, so $(\Gamma_e - \Gamma_o)/(\Gamma_e + \Gamma_o)$ is an irrelevant parameter.

(ii) In the one-channel case, weak RKKY interactions produce only small perturbations around the single-impurity behavior. In the two-channel case, by contrast, any interimpurity interaction drives one away from the single-impurity regime and radically alters the physics.

(iii) An isolated, unstable fixed point, at $I/T_K \simeq -1$ [15] and $\Gamma_e = \Gamma_o$, separates the one-channel Kondo and free-electron regimes. This non-Fermi-liquid fixed point disappears if the Hamiltonian's particle-hole symmetry is broken (by the introduction of potential scattering, for instance) [20]. We suspect that the two-channel marginal regime—which occupies a finite region of phase space, rather than a single point—is a more robust feature.

In summary, the behavior of the two-impurity, two-channel Kondo model is more complex than that of any Kondo system studied previously. We find that any interaction between the impurities, however weak, dominates the physics at sufficiently low temperatures. A novel regime of non-Fermi-liquid behavior which occurs for weak antiferromagnetic RKKY interactions is probably associated with nonuniversal critical properties.

We thank I. Affleck, D. Cox, A. Ludwig, and H. Pang for useful discussions. This work was supported in part by the U.S. DOE—Basic Energy Sciences, Division of Materials Sciences (J.W.W. and K.I.), and in part by the

National Science Foundation under Grant No. PHY89-04035 (B.A.J.). One of us (K.I.) gratefully acknowledges receipt of an IBM Postdoctoral Fellowship during the early stages of this work. Computer time was provided by the Ohio Supercomputer Center and the Cornell National Supercomputing Facility.

---

[a]Present address: Department of Physics, University of Florida, Gainesville, FL 32611.

[1] P. Nozières and A. Blandin, J. Phys. (Paris) **41**, 193 (1980); P. B. Wiegmann and A. M. Tsvelik, Pis'ma Zh. Eksp. Teor. Fiz. **38**, 489 (1983) [JETP Lett. **38**, 591 (1983)]; Z. Phys. B **54**, 201 (1984); N. Andrei and C. Destri, Phys. Rev. Lett. **52**, 364 (1984).

[2] A. M. Tsvelik, J. Phys. C **18**, 159 (1985); J. Phys. Condens. Matter **2**, 2833 (1989); P. D. Sacramento and P. Schlottmann, Phys. Lett. A **142**, 245 (1989); Phys. Rev. B **43**, 13 294 (1991).

[3] D. L. Cox, Phys. Rev. Lett. **59**, 1240 (1987); Physica (Amsterdam) **153-155C**, 1642 (1987).

[4] I. Affleck and A. W. W. Ludwig, Nucl. Phys. **B360**, 641 (1991); A. W. W. Ludwig and I. Affleck, Phys. Rev. Lett. **67**, 3160 (1991).

[5] D. L. Cox (to be published).

[6] C. M. Varma, P. B. Littlewood, S. Schmitt-Rink, E. Abrahams, and A. E. Ruckenstein, Phys. Rev. Lett. **63**, 1996 (1989).

[7] V. J. Emery and S. Kivelson (to be published).

[8] A. Zawadowski and K. Vladár, Solid State Commun. **35**, 217 (1980); A. Muramatsu and F. Guinea, Phys. Rev. Lett. **57**, 2337 (1986).

[9] C. L. Seaman *et al.*, Phys. Rev. Lett. **67**, 2882 (1991).

[10] B. Andraka and A. M. Tsvelik, Phys. Rev. Lett. **67**, 2886 (1991).

[11] S. Katayama, S. Maekawa, and H. Fukuyama, J. Phys. Soc. Jpn. **56**, 697 (1987).

[12] T. Ishiguro *et al.*, Phys. Rev. Lett. **69**, 660 (1992).

[13] D. C. Ralph and R. A. Buhrman (to be published).

[14] B. A. Jones and C. M. Varma, Phys. Rev. Lett. **58**, 843 (1987); B. A. Jones, thesis, Cornell University, 1987 (unpublished); B. A. Jones, C. M. Varma, and J. W. Wilkins, Phys. Rev. Lett. **61**, 125 (1988).

[15] The conventional (*one-channel*) Kondo temperature is defined to be $T_K \approx \Gamma^{1/2}\exp(-1/\Gamma)$.

[16] K. G. Wilson, Rev. Mod. Phys. **47**, 773 (1975).

[17] A third axis, measuring the exchange coupling Γ, has been suppressed in Fig. 1. Constant-Γ planes for Γ between 0.25 and 0.9 all show the same topology. Thus, Γ seems to be largely irrelevant in this problem.

[18] We find that, as in the one-channel case, the ground-state expectation value $\langle \mathbf{S}_I \cdot \mathbf{S}_c \rangle$ increases smoothly from $-\frac{1}{4}$ (triplet) to $+\frac{1}{4}$ (singlet) as the bare value of I/T_K increases from $-\infty$ to $+\infty$.

[19] I. Affleck and A. W. W. Ludwig, Phys. Rev. Lett. **68**, 1046 (1992).

[20] B. A. Jones, Physica (Amsterdam) **171B**, 53 (1991).

RJ 9566 (83572) October 22, 1993
Solid State Physics

Low-Temperature Physics of the Two-Impurity, Two-Channel Kondo Model

Kevin Ingersent

Department of Physics
University of Florida
215 Williamson Hall
Gainesville, FL 32611

Barbara A. Jones

IBM Research Division
Almaden Research Center
650 Harry Road
San Jose, CA 95120-6099

Abstract:
Numerical renormalization group calculations have shown that any non-zero RKKY coupling between a pair of spin-½ impurities destroys the zero-temperature critical point responsible for the marginal-Fermi-liquid behavior of the single-impurity, two-channel Kondo model. Here we report recent progress on calculating the low-temperature properties of the two-impurity model.

Introduction. The multi-channel Kondo Hamiltonian has received much recent attention as a possible description of a number of physical systems. The most intensive study has gone into a possible two-channel description [1] of certain uranium- and cerium-based compounds which exhibit anomalous (non-Fermi-liquid) behavior at low temperatures [2,3]. While some properties of these systems seem to be well-described by the two-channel Kondo model for a single impurity, several features cannot be accounted for within this framework. These include an upturn in the specific heat below 0.2K [2], the suppression of the specific heat in an applied magnetic field [3], and the linear temperature-dependence of the resistivity at temperatures T much below the Kondo temperature [2]. One factor which may contribute to these behaviors is interaction between impurities. The $1/T$ divergence in the single-impurity spin correlation length [4] hints at the importance of such interactions at low temperatures.

The simplest model that can be used to explore the competition between magnetic ordering of the impurities and the formation of a Kondo critical state around each impurity is one containing two impurities. In this paper we discuss ongoing work to understand the physical properties of this model.

The two-impurity, two-channel Kondo model is described by the Hamiltonian[2]

$$H = \sum_c \int d^3\mathbf{k}\, \epsilon_{\mathbf{k}\mu} c^\dagger_{\mathbf{k}c\mu} c_{\mathbf{k}c\mu} - J \sum_{c,i} \mathbf{s}_c(\mathbf{r}_i) \cdot \mathbf{S}_i, \tag{1}$$

where $\mathbf{S}_i$, $i = l, r$, represents the "left", "right" spin-$\frac{1}{2}$ impurity, located at position $\mathbf{r}_i$, and $\mathbf{s}_c(\mathbf{r})$, $c = 1, 2$, represents the spin of channel-c conduction electrons at position $\mathbf{r}$. We are interested in negative values of J.

Assuming the conduction bands to be isotropic, and utilizing the symmetry of the model,

[2]Summation over repeated spin indices is assumed throughout.

the Hamiltonian can be rewritten in one-dimensional form,

$$H/D = \sum_{c,p} \int d\epsilon\, \epsilon\, c^{\dagger}_{\epsilon cp\mu} c_{\epsilon cp\mu} - \sum_{c} \int d\epsilon \int d\epsilon' \left\{ \left[\Gamma_e(\epsilon,\epsilon')\, c^{\dagger}_{\epsilon ce\mu} c_{\epsilon' co\mu'} + \Gamma_o(\epsilon,\epsilon')\, c^{\dagger}_{\epsilon co\mu} c_{\epsilon' ce\mu'} \right] \times \right.$$
$$\left. \tfrac{1}{2}\sigma_{\mu\mu'} \cdot (\mathbf{S}_l + \mathbf{S}_r) + \left[\Gamma_m(\epsilon,\epsilon')\, c^{\dagger}_{\epsilon ce\mu} c_{\epsilon' co\mu'} + \Gamma_m(\epsilon',\epsilon)\, c^{\dagger}_{\epsilon co\mu} c_{\epsilon' ce\mu'} \right] \tfrac{1}{2}\sigma_{\mu\mu'} \cdot (\mathbf{S}_l - \mathbf{S}_r) \right\}, \quad (2)$$

where ϵ is the reduced energy, measured from the Fermi level in units of D, the conduction half-bandwidth, and the operators $c^{\dagger}_{\epsilon pc\mu}$, $p = e, o$, create states of even, odd parity about the mid-point between the impurities. The dimensionless couplings Γ_e, Γ_o and Γ_m depend on J/D, on the separation between the impurities, and on the conduction band density of states evaluated at the energies ϵ and ϵ'.

Solution of the Particle-Hole-Symmetric Problem. Following a previous treatment of the two-impurity, *one*-channel Kondo Hamiltonian [6], the couplings entering Eq. (2) can be averaged over their energy arguments, thereby reducing the problem to one with just three parameters, Γ_e, Γ_o and Γ_m. In this "energy-independent couplings approximation" the Hamiltonian is particle-hole symmetric.

The parameters Γ_e, Γ_o and Γ_m can be replaced by an equivalent, but more intuitive, set: (i) the Kondo temperature, T_K, the characteristic energy scale for the single-impurity Kondo effect; (ii) the RKKY coupling strength, I, the coefficient of the effective Hamiltonian $-I\mathbf{S}_l \cdot \mathbf{S}_r$ obtained by perturbatively integrating out all electronic degrees of freedom in Eq. (2); and (iii) $\alpha \equiv (\Gamma_e - \Gamma_o)/(\Gamma_e + \Gamma_o)$, the relative asymmetry between the coupling of even- and odd- parity combinations of electrons to the net impurity spin.

Ingersent, Jones and Wilkins [7] used Wilson's numerical renormalization-group (NRG) method [5] to solve the particle-hole-symmetric version of the model. Figure 1 provides a schematic phase diagram for cases where the RKKY interaction is antiferromagnetic — the situation of greatest relevance to heavy fermion compounds. The 3D parameter space has

been collapsed onto two dimensions by plotting the ratio I/T_K versus α. The NRG results can be interpreted in terms of the renormalization of I/T_K and α from their "bare" values as the temperature $T \to 0$. There are four types of stable zero-temperature ground state:

(a) *Even-parity Kondo.* For $\Gamma_e > \Gamma_o$ and weak antiferromagnetic RKKY interactions, the impurity spins are completely quenched by even-parity conduction electrons, while odd-parity electrons near the Fermi-energy are totally decoupled from the impurities (i.e., Γ_e renormalizes to infinity, Γ_o renormalizes to zero). The low-energy behavior can be described by local Fermi-liquid theory with the even[odd]-parity electrons undergoing a phase-shift $\delta_e = \pi/2$ [$\delta_o = 0$] at the Fermi surface.

(b) *Odd-parity Kondo.* A region analogous to (a) is obtained by exchanging even and odd parity labels.

(c) *Free-electron.* For large antiferromagnetic RKKY interactions, the impurity spins undergo no Kondo effect. The low-energy electrons completely decouple from the impurities, corresponding to a local Fermi liquid with phase shifts $\delta_e = \delta_o = 0$.

(d) *Marginal.* The three regions (a)–(c) surround a fourth within which the low-temperature behavior is not that of a Fermi liquid. Each set of initial conditions within the marginal region seems to flow to a distinct fixed point. The RKKY interaction and the asymmetry between the coupling of even- and odd-parity electrons to the impurities act as marginally relevant operators connecting these fixed points.

The fixed point corresponding to two completely independent impurities lies at I=0, α=0, on the border between the marginal region and the even- and odd-parity Kondo regions. Thus, there is no finite domain of stability for single-impurity behavior [8].

Low-Temperature Properties. The local deviations from any stable Fermi-liquid fixed

point can be expressed in terms of an effective Hamiltonian of the form

$$H_{eff}(T) = H_0 + \sum_i c_i \, (T/D)^{\lambda_i} \, \hat{O}_i, \tag{3}$$

where operator $\hat{O}_i$ respects all symmetries of the full Hamiltonian but breaks the higher symmetry of the fixed-point Hamiltonian H_0. The exponents λ_i are positive, i.e., all the operators $\hat{O}_i$ are irrelevant in the renormalization-group sense. At temperatures $T \ll D$, only the leading irrelevant operators — those with the smallest exponents — are physically important. The coefficients c_i vary with the bare parameters T_K, I and α.

The NRG Hamiltonian can be solved exactly at any Fermi-liquid fixed point, and expressions obtained for the eigenenergies in terms of the coefficients of the leading irrelevant operators. The c_i's can be extracted by fitting energies obtained numerically. The resulting coefficients can then be inserted into analytical (perturbative) expressions for thermodynamic quantities in the vicinity of the fixed point.

For the present problem we have identified seven leading irrelevant operators that preserve the full spin, axial-charge [6] and $Sp(4)$ [9] symmetries of the two-channel Kondo Hamiltonian. Two of these are simple operators that allow for hopping of electrons on and off the impurity sites. The remaining five operators mix channel 1 and 2 in a non-trivial way, e.g.,

$$\hat{O}_p = |\mathbf{s}_{1p} + \mathbf{s}_{2p}|^2, \qquad p = e, o, \tag{4}$$

and

$$\hat{O}_m = (\mathbf{s}_{1e} + \mathbf{s}_{2e}) \cdot (\mathbf{s}_{1o} + \mathbf{s}_{2o}), \tag{5}$$

where $\mathbf{s}_{cp}$ is the net spin of channel-c, parity-p conduction electrons localized about the impurity sites.

For the particle-hole-symmetric version of the problem, most of the coefficients c_i entering Eq. (3) diverge as the bare parameters I/T_K and α approach the borders of the marginal region. This is to be expected, since the marginal region is non-Fermi-liquid-like and hence cannot be related perturbatively to any Fermi-liquid fixed point.

One thermodynamic quantity of interest is the Wilson (or Sommerfeld) ratio, R. For single-impurity Kondo models, R is a universal quantity, taking the values 2 and 8/3 for one and two channels, respectively. Figure 2 shows the variation of R with I/T_K in the free-electron regime. The plot is for α=0, but similar results are obtained for non-zero α throughout the free electron regime. For large antiferromagnetic RKKY couplings, R tends to unity, the value appropriate for a free electron gas. As the bare parameters approach the left boundary of the marginal region in Fig. 2, the Wilson ratio decreases. However, since calculation of R involves taking the small difference of diverging coefficients, errors grow rapidly in this region of the parameter space. Further work is in progress to determine R more accurately all round the borders of the marginal region.

In the particle-hole-symmetric version of the two-impurity, *one*-channel Kondo model, there is an unstable, marginal-Fermi-liquid fixed point reached from one critical value of I/T_K on the antiferromagnetic side of the phase diagram [6]. This fixed point is completely wiped out by potential scattering [10]. It is natural to ask whether the same is true for the marginal region of the two-channel model. Calculations are presently being carried out to address this question.

A more general treatment of Equation (2) is also under way. This involves the reformulation of Wilson's NRG procedure [5] to permit an essentially exact solution of Eq. (2) — without relying on the energy-independent couplings approximation — for an isotropic, but otherwise arbitrary, electronic dispersion.

Acknowledgements. Computer time for this work was provided by the Ohio Supercomputer Center.

References

[1] D. L. Cox, Physica B 186-188 (1993) 312; D. L. Cox and M. Makivic, in these proceedings.

[2] C. L. Seaman, *et al.*, Phys. Rev. Lett. 67 (1991) 2882; C. L. Seaman and M. B. Maple, in these proceedings.

[3] B. Andraka and A. M. Tsvelik, Phys. Rev. Lett. 67 (1991) 2886; B. Andraka, in these proceedings.

[4] A. A. Ludwig and I. Affleck, Phys. Rev. Lett. 67 (1991) 3160.

[5] K. G. Wilson, Rev. Mod. Phys. 47 (1975) 773.

[6] B. A. Jones and C. M. Varma, Phys. Rev. Lett. 58 (1987) 843; B. A. Jones, C. M. Varma, and J. W. Wilkins, Phys. Rev. Lett. 61 (1988) 125.

[7] K. Ingersent, B. A. Jones, and J. W. Wilkins, Phys. Rev. Lett. 69 (1992) 2594.

[8] For more details see B. A. Jones and K. Ingersent, in these proceedings.

[9] I. Affleck, *et al.*, Phys. Rev. B 45 (1992) 7918.

[10] B. A. Jones, Physica B 171 (1991) 53.

Figure Captions

Fig. 1: Schematic renormalization-group phase diagram for the particle-hole symmetric version of the two-impurity, two-channel Kondo Hamiltonian, parametrized by I/T_K, the ratio of the interimpurity coupling to the single-impurity Kondo temperature, and α, the fractional difference between the coupling of the total impurity spin to even- and odd-parity conduction states. Only the quadrant corresponding to $I \leq 0$, $\alpha \geq 0$ is shown. Thin curves represent renormalization-group flows. Thick lines demarcate distinct regimes of low-temperature behavior. Circles indicate Fermi-liquid fixed points, and a square marks the fixed point corresponding to non-interacting impurities.

Fig. 2: The Wilson (or Sommerfeld) ratio as a function of I/T_K, the ratio of the interimpurity coupling to the single-impurity Kondo temperature, calculated for $\alpha = 0$. Errors in R accumulate rapidly as I/T_K approaches the border of the marginal region. (Within the interior of this region, R cannot be calculated via the method described in the text.) A cross marks the value of R for non-interacting impurities.

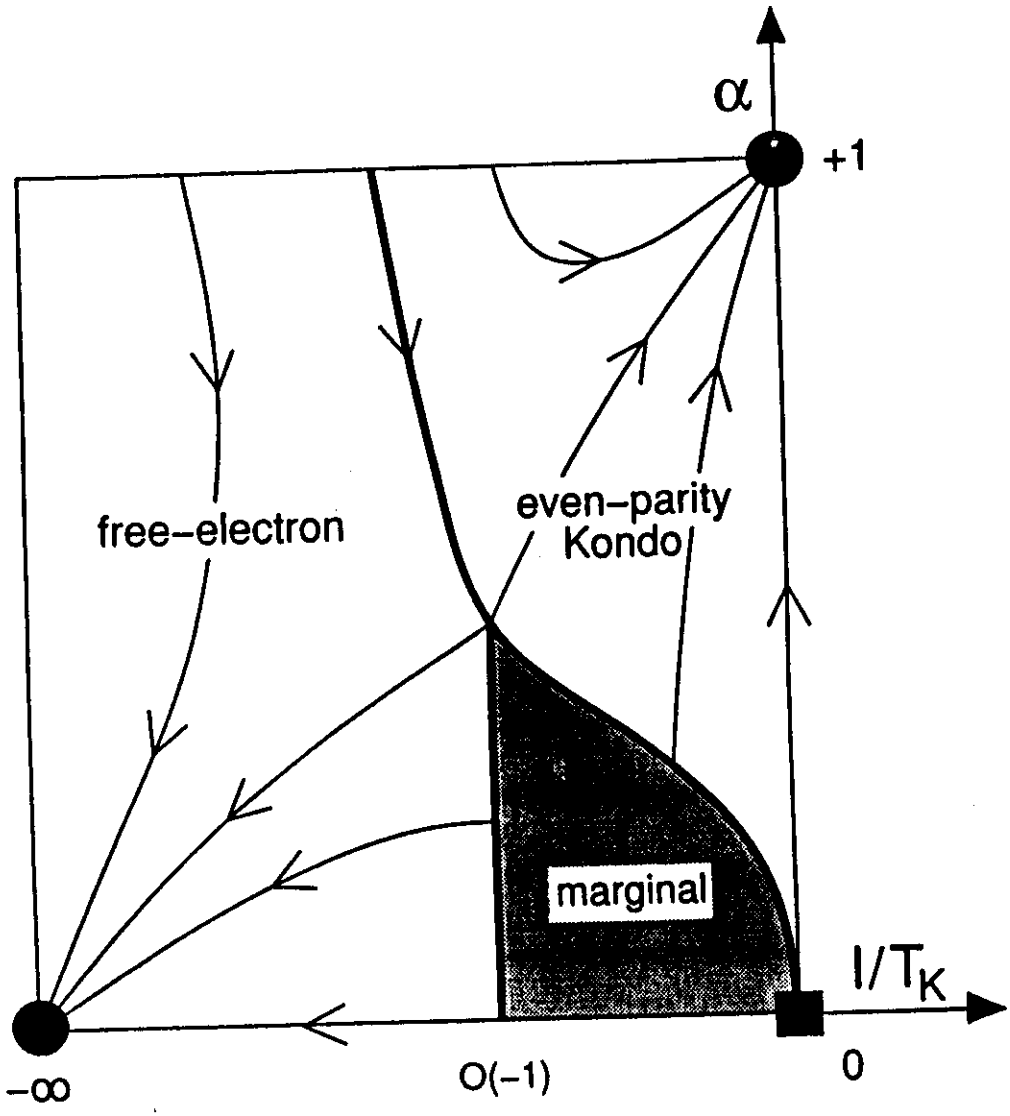

Fig. 1

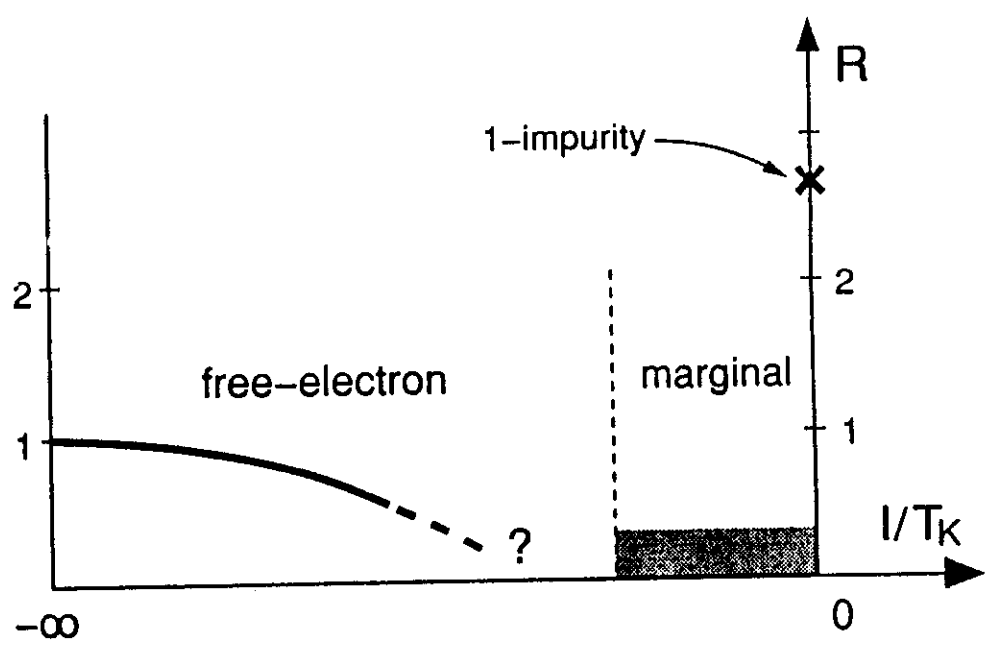

Fig. 2